Substrate recognition determinants of benzylsuccinate synthase and other fumarate-adding glycyl radical enzymes

Philipps Universität Marburg

Dissertation

zur Erlangung des Doktorgrades

der Naturwissenschaften

(Dr. rer. nat.)

dem Fachbereich Biologie der Philipps-Universität Marburg

vorgelegt von

Iryna Salii

aus Lwiw, Ukraine

Marburg/Lahn, Januar 2019

Die Untersuchungen zur vorgelegten Arbeit wurden von Oktober 2015 – Dezember 2018 am Fachbereich Biologie der Philipps-Universität Marburg unter der Leitung von Herrn Prof. Dr. Johann Heider durchgeführt.

Vom Fachbereich Biologie
der Philipps-Universität Marburg als Dissertation am _____ angenommen.

Erstgutachter: Prof. Dr. Johann Heider
Zweitgutachter: Prof. Dr. Wolfgang Buckel

Tag der mündlichen Prüfung: _____

Im Rahmen dieser Arbeit entstandene Publikationen:

Determinants for substrate recognition in the glycyl radical enzyme benzylsuccinate by targeted mutagenesis. Salii I., Seyhan D., Salieniec M., Schühle K., Heider J. Prepared for the submission to Angewandte Chemie International Edition.

Table of Contents

I. SUMMARY

The pathway of anaerobic toluene degradation is initiated by a radical-type fumarate addition, catalyzed by the remarkable glycyl radical enzyme benzylsuccinate synthase (BSS). It has been found that benzylsuccinate synthase is a member of fumarate-adding enzymes (FAEs), which are involved in the anaerobic biodegradation pathways of various hydrocarbons, both aromatic and aliphatic. 2-naphthyl(methylsuccinate) synthase (NMS) is a member of the FAE family, which is predicted to catalyze a similar radical type addition reaction, using 2-methylnaphthalene as substrate. In this study we have shown structure-functional characterization of recombinant BSS from *Thauera aromatica* K172 and NMS from the 2-methylnaphthalene degrading enrichment culture N47. We have established the first recombinant overproduction system of active benzylsuccinate synthase and present initial data on the effects of some constructed active-site mutants in the alpha subunit of the enzyme. We demonstrate that a single isoleucine substitution to valine inside the hydrophobic pocket of the active site of BSS leads to an extended substrate range of the mutated variant including conversion of *m*-xylene. Moreover, we show that a mutation of a highly conserved arginine to lysine or glutamine significantly decreases or eliminates the activity of BSS, proving the importance of this arginine in fumarate binding during catalysis. Remarkably, we demonstrate that an arginine to lysine substitution enables the conversion of a fumarate analogue – 3-acetyl acrylate, which is not converted by the wild type BSS. Overall, this study provides new insight on the reaction mechanism and catalytic parameters of BSS and elucidates the roles of certain amino acids in substrate recognition and binding. Subsequently, we have implemented our overproduction system and produced active NMS, which displayed low reactivity with toluene.

This data serve as an initial proof of the fumarate addition nature of NMS - previously a putative candidate to perform this chemical reaction. Moreover, we have overproduced and purified non-activated forms of BSS and NMS in *E. coli* in order to further characterize the protein complexes by X-Ray crystallography and EPR-spectroscopy.

II. ZUSAMMENFASSUNG

Der Weg des anaeroben Toluolabbaus wird durch eine radikalische Fumarataddition initiiert, die durch das Glycylradikalenzym Benzylsuccinatsynthase (BSS) katalysiert wird. Es wurde gefunden, dass Benzylsuccinatsynthase ein Mitglied der Fumarat-addierenden Enzyme (FAEs) ist, die an den anaeroben Abbauwegen verschiedener Kohlenwasserstoffe beteiligt sind, sowohl aromatischen als auch aliphatischen. Die 2-Naphthyl(methylsuccinat)-Synthase (NMS) ist ein Mitglied der FAE-Familie, von der vorhergesagt wird, dass sie eine ähnliche radikalische Additionsreaktion unter Verwendung von 2-Methylnaphthalin als Substrat katalysiert. In dieser Studie haben wir die Struktur-Funktions-Beziehung rekombinanter BSS aus *Thauera aromatica* K172 und NMS aus der 2-Methylnaphthalin-abbauenden Anreicherungskultur N47 untersucht. Wir haben das erste rekombinante Überproduktionssystem für aktive Benzylsuccinatsynthase etabliert und präsentieren erste Daten zu den Auswirkungen einiger konstruierter Mutanten des aktiven Zentrums in der alpha-Untereinheit des Enzyms. Wir zeigen, dass eine einzelne Isoleucin-Substitution gegen Valin in der hydrophoben Tasche des aktiven Zentrums von BSS zu einem erweiterten Substratbereich der mutierten Variante führt, einschließlich der Umwandlung von *m*-Xylol. Darüber hinaus zeigen wir, dass eine Mutation eines hochkonservierten Arginins zu Lysin oder Glutamin die Aktivität von BSS signifikant verringert oder eliminiert, was die Bedeutung dieses Arginins für die Bindung des Fumarats während der Katalyse belegt. Bemerkenswerterweise zeigen wir, dass eine Arginin-Lysin-Substitution die Umwandlung des Fumarat-Analogons - 3-Acetylacrylat ermöglicht, dass von Wildtyp-BSS nicht umgesetzt wird. Insgesamt liefert diese Arbeit neue Einblicke in den Reaktionsmechanismus und die katalytischen Parameter von BSS und verdeutlicht die Rolle bestimmter Aminosäuren bei der Erkennung und Bindung von Substraten. Anschließend haben wir unser Überproduktionssystem implementiert und aktive NMS produziert, die eine geringe Reaktivität mit Toluol als alternativem Substrat aufweist. Diese Daten dienen als erster Nachweis der Fumarataddition von NMS - zuvor ein mutmaßlicher Kandidat für die Durchführung dieser chemischen Reaktion. Darüber hinaus haben wir nicht aktivierte Formen von BSS und NMS in *E. coli* überproduziert und gereinigt, um die Proteinkomplexe durch Röntgenkristallographie und EPR-Spektroskopie weiter zu charakterisieren.

III. INTRODUCTION

Aromatic hydrocarbons

The group of hydrocarbons consists exclusively of carbon and hydrogen atoms and is divided into several subgroups such as aliphatic, alicyclic and aromatic. Aliphatic compounds are linear or branched compounds which may be saturated or unsaturated (e.g., *n*-hexane or 2-methyl pentane). Alicyclic compounds, on the other hand, contain a ring-shaped structure that, in contrast to the aromatic hydrocarbons, such as benzene, is not completely conjugated to a π-electron system (e.g., cyclohexene). Hydrocarbon compounds belonging to the aromatic hydrocarbons, in contrast to the alicyclic and aliphatic ones, meet the aforementioned criteria for aromatic compounds. One of the representatives of aromatic compounds, used in this work – toluene, is the simplest representative of the alkyl benzenes and has one substituted methyl group in the aromatic ring. Furthermore, aromatic compounds are abundant and structurally diverse in nature. They are found in all organisms in the form of the three aromatic amino acids (phenylalanine, tyrosine and tryptophan) and can make up one-quarter of the biomass of land plants. In addition, BTEX (benzene, toluene, ethylbenzene and xylene, Fig. 1) shows common environmental pollutants that are derived from petroleum derivatives such as gasoline.

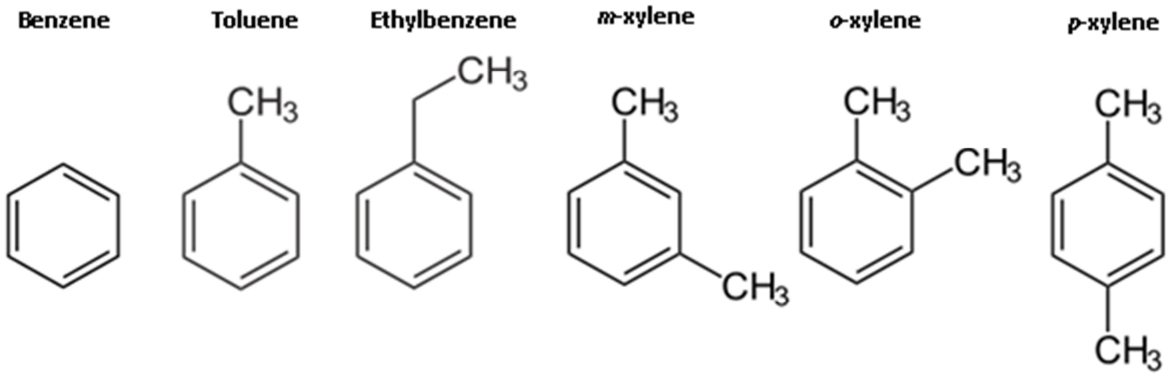

Figure 1: Members of BTEX group (Benzene, Toluene, Ethylbenzene*, m-, o-,* and *p*-xylene).

These substances are used industrially very commonly, e.g. in the manufacturing of various products such as plastic, agrochemicals as well as in the production of pharmaceuticals. Toluene is also used as a solvent, e.g. as component of paints and resins,

and serves as a starting material for the production of explosives (trinitrotoluene, TNT). BTEX hydrocarbons are classified as harmful to the environment and human health and are only slowly degraded (Service, 1989). The persistence of these molecules is due to their low solubility and chemical inertness: compounds such as toluene, phenol, and ethylbenzene contain no easily oxidized carbons, and dearomatization of these compounds requires strong oxidants or reductants. The human organism can take these substances up through the respiratory and digestive tract or via the skin. Toluene, due to the methyl group attached to its aromatic ring, is mainly degraded by oxidation to benzoic acid in the human body, while only small amounts of an epoxide intermediate are formed. Later on, benzoic acid is added to Hippuric acid and excreted through urine. On the other hand, animals and plants have limited possibilities for metabolizing aromatic substances, except for aromatic amino acids and a few other compounds. Hence, the degradation of aromatic substances is dominated by aerobic and anaerobic bacteria and aerobic fungi.

Microbial degradation of aromatic hydrocarbons

Microorganisms have a central role in the recycling of carbon from the aromatic ring. Interestingly, only a few archaea are known to degrade aromatic substrates, and they mainly use strategies that depend on the presence of molecular oxygen (O_2). Due to the low chemical reactivity, aromatic compounds are normally attacked by O_2 molecules and oxygenases, which form compounds such as catechol (1, 2-dihydroxybenzene) (in bacteria) or protocatechuate (3, 4-dihydroxybenzoate) (in most fungi and some bacteria) as central intermediates. This type of degradation is followed by central ring cleavage catalyzed by ring cleaving dioxygenases (Dagley, Evans *et al.,* 1960, Harayama, Kok *et al.,* 1992, Harwood and Parales, 1996, Butler and Mason, 1997, Gibson and Parales, 2000, Lipscomb, 2008).

In recent decades, various oxygen-independent reactions have been identified and characterized by the activation of diverse hydrocarbon substrates, depending on the organism and the respective hydrocarbon. Most studies of these strategies have been performed with denitrifying beta proteobacteria such as *Thauera aromatica* or *Azoarcus* spp., the phototrophic alphaproteobacterium *Rhodopseudomonas palustris* or strictly anaerobic deltaproteobacteria such as *Geobacter* spp.

Anaerobic degradation of toluene

Many ecosystems are contaminated with toluene, such as groundwater or deep soil layers in which no molecular oxygen is available as co-substrate for the activation of the aromatic ring for mono- or dioxygenases. The first pathway for the anoxic degradation of toluene was reported by Biegert *et al.* (1996) for the denitrifying beta-proteobacterium *Thauera aromatica*. This discovery was not only crucial from the environmental point of view but had an economic relevance to the oil industry due to the degradation of toluene in pipelines by sulfate-reducing bacteria, resulting in a release of toxic hydrogen sulfide. This creates dangerous working conditions and leads to corrosion of pipelines and oil tanks (Rabus, Fukui *et al.,* 1996). In recent years, a number of analogous pathways for anaerobic toluene degradation identified in various bacteria, which are represented by different phylogenetic groups and can be subdivided according to their respective metabolic type:

- Denitrifying bacteria (Rabus and Widdel, 1995, Zengler, Heider *et al.,* 1999);
- Iron (III) reducing (Lovley and Lonergan, 1990);
- Sulfate-reducing (Beller, Spormann *et al.,* 1996);
- Proton-reducing and phototrophic species (Zengler, Heider *et al.,* 1999).

The majority of isolated bacteria degrades toluene under denitrifying conditions and belongs to the β-proteobacteria. They include several strains of the genera *Thauera*, *Azoarcus*, *Georgfuchsia* and "*Aromatoleum*", which are abundant in nature (Anders, Kaetzke *et al.,* 1995, Rabus and Widdel 1995, Weelink, van Doesburg *et al.,* 2009). The strains used in our laboratory are *Thauera aromatica* strain K172 (Anders, Kaetzke *et al.,* 1995), *Azoarcus evansii* (Achong, Rodriguez *et al.,* 2001) and *Aromatoleum aromaticum* strain EbN1 (Rabus and Widdel, 1995).

To date, several species of sulfate-reducing toluene-degrading bacteria have also been added to our laboratory collection and cultivated, such as *Desulfobacula toluolica*, which oxidize different aromatic compounds, including toluene, to CO_2. Another model organism, tested in our laboratory is the iron (III) reducing bacterium *Geobacter metallireducens* (Lovley and Lonergan, 1990), which may also use toluene as an electron donor. This organism could be used in environmental protection for the decontamination of polluted

waters since these - due to additional pollution - often have high iron content. In addition to the genera mentioned above, there have been species of toluene-degrading bacteria identified that do not conserve energy by anaerobic respiration, but by fermentation. These bacteria can only be co-cultured with sulfate-reducing bacteria or methanogenic archaea, which are capable to keep hydrogen concentrations in the environment low enough to meet the thermodynamic requirements of the fermentation process (Vogel and Grbic-Galic, 1986). Moreover, phototrophic bacteria have been further identified to degrade aromatic hydrocarbons under anoxic conditions. A known member of this group is *Blastochloris*, which utilizes sunlight energy to allow the use of toluene as sole carbon and electron source (Zengler *et al.,* 1999). In the process of anaerobic toluene degradation, all oxygen-dependent steps of aerobic degradation are replaced by alternative enzymatic reactions in which no molecular oxygen as co-substrate is necessary.

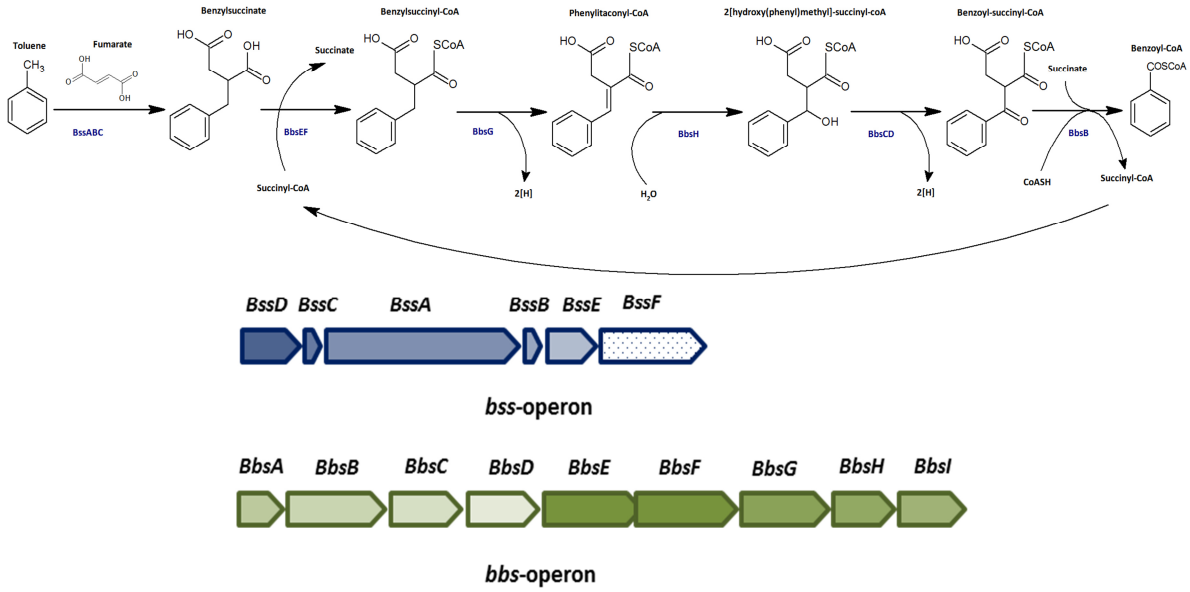

Figure 2: Anaerobic toluene metabolic pathway and gene organization. The reactions of benzylsuccinate synthase (BssDABC) and the enzymes of the further -oxidation pathway are indicated by the respective gene products. Arrows indicate the reversibility or irreversibility of the respective steps. The operon organization of the *bss* and *bbs* operons is indicated below. Enzymes, encoded by the bbs operon: succinyl-CoA: benzyl succinate-CoA transferase (BbsEF), benzylsuccinyl-CoA dehydrogenase (BbsG), (E)-phenylitaconyl-CoA hydratase (BbsH), 2- (hydroxymethylphenyl)-succinyl-CoA dehydrogenase (BbsCD), benzoylsuccinyl-CoA-thiolase (BbsAB) and succinate dehydrogenase (SDH).

Benzylsuccinate has previously been observed as excreted metabolite in supernatants of many toluene-degrading anaerobes, but was regarded as dead-end metabolite indicative of other metabolic pathways because it did not support growth of any known anaerobic

toluene degrader (Beller, Reinhard *et al.,* 1992, Evans, Ling *et al.,* 1992, Seyfried, Glod *et al.,* 1994, Frazer, Coschigano *et al.,* 1995). The role of benzylsuccinate as a true intermediate in anaerobic toluene metabolism and the necessity of a fumarate co-substrate was first demonstrated by in vitro experiments with extracts of the denitrifying bacterium *Thauera aromatica* (Biegert, Fuchs *et al.,* 1996). These findings were confirmed with toluene-degrading strains affiliated to the closely related genera *Azoarcus* and *Aromatoleum*, sulfate-reducing strains affiliated to the genus *Desulfobacula* and the anoxygenic phototroph *Blastochloris sulfoviridis* (Beller and Spormann, 1997, Zengler, Heider *et al.,* 1999). Subsequently, the reaction was shown to be stereospecific as *(R)*-benzylsuccinate was exclusively generated (Beller and Spormann 1998, Leutwein and Heider 1999, Seyhan, Friedrich *et al.,* 2016). Further studies have shown that benzylsuccinate is indeed the product of the initial reaction of toluene degradation pathway, catalyzed by the GRE enzyme *(R)*-benzylsuccinate synthase (Fig. 2).

Benzylsuccinate synthase: genetic organization and reaction mechanism

BSS was first purified and characterized from the β-proteobacteria *T. aromatica* and *Azoarcus* strain T (Leuthner, Leutwein *et al.,* 1998, Beller and Spormann, 1999). Moreover, all analyzed BSS enzymes accepted a number of substituted toluene derivatives, such as fluorotoluenes (Biegert, Fuchs *et al.,* 1996), *o*-xylene (Beller and Spormann, 1997), all three cresol isomers and *o*-toluidine (Lippert and Heider, unpubl. data). Importantly, BSS from *Azoarcus* strain T has been confirmed to convert all xylene isomers together with toluene and cresols (Verfurth, Pierik *et al.,* 2004).

Genetic organization. Genes coding for BSS and its activating enzyme are organized in a common operon, which was assigned as the *bss* operon (Fig. 2, 3) (Coschigano, Wehrman *et al.,* 1998, Leuthner, Leutwein *et al.,* 1998, Achong, Rodriguez *et al.,* 2001, Kube, Heider *et al.,* 2004, Aklujkar, Krushkal *et al.,* 2009). The gene order of the *bss* operon is *bssDCAB*, starting with the gene for the activating enzyme and followed by those for the β-, α- and γ-subunits. Moreover, the known *bss* operons continue with at least two or even more conserved genes of unknown function that have been labelled *bssE* , *bssF* , etc. (Fig. 2, 3) (Hermuth, Leuthner *et al.,* 2002, Kube, Heider *et al.,* 2004).

Figure 3: Structural organization of the genes of BSS from *Thauera aromatica* K172: *bssC*, *bssA* and *bssB* together with the gene *bssD* for the activating protein *BssD* and the genes *bssE, F, G* and *H* are summarized in an operon produced by the two-component regulatory system TdiSR encoded by *tdiS* and *tdiR.*

Together with the *bbs* operon coding for the enzymes of further degradation of benzylsuccinate and a putative operon involved in solvent resistance, the *bss* operon was shown to be exclusively expressed under anoxic conditions in the presence of toluene (Coschigano, 2000, Achong, Rodriguez *et al.,* 2001, Hermuth, Leuthner *et al.,* 2002, Kube, Heider *et al.,* 2004, Kuhner, Wohlbrand *et al.,* 2005), (Fig. 2).

Reaction mechanism. The reaction is initiated by the glycyl radical-dependent generation of a thiyl radical at the conserved Cys493, which is in close proximity to the active site Gly829. Due to the relative stability of glycyl radicals under anaerobic conditions (Knappe and Sawers, 1990, Buckel and Golding, 2006) and the distance to the putative active site (Funk, Judd *et al.,* 2014), it is believed that the radical located on glycine Gly829 only represents a low-reactive transition form of the activated enzyme until both substrates are bound in the catalytic centre, with monoprotonated fumarate binding first and taking the thermodynamically favourable pro-*(R)* orientation (Funk, Marsh *et al.,* 2015, Szaleniec and Heider, 2016). After subsequent binding of the toluene, the enzyme may undergo a structural change that closes access to the active site (Funk, Judd *et al.,* 2014), so that all further steps of catalysis take place in a closed-pocket environment in order to remove highly reactive intermediates involved in the reaction in order to prevent unwanted reactions. Inter alia, due to the spatial removal of the glycine residue from the putative active site of the enzyme, it is believed that the radical is first transferred from the glycine residue to a conserved cysteine present in all glycyl radical enzymes to give a thiyl radical (Fig. 4). This newly formed thiyl radical then participates in the reaction by abstracting a hydrogen atom from the methyl group of toluene to form a benzyl radical intermediate. This benzyl radical reacts in the addition to the distal C3 atom of the fumarate to form a benzylsuccinyl radical (Fig. 4) (Bharadwaj, Dean *et al.,* 2013, Szaleniec and Heider, 2016). At this point in the reaction, the hydrogen atom is re-abstracted from Cys493 and attached in a *syn*-addition to the proximal C2 atom of the fumarate (Qiao and Marsh, 2005, Szaleniec and

Heider, 2016), forming exclusively *(R)*-benzylsuccinate (Beller and Spormann, 1998, Leutwein and Heider, 1999) and regenerating the thiyl radical (Fig. 4). The resulting radical is transferred back to the glycine residue before the active site is opened. The product - *(R)*-benzylsuccinate is released, which presumably opens the active site cavity for the next round of reaction.

This mechanism has been supported by the studies of Beller and Spormann using D_3-methyl labelled toluene. As it is illustrated in Fig. 4, the abstracted hydrogen atom at the initial stage of the reaction can be recovered in the product benzylsuccinate (Beller & Spormann, 1999).

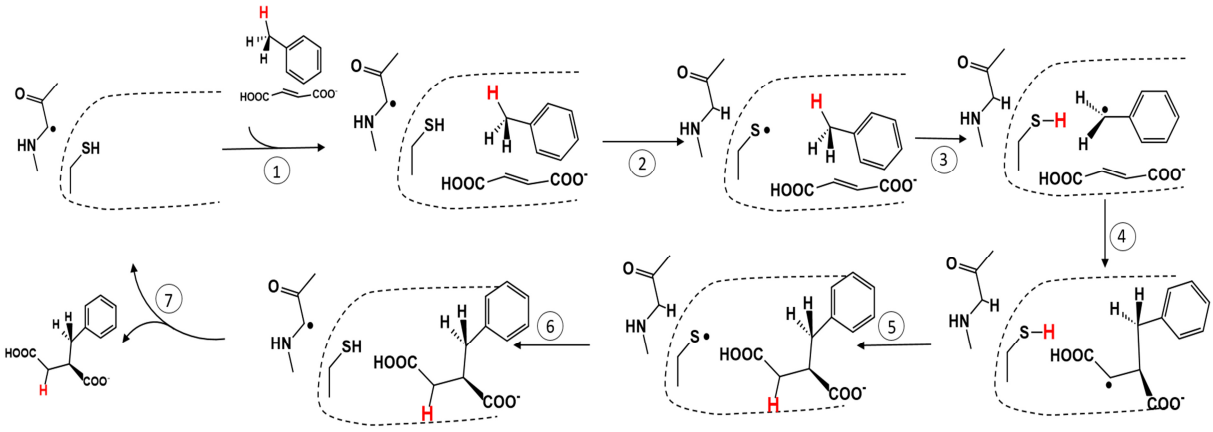

Figure 4: Proposed reaction mechanism of benzylsuccinate synthase. The dashed lines indicate the active site of the enzyme with binding sites for fumarate and toluene. 1: Of the two substrates, monoprotonated fumarate binds in pro- (R) orientation and then toluene. 2: Once the substrates have bound, the radical is transferred from the glycine residue Gly829 to the cysteine residue Cys493. 3: The resulting thiyl radical abstracts a hydrogen atom from the methyl group of toluene to produce a benzyl radical. 4: The benzyl radical adds to the double bond of fumarate. 5: The previously abstracted hydrogen atom is added in a syn addition to the proximal C2 atom. 6: Before the active site opens to release (R) -benzylsuccinate, the radical is transferred from the cysteine residue back to the glycine residue. 7: With the release of (R) -benzylsuccinate, the enzyme is available for the next reaction cycle (Heider, Szaleniec *et al.,* 2016).

Moreover, Himo's DFT calculations also confirmed the plausibility of the suggested mechanism described with the attack of the methyl group by the thiyl radical with the subsequent C-C bond formation, and the dissolution of the benzylsuccinyl radical by abstraction of the hydrogen from the cysteine residue Cys493 (Himo, 2002, Himo, 2005).

Significant differences from Himo's studies were identified by Szaleniec and Heider in 2016 regarding the relative heights of the energetic barriers to the individual steps of the reaction mechanism (Szaleniec and Heider, 2016). According to DFT modeling data based on

the crystal structure of (Funk, Judd *et al.,* 2014), it is no longer assumed that the formation of the C-C bond (TS2 in Fig. 5, TS3 in Himo, 2005) represents the limiting step of the reaction. Instead, the new data suggest that the turnover rate is mainly regulated by the C-H activation (TS1 in Fig. 5, TS2 in Himo, 2005), and that the calculated energy barriers of TS1 and TS2 differ by 4.8 kcal/mol (Fig. 5). The step of re-abstracting the hydrogen from Cys493-SH, which was assigned by Himo (2005) to a comparatively low energy level, is more energy-consuming than the addition of the benzyl radical to fumarate (15.2 vs. 13.6 kcal/mol, Fig. 5) (Szaleniec and Heider, 2016).

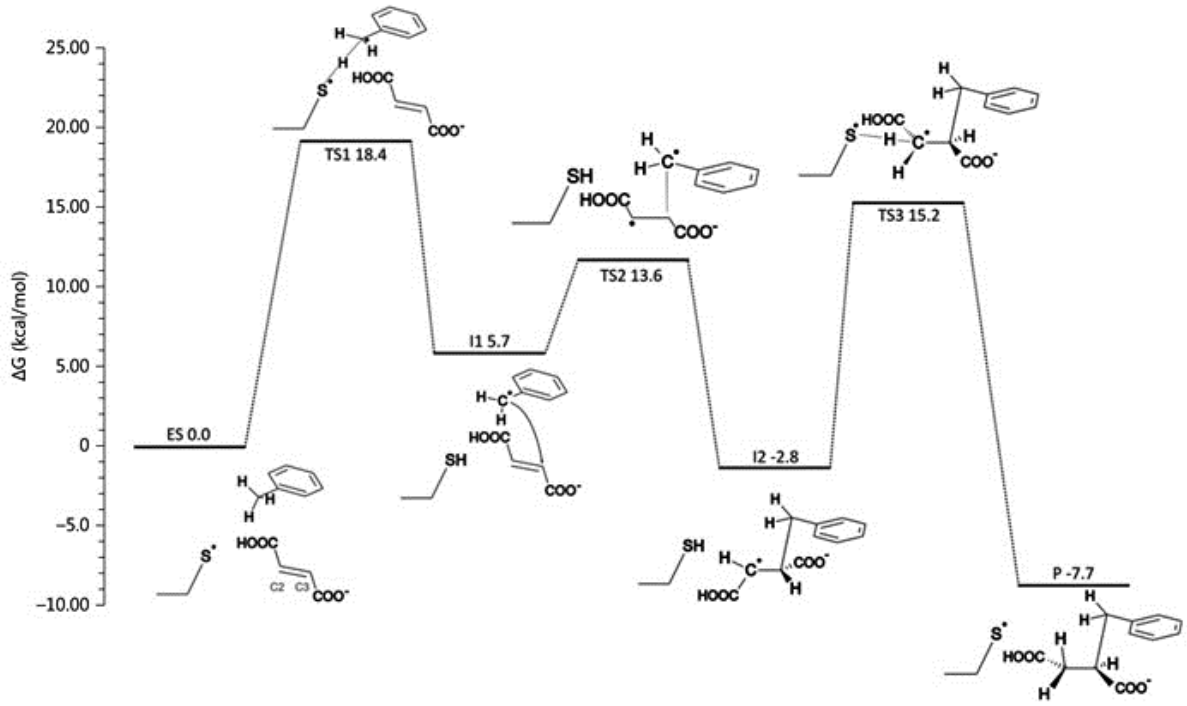

Figure 5: DFT model of Gibbs free enthalpy for the reaction mechanism of BSS (Heider, Szaleniec *et al.,* 2016). Starting from the enzyme-substrate complex (ES), activation of toluene by the thiyl radical leads through transition state TS1 to stage I1 (intermediate 1), the formation of the benzyl radical intermediate. The formation of the C-C bond between benzyl radical and fumarate leads to stage I2, the benzylsuccinyl radical, through the attack of the distal C3 atom of fumarate as transitional state 2 TS2. The third energy barrier, with the transition state TS3, represents the extinction of the benzylsuccinyl radical by abstraction of the hydrogen atom from the Cys493-SH group, resulting in the formation of the benzylsuccinate-linked enzyme-product complex P. The overall reaction is -7.7 kcal/mole exergonic.

The activating enzyme BssD is responsible for the generation of a glycyl radical in BSS

Post-translational activation of BSS requires the presence of an additional activating enzyme BssD which, as in all known fumarate-adding enzymes, is encoded in the *bss* operon together with the three subunits of BSS (Fig. 2, 3), (Coschigano, Wehrman *et al.,* 1998, Leuthner, Leutwein *et al.,* 1998, Achong, Rodriguez *et al.,* 2001, Kube, Heider *et al.,* 2004).

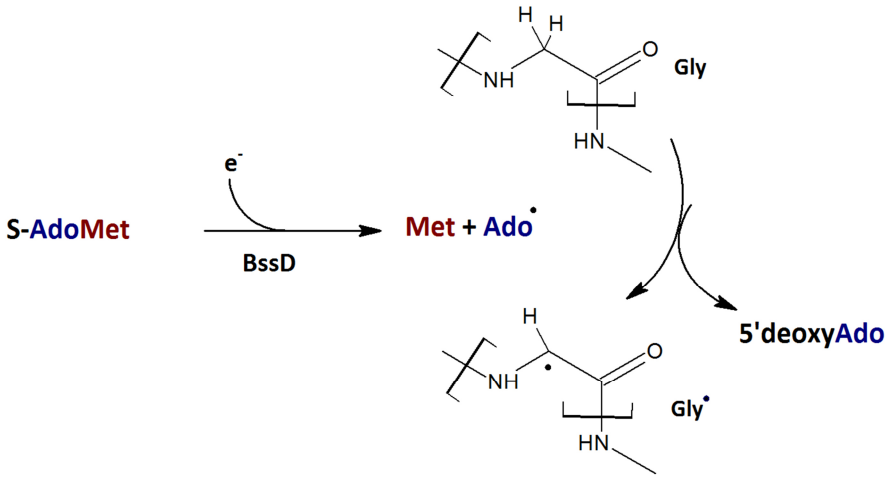

Figure 6: Activating enzyme BssD generates a Gly radical on BSS via SAM-dependent mechanism.

BssD is very similar to other glycyl radical activation enzymes and belongs to the family of S-adenosylmethionine-dependent radical enzymes (SAM) (Sofia, Chen *et al.,* 2001). In contrary to the activating enzymes of 4-hydroxyphenylacetate decarboxylase and most other known glycyl radical enzymes, it differs from the previously investigated activating proteins (pyruvate formate lyase and anaerobic ribonucleotide reductase) by an additional domain containing two additional ferredoxin-like Fe_4S_4 clusters of unknown function (Leuthner, Leutwein *et al.,* 1998, Selmer, Pierik *et al.,* 2005). Similar to all activating enzymes, the Fe_4S_4 cluster is unusually coordinated by a cysteine motif of only three conserved cysteine residues. This leaves the fourth coordination site of the cluster vacant and serves to bind the co-substrate S-adenosylmethionine (SAM), which is used to generate a glycyl radical (Fig. 6). In this case, an electron is transferred from the iron-sulfur cluster to the co-substrate SAM, so that it is homolytically cleaved to form an adenosyl radical and methionine. The adenosyl radical is used to generate the glycyl radical in the active site of the BSS (Fig. 6).

Further degradation of *(R)*-benzylsuccinate via β-oxidation pathway

The subsequent degradation of *(R)*-benzylsuccinate is followed by the so-called β-oxidation pathway. The enzymes of this route are encoded in a toluene-induced *bbs* operon (Fig. 2) (stands for β-oxidation of benzylsuccinate) (Leuthner and Heider, 2000, Kube, Heider *et al.,* 2004).

The succinyl-CoA: benzylsuccinate-CoA transferase (BbsEF) together with succinyl-CoA forms *(R)*-benzylsuccinyl-CoA, which is oxidized by the benzylsuccinyl-CoA dehydrogenase (BbsG) and hydrated to the corresponding alcohol (2-hydroxymethylphenyl)-succinyl-CoA by *(E)*-phenylitaconyl-CoA hydratase (BbsH). In the next step, the hydroxyl group is oxidized by 2-(hydroxymethylphenyl)-succinyl-CoA dehydrogenase BbsCD (alcohol dehydrogenase) to form benzoylsuccinyl-CoA. Finally, the thiolytic cleavage of benzoylsuccinyl-CoA is catalyzed by thiolase BbsAB and the subsequent reaction leads to benzoyl-CoA and succinyl-CoA intermediates (Leuthner and Heider, 2000). Benzoyl-CoA is a common intermediate in most anaerobic degradation pathways of aromatic hydrocarbons and is later metabolized to acetyl-CoA by a highly conserved degradation pathway initiated by benzoyl-CoA reductase (Boll, Albracht *et al.,* 1997, Boll, 2005, Peters, Shinoda *et al.,* 2007, Fuchs, Boll *et al.,* 2011). Succinyl CoA is used to activate benzylsuccinate and the resulting succinate is oxidized to fumarate by succinate dehydrogenase and is thus available again to benzylsuccinate synthase as a co-substrate (Fig. 7).

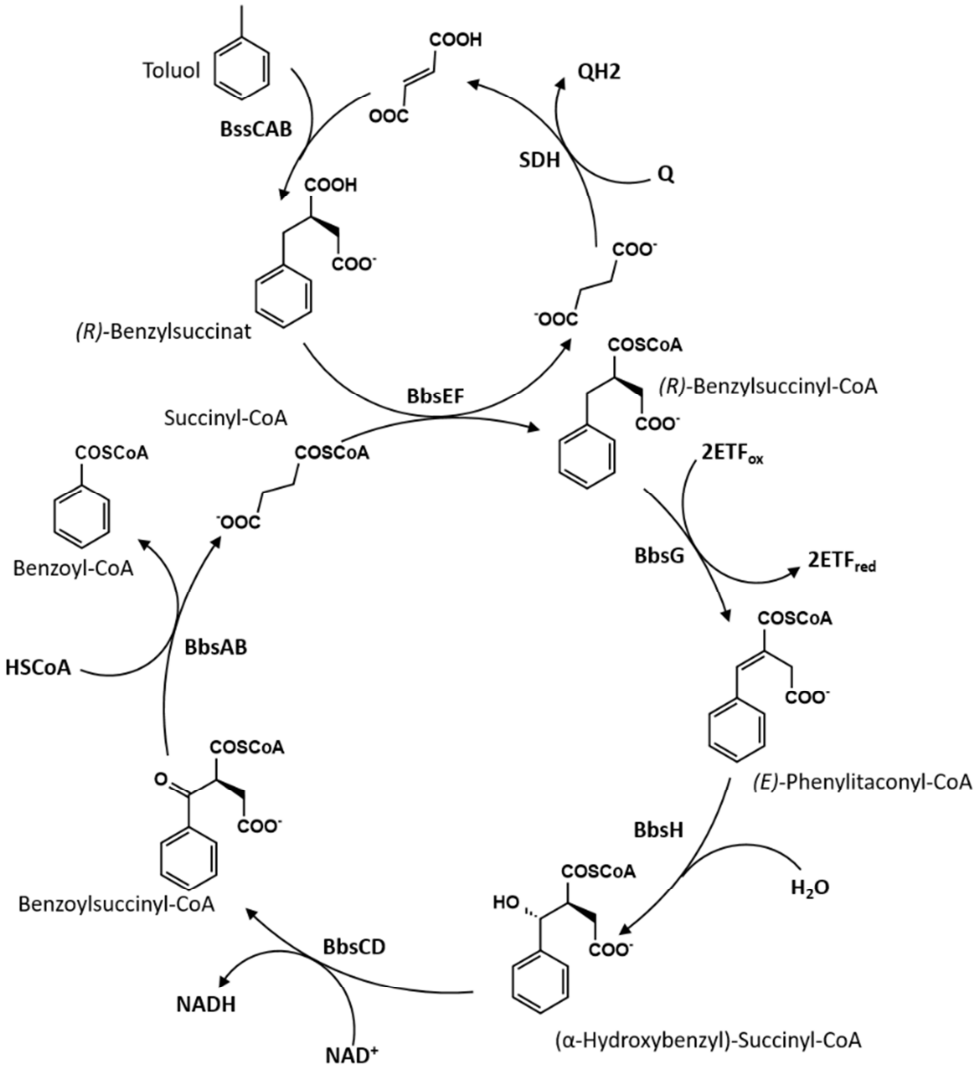

Figure 7: Initiation of the degradation of toluene by benzylsuccinate synthase followed by β-oxidation of benzyl succinate in *T. aromatica* (after Hilberg, 2012, Seyhan, 2016, non-modified). The initial step in the anaerobic degradation of toluene, the formation of *(R)*-benzylsuccinate, is catalyzed by *(R)*-benzyl succinate synthase (BssCAB). Succinyl-CoA: benzylsuccinate-CoA transferase (BbsEF) then forms with succinyl-CoA to form succinate the CoA thioester *(R)*-benzylsuccinyl-CoA, which is oxidized by the benzylsuccinyl-CoA dehydrogenase (BbsG) and passed through the *(E)*-phenylitaconyl-CoA hydratase (BbsH) is hydrated. The 2-(hydroxymethylphenyl) succinyl-CoA dehydrogenase (BbsCD) oxidizes the alcohol group to form benzoylsuccinyl-CoA to the keto group. Benzoylsuccinyl-CoA thiolase (BbsAB) cleaves one thioester bond to form a new one, generating benzoyl-CoA and succinyl-CoA and starting a new cycle. Fumarate can be regenerated from succinate by succinate dehydrogenase.

Structural insights into the active center of BSS

The structure of benzylsuccinate synthase from *T. aromatica* strain T1, which is a highly related to strain K172, was recently published by (Funk, Judd *et al.,* 2014). It

confirmed, that BSS consists of three subunits of 98, 8.5 and 6.5 kDa, which form an heterohexamer of 220 kDa. The sequence of the large subunit includes a conserved Gly residue close to the C-terminus involved in generating and carrying the glycyl radical and a structurally adjacent conserved Cys in the middle of the sequence, which is supposed to be involved in the reaction in the form of a reactive thiyl radical (Gly829 and Cys493 for BSS from *T. aromatica*, respectively) (Leuthner, Leutwein *et al.,* 1998, Selmer, Pierik *et al.,* 2005) . Furthermore, the active site of the BSS α-subunit is consistent with the general glycyl radical enzyme fold, which consists of a β/α barrel domain with two inward-facing finger loops carrying the catalytically important amino acids Cys493 and Gly829 at their tips. Both small subunits contain a Fe_4S_4 cluster of very low redox potential, which is coordinated by four cysteine residues, respectively (Hilberg, unpublished data). In the available crystal structures, the Fe_4S_4 cluster of the γ-subunit is missing, whereas the coordination of the cluster of the β-subunit is reminiscent to that of high potential iron-sulfur protein. However, the relatively large distances between the small subunits and the active site indicate that they have no direct role in catalysis. The β-subunit of BSS has been proposed to play a potential role in enabling access of the substrates to the active site, whereas the loss of the Fe_4S_4 cluster of the γ-subunit in the crystallized enzyme precludes the assignment of a functional role. Despite having no recognizable sequence homology to any protein of known structure, BSSβ adopts a fold similar to that of a high potential iron-sulfur protein (HiPIP). Three short β-strands make a stable platform for the coordination of the [4Fe-4S] cluster by four Cys ligands.

It has recently been shown that each of the small subunits of BSS contains a very low potential Fe_4S_4 cluster of as yet unknown function (Li, Patterson *et al.,* 2009, Hilberg, Pierik *et al.,* 2012, Funk, Judd *et al.,* 2014), which is most likely responsible for the oxygen sensitivity of the enzyme even in the non-activated state. The active, radical-containing form of BSS requires an additional activating enzyme, BssD, which is encoded in a common operon with the three subunits of BSS (Bss-CAB) and belongs to the family of S-adenosyl methionine radical enzymes (Coschigano, Wehrman *et al.,* 1998, Leuthner, Leutwein *et al.,* 1998, Achong, Rodriguez *et al.,* 2001, Sofia, Chen *et al.,* 2001, Kube, Heider *et al.,* 2004).

Recent studies (Bharadwaj, Dean *et al.,* 2013, Funk, Marsh *et al.,* 2015, Szaleniec and Heider, 2016) have predicted several amino acids that may play key roles in the reaction

mechanism of BSS, either by providing hydrophobic interaction for the correct positioning of toluene or by hydrogen bonding to position and fixing of fumarate.

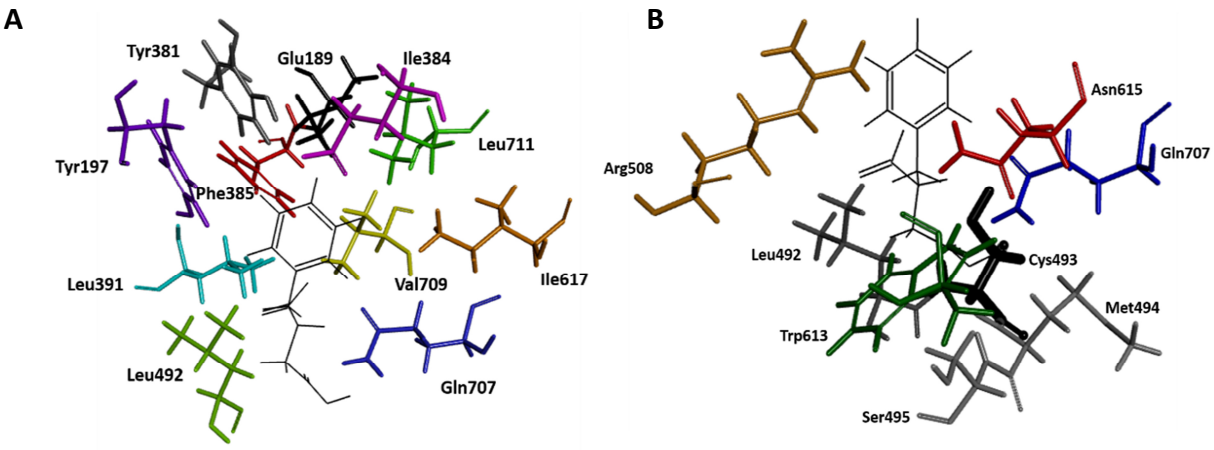

Figure 8: (Seyhan, 2016) BSS activity center models containing benzylsuccinate, calculated by Maciej Szaleniec, optically modified for this work. (A) Amino acids, which are considered by their non-polar properties as likely candidates for the correct positioning and binding of toluene. (B) Amino acids whose polar properties make them suitable for the positioning and binding of fumarate. Calculated electrostatic and hydrogen-bonded interaction energies: Arg508 (-11.94 kcal / mol), Tyr197 (-3.16 kcal / mol), Trp613 (-2.52 kcal / mol), Gln707 (-0.85 kcal / mol), Cys493 (-0.25 kcal / mol); Calculated van der Waals-based interactions: Ile384 (-2.39 kcal / mol), Leu492 (-2.34 kcal / mol), Leu391 (-1.45 kcal / mol), Val709 (-1.99 kcal / mol), Leu711 (-1.90 kcal / mol).

Docking studies based on (Funk, Judd *et al.,* 2014) suggest the attachment of the carboxyl group of fumarate by the positively charged arginine residue Arg508. On the other side of the BSS putative active site, a number of hydrophobic amino acids have been identified that could play a role in the binding of toluene. Quantum-mechanical (QM) cluster models indicate 9 amino acid residues in the putative centre surrounding the bound substrates: Glu189, Tyr197, Ser199, Ile384, Leu391, Leu492, Cys493, Arg508, and Val709 (Fig. 8).

Toluene contains no polar functional groups to facilitate its positioning during catalysis. The binding site is created primarily by aliphatic and aromatic residues. Residues from two regions, α-helix loop 3’ (Ile384, Phe385, Leu391) and the α-helix loop 8’and β-sheet 8 (Val-709, Leu-711), create what is called a “hydrophobic wall” (Funk, Judd *et al.,* 2014) that forms one side of the active site, opposite fumarate, thereby making the Gly radical domain considerably less solvent-accessible than in the other enzymes in GRE family. A ring of hydrophobic (Tyr197, Tyr381, Leu492, Ile617) and polar (Glu189, Gln707) residues forms the sides of the toluene binding pocket, matching the toluene molecule.

The final side of the binding pocket is created by fumarate itself, with the methyl group of toluene stacked against C2 of fumarate and the aromatic ring of toluene stacked against the C1 carboxylate of fumarate (Funk, Marsh *et al.,* 2015).

This orientation of toluene is consistent with the production of (*R*)-benzylsuccinate, as previously observed (31, 32), as it places C1 of toluene directly adjacent to C2 of fumarate (Qiao and Marsh, 2005, Li and Marsh, 2006).

Paralogous fumarate addition enzymes

Anaerobic toluene-degrading bacteria occur in many physiological groups of microorganisms, especially denitrifying bacteria, metal ion and sulfate-reducing species. Most of the known toluene-degrading denitrifying bacteria belong to the genera *Thauera*, *Azoarcus*, *Georgfuchsia* and *Aromatoleum* within the betaproteobacterial family *Rhodocyclaceae* (Fig. 9). Three additional subfamilies of paralogous FAE isoenzymes catalyzing fumarate addition to various aromatic or aliphatic compounds other than toluene were identified in diverse bacteria: for example, the sulfate-reducing species *Desulfobacula toluolica* contains a second operon coding for an FAE apparently specific for *p*-cresol activation (HBSS) next to the normal *bss* operon involved in toluene metabolism.

The derived sequence of the large subunit of HBSS forms a separate cluster in the phylogenetic tree together with the sequences of some closely related uncharacterized FAEs, which can now be assigned as *p*-cresol-specific *p*-hydroxybenzylsuccinate synthases (HBSS; Fig. 9). Alkane-degrading species of nitrate- or sulfate-reducing bacteria have been shown to use a special clade of FAE (alkanesuccinate synthase, ASS, or 1-methyl alkyl) succinate synthase, MASS) for the initial step of alkane activation, forming alkyl succinate adducts at the methylene group of the alkane (Rabus, Wilkes *et al.,* 2001, Callaghan, Wawrik *et al.,* 2008, Grundmann, Behrends *et al.,* 2008, Callaghan, Davidova *et al.,* 2010). Genes coding for another enzyme involved in the degradation of *p*-cymene have also been identified in a nitrate-reducing strain (Strijkstra *et al.*).

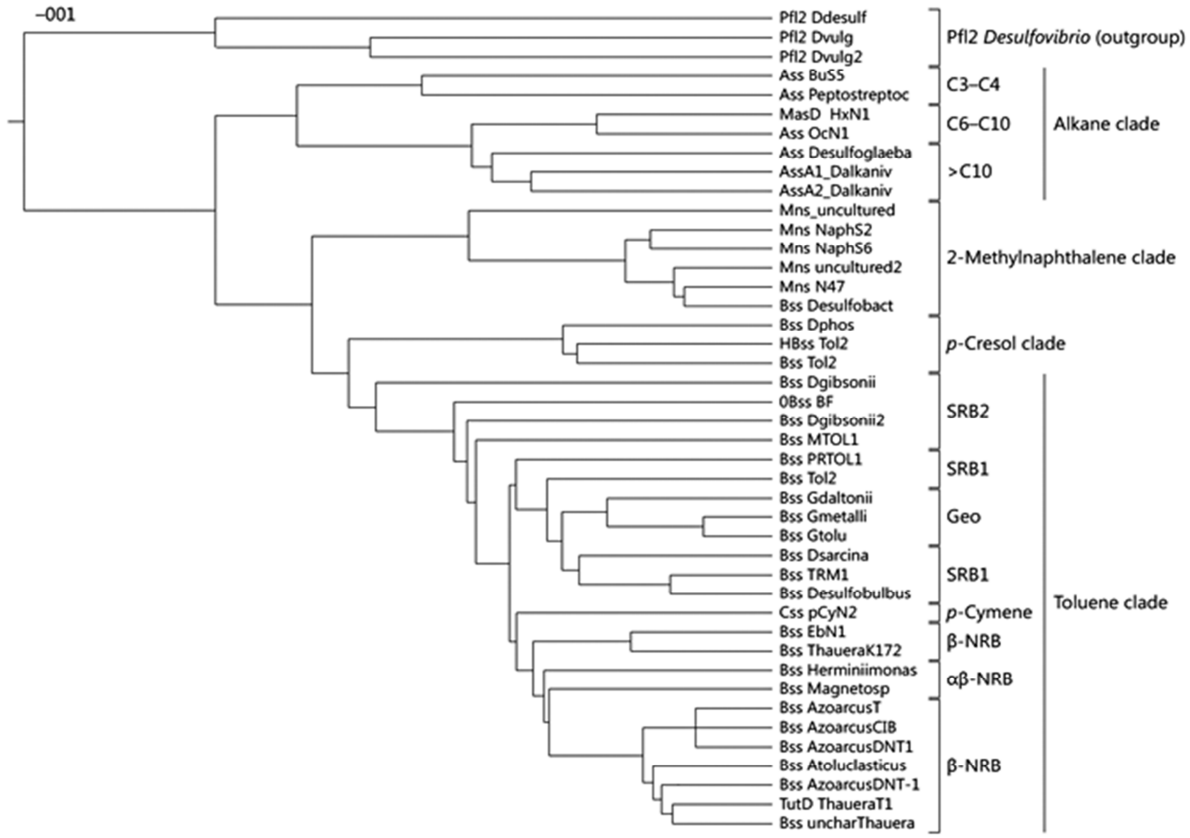

Figure 9: (Heider, Szaleniec *et al.,* 2016) Phylogenetic tree of FAEs. SRB1 and SRB2 = Sulfate-reducing bacteria affiliated to the Deltaproteobacteria or the Firmicutes, respectively; Geo = Geobacter strains. As the outgroup, a number of similar uncharacterized GREs from Desulfovibrio strains have been used, which belong to the 'Pfl2' group of GREs but are not members of the FAE group (based on missing active-site residue homologs, such as the universally conserved Arg508 or the amino acids surrounding Cys493, and the lack of genes for small subunits in their respective operons).

More importantly, FAEs have been also found in several naphthalene and 2-methylnaphthalene-degrading sulfate-reducing isolates and enrichment cultures (NaphS6, N47) to effect 2-methylnaphthalene activation, generating a 2-(2-methylnaphthyl) succinate intermediate (Galushko, Minz *et al.,* 1999, Selesi, Jehmlich *et al.,* 2010), (Fig. 10). Phylogenetic analysis with the sequences of the respective large subunits of these enzymes (naphthyl-2-methyl succinate synthase, NMS) indicates that they form another homology cluster, representing a distinct NMS clade with less sequence conservation to the BSS and HBSS paralogs.

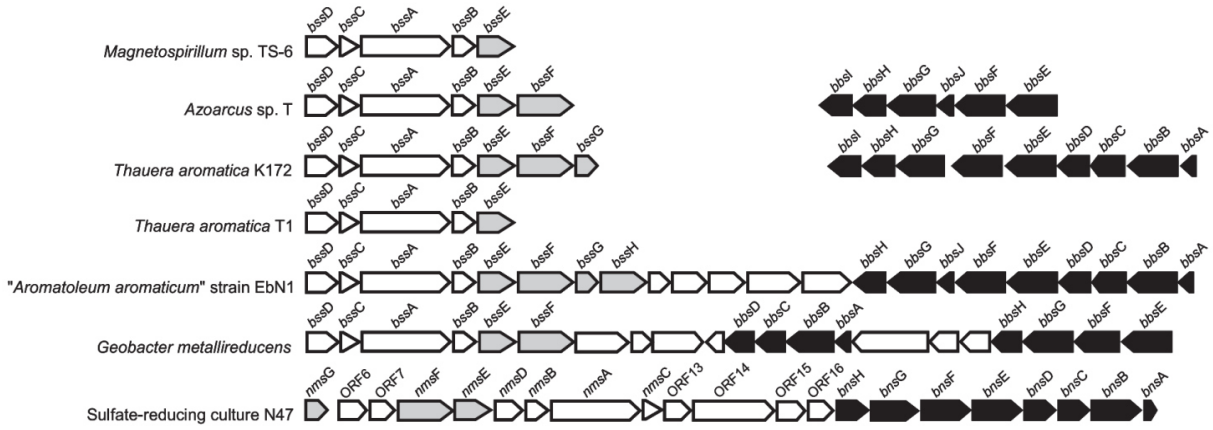

Figure 10: (Selesi, Jehmlich *et al.,* 2010) Organization of the *nms* and *bns* gene clusters of anaerobic 2-methylnaphthalene catabolism in the sulfate-reducing culture N47 in comparison with those of the *bss* and *bbs* genes for anaerobic toluene degradation in *Magnetospirillum* sp. strain TS-6, *Azoarcus* sp. strain T, *T. aromatica* strain K172, *T. aromatica* strain T1, *A. aromaticum* strain EbN1, and *G. metallireducens* strain GS15. Genes are depicted as arrowheads. Genes for anaerobic toluene degradation are as follows: *bssABCD*, encoding benzylsuccinate synthase and the activating enzyme; *bssE*, encoding a putative chaperone; *bssH*, encoding a putative transporter; *bbsEF*, encoding succinyl-CoA:(*R*)-benzylsuccinate CoA-transferase; *bbsG*, encoding (*R*)-benzylsuccinyl-CoA dehydrogenase; *bbsH*, encoding phenylitaconyl-CoA hydratase; *bbsCD*, encoding 2-[hydoxy(phenyl)methyl]-succinyl-CoA dehydrogenase; *bbsAB*, encoding benzoylsuccinyl-CoA thiolase; and *bssF*, *bssG*, *bbsI*, and *bbsJ*, encoding hypothetical proteins.

Methylnaphthalene and phenanthrene degradation under sulfate reducing conditions

Marine sediment incubations and enrichments showed degradation of naphthalene, methylnaphthalene or phenanthrene with sulfate as electron acceptor (Galushko, Minz *et al.,* 1999, Musat, Galushko *et al.,* 2009) and even pure cultures were obtained that can degrade naphthalene and 2-methylnaphthalene. ^{14}C-labeled compounds were used to show the mineralization of naphthalene or phenanthrene to CO_2. Zhang and Young (1997) also incubated the enrichments with ^{13}C-bicarbonate and naphthalene or phenanthrene, and observed the incorporation of the ^{13}C-label into naphthoic and phenanthroic acid.

Active biodegradation with sulfate was also reported for incubations from contaminated aquifers (Annweiler, Materna *et al.,* 2000, Meckenstock, Annweiler *et al.,* 2000, Kummel, Herbst *et al.,* 2015). The peripheral pathway of 2-methylnaphthalene degradation was elucidated in culture N47, which was enriched from contaminated groundwater.

The culture consisted mainly of a Deltaproteobacterium and to a minor extent of a *Spirochaeta*. 2-methylnaphthalene is activated by fumarate addition to the methyl group analogous to anaerobic toluene degradation. The reaction is catalyzed by the glycyl radical enzyme naphthyl-2-methyl-succinate synthase (Annweiler *et al.,* 2000; Safinowski and Meckenstock, 2004). After activation with coenzyme (Co)A, the degradation pathway proceeds via β-oxidation on the methylene carbon finally leading to the central metabolite 2-naphthoyl-CoA (Meckenstock *et al.,* 2000; Safinowski and Meckenstock, 2004).

Methylphenanthrene succinate synthase

Methylphenanthrene succinate synthase (MPS) is a putative glycyl radical FAE, which has not been yet described in the literature and has been found in the metagenome sequence of an anaerobic phenanthrene degrading enrichment culture. It is proposed to be encoded in the phenanthrene-degrading microorganism together with the genes for anaerobic phenanthrene degradation (Davidova, Gieg *et al.,* 2007, Himmelberg, Bruls *et al.,* 2018), allowing the strain more metabolic flexibility to degrade naturally occurring substrate mixtures. Due to the phylogenetic tree alignments, the sequence of a putative MpsA subunit forms a separate cluster, implicating a separate position within the fumarate-adding enzymes (Fig. 32). In contrast to *bss* and *nms* operons, the available genes for the putative *mps* operon encode only α and β subunits, but no γ subunit. However, no sequences for further β-oxidation of the succinate adduct of 2-methylphenanthrene have been detected in the metagenome. Although, regarding the BSS-like nature of this enzyme, as a careful examination of its sequence might provide some clues towards its substrate preference (Fig. 11). Moreover, the gene content of this organism suggests it is active towards a large spectrum of PAH (polycyclic aromatic hydrocarbons) substrates.

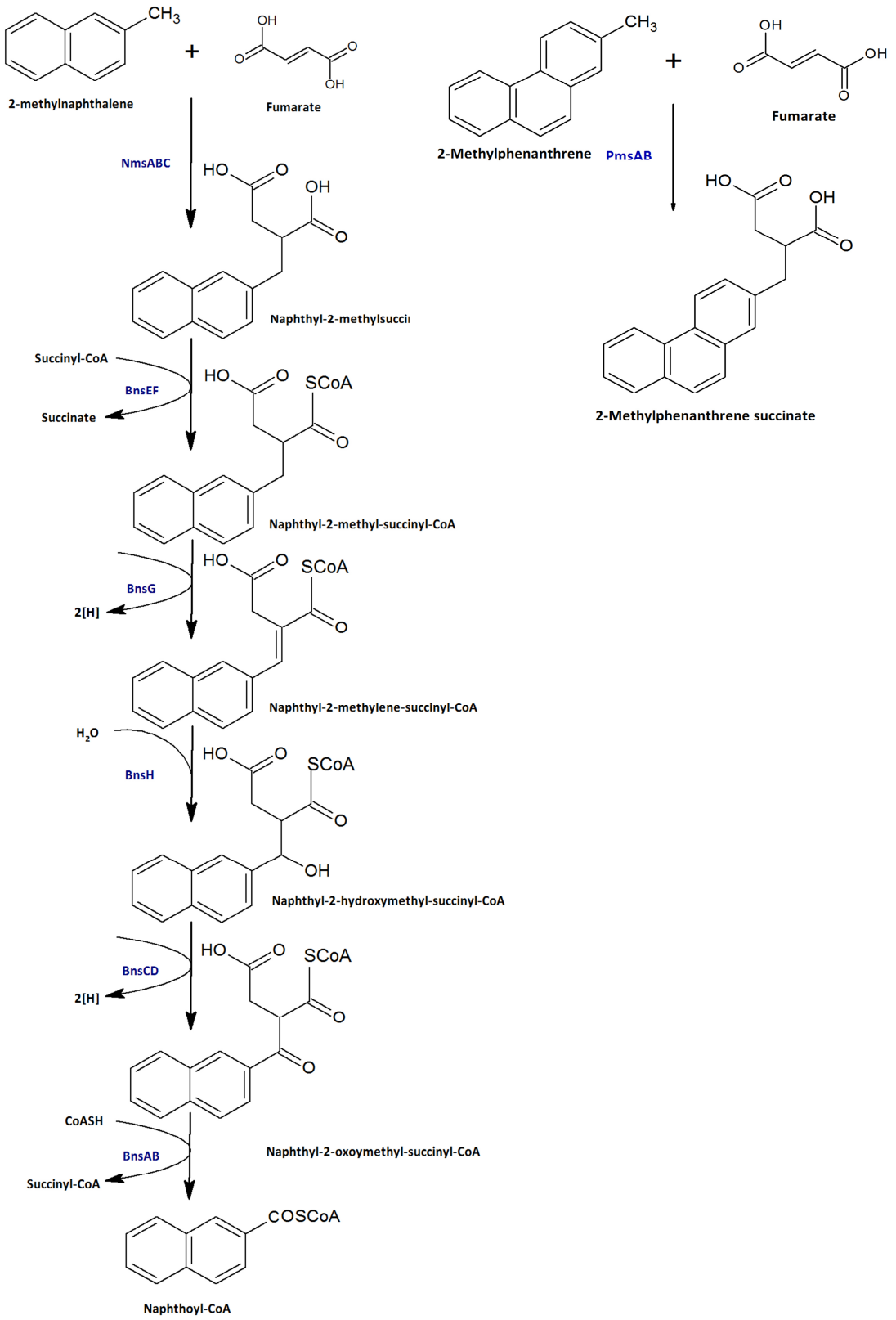

Figure 11: (A) Predicted anaerobic 2-methylnaphthalene degradation pathway, performed by naphthyl-2-methyl succinate synthase (NMS). The reactions of (NmsABC) and the enzymes of the further β-oxidation pathway (Bns) are indicated by the respective gene products. Genes found in the N47 genome encode the following enzymes (shown in gray boxes): NmsABC, naphthyl-2-methyl-succinate synthase; BnsEF, naphthyl-2-methyl-succinate CoA transferase; BnsG, naphthyl-2-methyl-succinyl-CoA dehydrogenase; BnsH, naphthyl-2-methylene-succinyl-CoA hydratase; BnsCD, naphthyl-2-hydroxymethylsuccinyl-CoA dehydrogenase; BnsAB, naphthyl-2-oxomethyl-succinyl-CoA thiolase; and NcrABCD, 2-naphthoyl-CoA reductase. (B) Putative fumarate addition reaction to the methyl group of 2-methylphenanthrene, catalyzed by phenanthrene-2-methyl-succinate synthase (PmsAB or MpsAB), derived from phenanthrene degrading metagenome.

IV. PROJECT OBJECTIVES

In the context of my PhD thesis, I have performed the structure-functional analysis of two fumarate addition enzymes: benzylsuccinate synthase and 2-naphthyl-methylsuccinate synthase, involved in the anaerobic toluene and 2-methylnaphthalene degradation. The main focus was to establish a near-homologous expression system for these enzymes to allow their biochemical characterization and to apply certain protein engineering strategies, which will lead to industrially applicable enzyme variants.

In order to further characterize benzylsuccinate synthase from *Thauera aromatica* K172 and 2-naphthyl-methylsuccinate synthase derived from the sulfate-reducing enrichment culture N47 several strategies were applied:

- **Establishment of the near-homologous overexpression** system of active benzylsuccinate synthase and naphthyl-2-methyl-succinate synthase in *Azoarcus evansii* and estimation of the substrate specificities of recombinant proteins*;*

- **Examination of the first kinetic parameters of the recombinant BSS;**

- **Further elucidation of the determinants of the substrate specificity of BSS by targeted mutagenesis.** Altering of crucial amino acids inside the active site of the BSSα subunit would have an effect on the benzylsuccinate synthase activity and give an information about different substrate specificities and substrate discrimination;

- **Purification of BSS and NMS in *E.coli* DH5α** for further X-ray crystallography studies and first structural characterization of the non-active form of 2-naphthyl(methyl)succinate synthase

V. MATERIALS AND METHODS

1. Chemicals and enzymes

The chemicals used in this work were purchased from Alpha Aesar (Karlsruhe), AppliChem GmbH (Darmstadt), DIFCO Becton Dickinson (Detroit, USA), Merck (Darmstadt), Fluka (Buchs), Roche Diagnostics GmbH (Mannheim), Roth (Karlsruhe), Serva Feinbiochemika (Heidelberg) and Sigma-Aldrich (Taufkirchen). Gases were purchased from Praxair (Dusseldorf). Enzymes were from New England Biolabs (Frankfurt), Thermo Fisher Scientific (Waltham, MA) and Roche Diagnostics GmbH (Mannheim).

2. Microbiological Methods

2.1 Microorganisms

The microorganisms strains, used in this work, are listed in Table 1.

Table 1: Bacterial strains used in this work.

Strain	Genotype	Reference
Thauera aromatica K172	Wild type (DSM-Nr. 6984)	(Anders, Kaetzke *et al.,* 1995)
Escherichia coli DH5α	F^- *endA1 glnV44 thi-1 recA1 relA1 gyrA96 deoR nupG purB20* ϕ80d*lacZ*ΔM15 Δ(*lacZYA-argF*)U169, hsdR17($r_K^-m_K^+$), λ^-	(Woodcock *et al.,* 1989)
Escherichia coli BL21 (DE3)	F^- *ompT gal dcm lon hsdS*$_B$($r_B^-m_B^-$) λ (DE3 [*lacI lacUV5-T7p07 ind1 sam7 nin5*]) [*malB*$^+$]$_{K\text{-}12}$(λ^S)	(Studier und Moffatt, 1986)
Escherichia coli S17-1	*hsdr*17, *end*A, *pro*, *rec*A, NxS, integrated RP4-2 (Tc::Mu,	(Simon *et al.,* 1983)

	Km,::Tn7), mobilizer strain	
Escherichia coli WM3064	thrB1004 pro thi rpsL hsdS lacZΔM15 RP4-1360 Δ(araBAD)567 ΔdapA1341::[erm pir]	(Dehio and Meyer, 1997)
Azoarcus evansii KB 740^T	wild type (DSM-Nr. 6898)	(Anders, Kaetzke *et al.,* 1995)
Aromatoleum aromaticum EbN1 SR-7	Spontaneous mutant, isolated after growth on Streptomycin	(Wöhlbrand and Rabus, 2009)

2.2 Anaerobic work

The anaerobic cell extracts of *Thauera aromatica* K172 and *Azoarcus evansii* KB 740^T were harvested and prepared in the anaerobic tent (Coy Laboratory Products, MI, USA). The atmosphere in the tent consists of 95% N2 and 5% H2. Traces of oxygen were removed by palladium catalysts, where a controlled oxyhydrogen gas reaction takes place. The oxygen and hydrogen content in the anaerobic tent was measured by a H2/O2 sensor (Coy Laboratory Products, MI, USA). Solutions were anaerobized by cyclic vacuumization and adding nitrogen and further autoclaved.

2.3 Cultivation of microorganisms

Organisms *Escherichia coli*, *Thauera aromatica* K172 and *Azoarcus evansii* were cultured in the respective media listed below. To quantify microbiological growth, cell density was determined by measuring light absorption at 578 nm using the Cary 60 UV-Vis (Agilent, Santa Clara, CA) photometer. If necessary, the cell suspension was diluted appropriately to obtain readings ranging between 0.1 and 0.3.

2.4 Cultivation of Escherichia coli

E. coli was aerobically cultured by agitation in LB medium (Lysogeny Broth(Bertani 1951), 10 g / L tryptone, 5 g / L yeast extract, 10 g / L NaCl) at 37 ° C. After induction of the

recombinant genes, the cultures were further incubated at the room temperature. For the preparation of solid nutrient media, 1.5% (w/v) agar was added to the LB medium (Table 9).

2.5 Cultivation of Thauera aromatica K172

Cultivation of *T. aromatica* was carried out in anaerobic 2 L culture bottles in mineral salt medium (Tab. 2 and 3) at 28 ° C under agitation. The medium was treated with 2 mM toluene as carbon source and 4 mM nitrate as electron acceptor after autoclaving. Since toluene in a concentration of 1 - 2 mM is toxic to the cell growth, the medium was overlaid with 2% (v/v) paraffin oil, in which most of the toluene was dissolved and thus acted as a reservoir. The consumption of toluene was measured indirectly by the consumption of nitrate using Quantofix nitrate sticks (Macherey-Nagel, Düren). The cells were harvested in the exponential phase at an OD578 of 3-5 under anaerobic conditions (Section 2.2).

Table 2: Base medium for the cultivation of *T. aromatica*. ([1]): Addition of toluene as a substrate.

Stock solution	Composition per 1 L of the stock solution	Concentration in medium
Base medium, pH8	0,6 g $NaH_2PO_4 \cdot 2\ H_2O$	7,9 mM
	5,6 g K_2HPO_4	32,1 mM
	0,54 g NH_4Cl	10 mM
	20 ml/l paraffin oil [(1)]	2 % (v/v)

Table 3: Supplements added to the base medium after autoclaving the basal medium; ([2]): adjust pH to 6.5 with NaOH, ([3]): sterile filter with 0.2 µm sterile filter and add after autoclaving the basal medium; ([4]): Addition after autoclaving the base medium.

Supplement	Composition per 1 L of the stock	Additon per 1 L	Conc. in medium
0,8 M $MgSO_4$ –	197,18 g $MgSO_4 \cdot 7\ H_2O$	1 ml/l	0,8 mM
Stock solution	14,7 g $CaCl_2 \cdot 2H_2O$	1 ml/l	0,1 mM
0,1 M $CaCl_2$ -	169,98 g $NaNO_3$	2 ml/l	2 mM
Stock solution			
2 M $NaNO_3$ –			

Stock solution			
Trace element solution SL7 (1000 x) [2, 4]	3 g Fe (II) $Cl_2 \cdot 4\ H_2O$ 70 mg $ZnCl_2$ 100 mg $MnCl_2 \cdot 4\ H_2O$ 4 mg $CuCl_2 \cdot 2\ H_2O$ 24 mg $NiCl_2 \cdot 6\ H_2O$ 36 mg $Na_2MoO_4 \cdot 2\ H_2O$ 6 mg H_3BO_3	1 ml/l	1,5 µM 0,5 µM 0,5 µM 0,02 µM 0,1 µM 0,15 µM 0,01 µM
Vitamins solution VL7 (1000 x) [3, 4]	80 mg 4-aminobenzoate (H_1) 100 mg Ca (+)-pantothenate 100 mg cyanocobalamine (B_{12}) 20 mg D (+)-biotine 200 mg nicotinate 300 mg pyridoxine-HCl (B_6) 200 mg thiamine-HCl (B_1)	1 ml/l	0,8 mg/l 0,1 mg/l 0,1 mg/l 0,02 mg/l 0,2 mg/l 0,3 mg/l 0,2 mg/l
Sodium selenite / sodium tungstate stock solution [4]	2 mg $Na_2SeO_3 \cdot 5\ H_2O$ 4 mg $Na_2WO_4 \cdot H_2O$ 0,5 mg NaOH	1 ml/l	11,6 nM 12,1 nM 12,5 nM

2.6 Cultivation of Azoarcus evansii

A. evansii was cultured anaerobically at 28 ° C on two different mininal media (Tables 4 and 5) under agitation. The NM medium was treated with 4 mM benzoate as the carbon source and 4 mM nitrate as the electron acceptor after autoclaving. The ThB medium (ThB, Table 4) is also buffered by phosphate and is the standard medium for growth and cultivation methods. For growth in the solid medium and for conjugation purposes, a potassium phosphate-buffered normal medium was used (NM, Table 5).

Table 4: Composition of the ThB Medium for the cultivation of *A. evansii*. [(1)]: addition after autoclaving base medium.

Solution A	**Amount [mg/l]**
KH_2PO_4	816
K_2HPO_4	5920
Solution B	**Amount [mg/l]**
NH_4Cl	530
$MgSO_4$	200
KNO_3	1000
$CaCl_2$ x H_2O	25
Na-benzoate	500
Supplements	**Amount [ml/l]**
SL-10 (1000x)**[(1)]:** (Table 7)	10
VL-7 (1000x)**[(1)]:** (Table 7)	5
Sodium selenite: / sodium tungstate stock solution[(1)]: (1000x) (Table 7)	1

Table 5: Composition of a Normal Medium / Nitrate Reducing Medium (NM) for the cultivation of *A. evansii.* ([1]): addition on incubation on solid medium; ([2]): addition in preparation of mating solid medium.

Stock solution	**Composition per L of the Stock Solution**	**Conc. in medium**
Basic medium	0,23 g Na_2SO_4	1,6 mM
	1 g NaCl	17 mM
	2,55 g $NaNO_3$	30 mM
	1,6 g NH_4Cl	29,9 mM
	20 g Agar (AppliChem) [(1, 2)]	2 % (w/v)
	10 g tryptone [(2)]	10 g/l

Table 6: Supplements of the NM. ([1]): addition after autoclaving base medium; ([2]): addition during the preparation of mating solid medium.

Supplements	Composition per L of the Stock Solution	Addition to base medium	Conc. in medium
1 M $MgCl_2$-St.sol. (1000 x) [(1)]	95,21 g $MgCl_2 \cdot 6\ H_2O$	1 ml/l	1 mM
0,6 M $CaCl_2$- St.sol. (1000 x) [(1)]	88 g $CaCl_2 \cdot 2\ H_2O$	1 ml/l	0,6 mM
1 M KH_2PO_4- St.sol. [(1)]	136,09 g KH_2PO_4	4 ml/l	4 mM
1 M K_2HPO_4- St.sol. . [(1)]	174,18 g K_2HPO_4	16 ml/l	16 mM
1 M pyruvate- St.sol. [(1, 2)]	110,05 g sodium pyruvate	5 ml/l	5 mM
1 M acetate- St.sol. [(1, 2)]	82,03 g sodium acetate	5 ml/l	5 mM

Table 7: Supplements for NM. ([1]): After dissolving the supplements, the pH is adjusted to 6.5 with NaOH, the solution anaerobized and autoclaved. ([2]): After dissolving the supplements, the solution is sterile-filtered with a 0.2 µm sterile filter and anaerobized. ([3]): After dissolving the supplements, the solution is anaerobized and autoclaved. ([4]): The addition takes place after autoclaving the base medium.

Supplement	Composition per L of the St. Sol	Addition to BM	Conc. in medium
Trace element solution SL10 (1000 x) [(1, 4,)]	5,2 g Na_2EDTA	1 ml/l	5,2 mg/l
	2,1 g $FeSO_4 \cdot 7\ H_2O$		2,1 mg/l
	30 mg H_3BO_3		30 µg/l
	100 mg $MnCl_2 \cdot 4\ H_2O$		100 µg/l
	24 mg $CoCl_2 \cdot 6\ H_2O$		24 µg/l
	24 mg $NiCl_2 \cdot 6H_2O$		24 µg/l
	29 mg $CuCl \cdot H_2O$		29 µg/l
	144 mg $ZnSO_4 \cdot 7\ H_2O$		144 µg/l
	36 mg $Na_2MoO_4 \cdot 2\ H_2O$		36 µg/l
Vitamins solution VL7(1000 x) [(2, 4)]	80 mg 4-aminobenzoic acid	1 ml/l	0,08 mg/l
	100 mg Ca-D-(+)-pantothenate		0,1 mg/l
	100 mg cyanocobalamin (B_{12})		0,1 mg/l
	20 mg D (+) -biotin		0,02 mg/l
	200 mg nicotinic acid		0,2 mg/l
	300 mg pyridoxamin-HCl (B_6)		0,3 mg/l

	200 mg thiamin dichloride (B_1)		0,2 mg/l
Sodium selenite: / sodium tungstate stock solution (1000 x) [3, 4]	6 mg $Na_2SeO_3 \cdot 5\ H_2O$ 6 mg $Na_2WO_4 \cdot H_2O$ 0,4 g NaOH	1 ml/l	6 µg/l 6 µg/l 400 µg/l

Table 8: Carbon sources, used in this work. The addition of toluene requires the use of paraffin oil (see Table 2). The addition takes place in both cases after autoclaving the base medium and after complete consumption of the nitrate.

Carbon source	Composition per 1 l	Addition to BM	Conc. in medium
toluene	100 % toluene (9,1 M)	100 µl/l	0,91 µM
1 M Sodium benzoate	144,11 g/l	2 ml/l	2 mM

2.7 Antibiotics

The necessary antibiotics were added to the media from a stock solution before inoculation. To prepare the stock solutions, the respective antibiotic was dissolved in water and sterile filtered. The stock solutions were stored at -20 ° C until use.

Table 9: Used antibiotics. With the exception of chloramphenicol, the preparation of the stock solutions with H_2O. All stock solutions were sterile filtered and stored at -20 ° C until use in 1 ml portions. The addition to the medium takes place when it has cooled sufficiently.

Antibiotic	Stock solutions used	Concentration in medium
Ampicillin	100 mg/ml in H_2O	100 µg/ml
Streptomycin	50 mg/ml in H_2O	50 µg/ml

2.8 Transformation of microorganisms

Preparation of electrocompetent Escherichia coli cells

In order to prepare electrocompetent *E. coli* cells, an overnight culture was inoculated using a single colony and incubated overnight for approximately 16 hours. Subsequently, 100 ml of dYT medium (16 g/l tryptone, 10g /l yeast extract, 5 g/l NaCl) was inoculated with the overnight culture to an OD578 of 0.1 and the main culture was incubated under

agitation at the room temperature to an OD578 of 0.4. The cell culture was rapidly cooled in an ice bath with shaking, distributed to 50 ml screw-cap reaction tubes (Sarstedt, Nümbrecht) and incubated for further 30 minutes in an ice bath. The culture was centrifuged for 10 minutes at 4 °C and 3000 rpm (Universal 320R, Hettich, Tuttlingen) and the cell pellet resuspended in 50 ml of the ice-cold water. After repeating the centrifugation, the sedimented cells were taken up in 5 ml of ice-cold water and the contents of several vessels were combined. After two repetitions of the centrifugation, interrupted by another washing step, the cell pellet was resuspended in 1 ml of ice-cold 10% glycerol (w/v). The resulting cell suspension was frozen in 50 µl aliquots in liquid nitrogen and stored at -80 ° C until use.

Transformation of the electrocompetent Escherichia coli cells

The transformation of competent *E. coli* cells was carried out by electroporation at 2.5 kV, 200 Ω and 25 µF (Dower, Miller *et al.,* 1988) with plasmid DNA or ligation mixtures precipitated with 1-butanol. A 50 µl aliquot of electro competent *E. coli* cells was placed on ice and then spiked with 1 µl of plasmid DNA (10-40 ng) or 8 µl of the previously precipitated and H_2O resuspended ligation mixture. The batch was transferred to a 0.2 µm electroporation cuvette (peqlab, Erlangen) and exposed in an electroporator (MicroPulser, Bio-Rad, Hercules, CA, USA) to an electrical pulse with the parameters mentioned above. The cells were rinsed out of the electroporation cuvette using 500 µl of sterile LB medium and incubated at 37 ° C. for 30 (for ampicillin) under agitation (800-1000 rpm, Thermomixer 5436, Eppendorf, Hamburg). Subsequently, the entire batch was plated in 100 and 400 µl portions on two LB agar plates with a corresponding antibiotic and incubated at 37°C overnight.

Transformation of chemically competent Escherichia coli cells

A 100 µl aliquot of chemically competent cells stored at -80°C was placed on ice and mixed with 1 µl of plasmid DNA (10-40 ng). The batch was incubated on ice for 30 minutes. After a heat shock (42 °C, 30-45 seconds), the cells were incubated again for 5 minutes on ice and incubated after addition of 800 ul LB medium for 30-60 minutes at 37°C under

agitation (800 - 1000 rpm; Thermomixer 5436, Eppendorf, Hamburg). Next, the entire batch was plated on an LB agar plate with a corresponding antibiotic and incubated at 37°C overnight.

Conjugation of Azoarcus evansii

The constructed plasmids were first transferred by chemical transformation (Section 2.8.) into *E. coli* strains S17-1 or WM3064 (Dehio and Meyer, 1997). For subsequent conjugation, the resulting *E. coli* strains, S17 1 + plasmid 'or' WM3064 + plasmid 'were cultured in 5 ml of LB medium. *A. evansii* was used as an acceptor strain and SR-7 with a streptomycin resistance as a donor strain (Wohlbrand and Rabus, 2009). *A. evansii* was cultivated for 2 days in NM medium with benzoate for conjugation. In order to enable a conjugation event between two organisms *E. coli* S17-1/WM3064 and *A. evansii* were mixed in various ratios and centrifuged for 5 minutes at 15,000 x g. The supernatant was discarded, each sediment was washed twice with 500 µl of a supplemented NM medium (section 2.6) and centrifuged at 15,000 x g for 5 minutes. The sediment after the second wash was resuspended with 20 µL of NM medium and the resulting cell suspension was added as a blob to a NM "Mating" agar plate (section 2.6). The agar plate was incubated with the lid up for about 16 hours at 28 ° C and the cell blob then scraped with a microbiological loop off the plate. The cells attached to the inoculation loop were placed in a 1.5 ml reaction vessel into which 500 µl of NM medium had previously been introduced. After resuspension of the cells, a three-hour incubation was carried out at 28 ° C with slight agitation (400 rpm, Thermomixer 5436, Eppendorf, Hamburg). From this cell suspension, various dilution steps were plated on NM agar and incubated anaerobically for 8-12 days at 28 ° C. Since *A. evansii* strain does not harbor the genes for the Streptomycin resistance, the cells were separated from *E. coli* S17-1 or WM3064 by continuous inoculation into 5, 10 and 15 ml hungate tubes with NM medium under anaerobic conditions until no *E. coli* cells were detected.

3. Molecular biology methods

3.1 Plasmids and oligonucleotides

The plasmids used in this work are shown in Table 10, the oligonucleotides are represented in Table 11.

Table 10: Plasmids, used in this work.

Plasmid	Genotype, description	Reference
pASG3_mob^{+}_BSS-Strep+BssD-Txn (with *E. coli* ori)→in this work pASG3bssStrep+ori1	Amp^{R} (*bla)*, plasmid for homologous overproduction of BSS in *A. aromaticum* and *A. evansii*	Dissertation M. Hilberg, 2012
pASG3bssStrepIle617+620Val	Amp^{R} (*bla)*, pASG3bssStrep+ori1-derivative	Dissertation D. Seyhan, 2016
pASG3bssStrepIle620Val	Amp^{R} (*bla),* pASG3bssStrep+ori1-derivative	Dissertation D. Seyhan, 2016
pASG3bssStrepIle620Gln	Amp^{R} (*bla),* pASG3bssStrep+ori1-derivative	Dissertation D. Seyhan, 2016
pASG3bssStrepArg508Lys	Amp^{R} (*bla),* pASG3bssStrep+ori1-derivative	Dissertation D. Seyhan, 2016
pASG3bssStrepArg508Gln	Amp^{R} (*bla),* pASG3bssStrep+ori1-derivative	Dissertation D. Seyhan, 2016
pASG3bssStrepIle617Val	Amp^{R} (*bla),* pASG3bssStrep+ori1-derivative	This work
pASG_nmsAB_Strep_bssCD_DTxn-ori	Amp^{R} (*bla),* pASG3bssStrep+ori1-derivative	This work
pASG_mpsAB_Strep_bssCD_DTxn-ori	Amp^{R} (*bla),* pASG3bssStrep+ori1-derivative	This work

Table 11: Oligonucleotides, used in this work.

Nr.	Name	Sequence (5‘ → 3‘)
1	IS 011_Ile617_EcoRI_fw	GCAGCAGGATCCGTTCTCGTTGGCGACTTCCTCGG
2	IS 012_Ile617_MluI_rev	TCCATCGTCGCAGGGAATTCGCTCGTC
3	nmsFW_NheI	GC GCTAGC ATATCCACTTTACTCAACAGAGAAG
4	nmsRV_AatII	CC GACGTC TATTCCCTCTCTGATCTGTTGC
5	N47seq_fw	GACCAGTGTTGCGGCGCGTTCCAC
6	N47seq_rv	GCTCAGTTCGCCTTCCTCGTGAC
9	mps_seq_fw	GAACCATACGACAGAACAAGGTAGG
10	mps_seq_rv	CTCAGTTCGCCTTCCTCGTGAC

3.2 Isolation of plasmid DNA from Escherichia coli

Plasmid DNA was isolated from *E. coli* according to the modified method of (Birnboim and Doly 1979). The solutions used are listed in Table 12. Cells from a 5 ml overnight culture were centrifuged at 15800 x g for 2 minutes, the supernatant removed and the cell pellet resuspended in 200 µl of P1 solution and 5 µl of RNase A (10 mg/ml) (Table 12). After addition of 300 µl P2 solution, 300 µl ice-cold P3 solution and each subsequent inverting to mix the approach, a ten-minute incubation on ice and a likewise ten-minute centrifugation step at 15800 x g was carried out. The supernatant was removed, treated to precipitate the DNA with 750 ul of isopropanol and centrifuged at 15800 x g for 10 minutes. The precipitate was washed with 500 µl of ice-cold 70% (v/v) ethanol, then dried and finally dissolved in 50-100 µl of distilled H_2O. For higher purity of the plasmid preparation, the GeneJet Plasmid Miniprep Kit (Thermo Fisher Scientific, Waltham, MA, USA) was used according to the manufacturer's instructions.

Table 12: Solutions used for the preparation of plasmid DNA.

Solution	Composition
P1	50 mM Tris/HCl; EDTA, pH 8
P2	0,2 M NaOH, 1 % (w/v) SDS
P3	3 M potassium acetate, pH 5,5; stored by 4 °C
RNase A	10 mg/ml in 5 mM Tris/HCl, pH 8; 10 min. heated to 100 ° C and cooled on ice

3.3 Polymerase Chain Reaction (PCR)

DNA fragments were amplified by polymerase chain reaction (Mullis, Faloona *et al.,* 1986) in a thermocycler. For the construction of pASG_nmsAB(mpsAB)StrepbssCD_DTxn-ori, pASG3bssStrep+ori1 and derivatives, as well as for sequencing, the necessary fragments were amplified in preparative scale reactions (≥ 100 µl). For the verification the identity of the resulted vectors, reactions were carried out on an analytical scale (20 µl). In both applications, commercial (Thermo Fisher Scientific) or laboratory purified phage DNA polymerase was used at a 1:4 dilution. To generate point mutations on the plasmid pASG3bssStrep + ori1, the KOD polymerase (Merck, Darmstadt) was used, which is suitable for longer amplificates. The template used was previously designed pASG3bssStrep + ori1 plasmid (Seyhan 2016), 2 µl of which was used in the PCR reaction. Each reaction batch contained, in addition to the DNA polymerase, a suitable buffer and the corresponding template, 200 µM deoxyribonucleotides (dNTPs) and 0.2 µM each of an oligonucleotide pair (Table 11). The oligonucleotides for this work were purchased from biomers (Ulm) in dried form after cartridge cleaning. Prior to use, the oligonucleotides were distilled by resuspending with H_2O adjusted to a concentration of 100 µM. From these stock solutions, working dilutions were made at a concentration of 10 µM. The standard program of polymerase chain reaction is listed in Table 13. The duration of steps 3, 4 and 5 is 30 - 40 times. For purification of the amplified fragments, the PCR Purification Kit from Thermo Scientific was used according to the manufacturer's instructions.

Table 13: Standard programs for the polymerase chain reaction with the polymerases used in this work.

Reaction step		Phusion-Polymerase		KOD-Hot Start-Polymerase	
		Temperature (°C)	Time (s)	Temperature (°C)	Time (s)
1	Activation of pol.	-	-	94	120
2	Denaturation	98	30	94	30
3	Denaturation	98	10	94	15
4	Annealing	50 - 65	30	50 – 65	30
5	Elongation	72	15 – 30/kBp	72	20 – 40/kBp
6	Elongation	72	300	72	300
7	Cooling phase	4 - 10	variable	4 - 10	variable

Table 14: PCR reactions, performed in this work.

Components	Phusion-Polymerase		KOD-Hot Start-Polymerase
	100 µl-reaction	20 µl-reaction	50 µl-reaction
Buffer	20 µl 5 x GC buffer	4 µl 5 x GC-buffer	5 µl 10 x PCR-buffer KOD HS
10 mM dNTPs	2 µl (≙ 200 µM)	0,4 µl (≙ 200 µM)	2 µl (≙ 200 µM)
Primer A (10 µM)	2 µl (≙ 0,5 µM)	0,4 µl (≙ 0,5 µM)	1,5 µl (≙ 0,3 µM)
Primer B (10 µM)	2 µl (≙ 0,5 µM)	0,4 µl (≙ 0,5 µM)	1,5 µl (≙ 0,3 µM)
Matrix	50 – 100 ng gen. DNA	500 – 100 ng gen. DNA	1 ng plasmid-DNA
DMSO	3 µl (≙ 3 %)	0,6 µl (≙ 3 %)	1,5 (≙ 3 %)
$MgSO_4$	-	-	3 µl (≙ 1 mM)
DNA-Polymerase	1 – 2 µl (1 – 2 U)	0,4 – 0,8 µl (0,4 – 0,8 U)	2 µl KOD HS Pol. (1 U/µl→2 U)
H_2O dest.	adjust to 100 µl	adjust to 20 µl	adjust to 50 µl

3.4 DNA electrophoresis

DNA fragments were separated by electrophoreses on a 1% (w/v) agarose gel at 60-120 V using TAE (40 mM Tris, 11.42% acetic acid, 2 mM Na_2EDTA, pH 8.5) as a running

buffer. Agarose was dissolved by boiling in TAE buffer. The size standard used was the 'GeneRuler DNA Ladder Mix' from Thermo Scientific with fragments of 100 - 10,000 base pairs. By plotting the decadal logarithm of the DNA fragment sizes of the size standard against the associated run distance, the sizes of fragments obtained were determined. After the separation, the gel was incubated for 10 minutes in an aqueous solution of ethidium bromide (1 µg/ml) and the DNA then visualized under UV light. To isolate individual fragments from the agarose gel, the PCR Gel Extraction Kit from Thermo Fisher Scientific was used according to the manufacturer's instructions.

3.5 DNA ligation

DNA fragments were digested in 1 x T4 ligase buffer (40 mM Tris-HCl, pH 7.8 at 25 ° C, 10 mM MgCl2, 10 mM DTT and 1.8 mM ATP, Thermo Fisher Scientific) with 7.5U T4 DNA ligase (1.5 U / µl, Thermo Fisher Scientific) in a total volume of 15 µl. The ratio of vector DNA to insert DNA was about 1: 4 to 1: 5 (vector: insert). The incubation was either two hours at the room temperature or overnight at 16°C in a water bath. The volume was then adjusted to 50 µl and the DNA precipitated with 1-butanol.

3.6 DNA precipitation

The DNA from ligation mixtures were precipitated with 1-butanol. The mixture was scaled up to 50 µl with distilled water and treated with 500 µl of 1-butanol. After thorough mixing and a 10 minute centrifugation step at 12,000 x g, the precipitate was washed with 70% (v/v) ice-cold ethanol, then dried and dissolved in 8 µl of distilled H_2O. Subsequently, the entire approach was used for transformation of electrocompetent *E. coli* cells (Section 2.8).

3.7 DNA sequencing

For the DNA sequencing, approximately 720-1200 ng of plasmid DNA and 18 ng per 100 bp PCR fragment were mixed with 30 pmol of each oligonucleotide in 12 µl total

volume. Sequencing was then performed by the chain termination method of (Sanger, Nicklen *et al.,* 1977) by Seqlab (Göttingen).

3.8 DNA concentration determination

Concentrations of DNA solutions were determined with the NDrop 1000 NanoDrop Spectrophotometer (NanoDrop Technologies, Wilmington, DE, USA). 1 .mu.l of a DNA solution of unknown concentration was added to the measuring device of the spectrophotometer and the concentration and purity of nucleic acids were determined on the basis of the absorption at 260 nm and 280 nm. An absorbance of 1 at 260 nm corresponds to a concentration of 50 µg/ml of the double-stranded DNA. The quotient of the absorbance of 260 nm and 280 nm can be used for the purity of the solution, which has to be between 1.5 and 1.9 (Sambrook 1989).

3.9 Designing of pASG_nmsAB_Strep_bssCD_DTxn-ori and pASG_mpsAB_Strep_bssCD_DTxn-ori vectors

For the construction of the corresponding plasmids pASG_nmsAB_Strep_bssCD_DTxn-ori and pASG_mpsAB_Strep_bssCD_DTxn-ori, the genes nmsA and nmsB derived from the genomic DNA of sulfate reducing enrichment culture N47, which was kindly provided by the group of Prof. Dr. Rainer Meckenstock, Group of Aquatic Microbiology, University Duisburg-Essen. The gene sequences of mpsA and mpsB, together with the restriction sites NheI on the 5'-end and AatII on the 3'-end for the following insertion into the matrix vector, were artificially synthesized by Eurofins Genomics (Ebersberg, Germany). The NmsA and NmsB genes were amplified using oligonucleotides nmsFW_NheI and nmsRV_AatII (Table 10), which contained restriction sites NheI and AatII, which were subsequently used for the correct insertion of the amplified NmsAB fragment into the matrix plasmid pASG3_mob^{+}_BSS-Strep+BssD-Txn. The pASG3_mob^{+}_BSS-Strep+BssD-Txn vector was subjected to the preparative restriction digestion with NheI and AatII and BssAB fragment was cut eliminated from the construct and fused with amplified NmsAB and synthesized mpsAB fragments via ligation reaction (Section 3.5).The ligation mixtures were transformed to *E. coli* by chemical transformation. The plasmids isolated from DH5α were subjected to

restriction analysis with EcoRV and sequencing reactions (Section 3.7) to ensure their correctness (data not shown).

Table 15: Plasmids isolated from *E. coli* DH5α, which were digested with the restriction endonucleases and thus subjected to a preselection. All correctly identified candidates were clearly verified by DNA sequencing (Section 3.7).

Plasmid	Restriction enzyme	Expected fragments
pASG_nmsAB_Strep_bssCD_DTxn-ori pASG_mpsAB_Strep_bssCD_DTxn-ori	NheI, AatII	2640, 9312
	PstI	1399, 10553
	SmaI	1066, 1448, 5438
	XbaI	11952

bp = basepairs.

4. Biochemical methods

4.1 Overproduction of BSS and NMS in Azoarcus evansii

Azoarcus evansii, conjugated with pASG3bssstrep expression vectors was grown at 30 °C under denitrifying conditions in a mineral salt medium with benzoate as a sole substrate. Growth was monitored by measuring optical density at 578 nm. Cultures were grown in stoppered 2 l-bottles with discontinuous feeding of organic substrate and nitrate. Typical doubling time of *A. evansii* was 3 hours. Cultures were induced with 100 µmol of anhydrotetracycline at OD 0.7. The induced cell extracts containing active BSS were pooled for SDS-PAGE (7% Bis-acrylamide) and Western Blot analysis using α-Strep antibody and 3% chloronaphthol staining for further verification of the double band of α subunit. All following steps (except for centrifugations in air-tight beakers) were carried out at 25 °C under strictly anoxic conditions in a glove box with a N2/H2 (95:5 by volume) gas phase. Exponentially growing cells (at optical densities of 1,5-2) were harvested by centrifugation at 4 °C for 20 min (10,000 *g*), washed with anoxic growth media without organic substrate, suspended in 1 volume (w/v) of 10 mM triethanolamine buffer (pH 7.5), and transferred to a French pressure cell (Aminco). Cells were lysed by 3 passages at 137 MPa and directly

transferred into a degassed Hungate-tube, which had been connected to the French pressure cell in the glove box. The cell lysate was transferred into polycarbonate tubes and centrifuged for 60 min at 100,000 x g. Protein concentrations of the supernatants (cell extracts) were determined according to the method of Bradford (1976) using bovine serum albumin as a standard.

4.2 SDS-Polyacrylamide Gel Electrophoresis

The electrophoretic separation of proteins by their apparent molecular masses was carried out in denaturing 7-15% SDS-polyacrylamide gels by means of discontinuous SDS-polyacrylamide gel electrophoresis (SDS-PAGE) according to (Laemmli, 1970) at 16 mA in collecting gel and 26 mA in a separating gel. To separate the proteome from the cells, 1 ml cell culture of known optical density (OD578) was centrifuged for 5 minutes at 15,000 × g, the supernatant discarded and the cell sediment distilled in H_2Od together with 1 µg/ml DNaseI. This cell suspension was incubated with 4X SDS sample buffer (300 mM Tris, pH 6.8, 2.4% SDS (w/v), 37.8% (w/v) glycerol, 30% β-mercaptoethanol, 0.0032 % (w/v) (bromophenol blue) to give a volume corresponding to OD578 optical density of 10% of the original cell culture. The samples were boiled for 5 min at 95°C, cooled briefly on ice and then 15ul of the sample (25 µg per pocket) was applied to the SDS-polyacrylamide gel and gel electrophoresis in a 1 x SDS running buffer (25 mM Tris, 200 mM glycine, 0.1% SDS) at the room temperature. The protein standard used was PageRuler Prestained Protein Ladder ™ (Thermo Fisher Scientific, Waltham, Mass.) with protein fragments between 170 and 10 kDa. Following gel electrophoresis, the separated proteins in the separation gels were stained with either Coomassie staining solution (0.25% (w/v) Coomassie Blue R 250, 5% (v/v) acetic acid and 50% (v/v) ethanol) and non-protein bound dye with decolorizer solution (10% (v/v) ethanol, 7% (v/v) acetic acid) or the gels are further used for immunoblotting (Section 4.3).

Table 16: Composition of the polyacrylamide gels used in this work for the electrophoretic separation of proteins. After the preparation of the separation gel it is placed into the gel chamber and in order to exclude oxygen is overcoated with distilled H_2O or 2-propanol. After polymerizing the separation gel, the H_2O/2-propanol is removed, the collection gel is filled into the gel chamber and the comb used to form the order pockets. PAA: polyacrylamide; AA /BAA: acrylamide/bisacrylamide in a mixing ratio of 37.5: 1 (Rotiphoresis Gel 30®, ready for use, Carl Roth GmbH, Karlsruhe); SDS: sodium dodecyl sulfate; TEMED: tetramethylethyldiamine; APS: ammonium peroxodisulfate.

Components	**7 % PAA-Separation gel**	**10 % PAA-Separation gel**	**15 % PAA-Separation gel**	**7 % PAA-Stacking gel**
1 M Tris/HCl pH8,8	1,95 ml	1,95 ml	1,95 ml	-
1 M Tris/HCl pH 6,8	-	-	-	235 µl
H_2O d.	1,560 ml	1,058 ml	275 µl	1,27 ml
30 % AA/BAA	1,125 ml	1,627 ml	2,411 ml	480 µl
10 % SDS (w/v)	54,5 µl	54,5 µl	54,5 µl	20 µl
5 % TEMED	54,5 µl	54,5 µl	54,5 µl	20 µl
10 % APS	78 µl	78 µl	78 µl	40 µl

4.3 Immunological detection of BSS and NMS

For the detection of BSS and NMS in *A. evansii* proteomes of individual strains were separated by electrophoresis, analyzed by the 'Western Blot' method (Towbin, Staehelin *et al.,* 1979) and transferred in a semi-dry electroblotting chamber on a nitrocellulose membrane with 0.2 micron pore size (Sartorius, Göttingen). The membrane was blocked with 50 ml of 5% milk powder (L3, Table 17) in PBST (w/v) for 1 hour. Next, membrane was washed 3 times with 20 ml of PBST (L2, Table 17) for 5 minutes each. For the detection of BSS and NMS, monoclonal α-streptavidin antibodies coupled to a horseradish peroxidase (StrepMAB-Classic HRP Conjugate, Strep-tag® II specific monoclonal antibody, IBA GmbH, Gottingen) were used in a 1: 4000 dilution in 10 ml PBST (2.5 µl L4) with the incubation time for 1 hour. After two washes with PBST and with 20 ml PBS, the Western blot was developed with 20 ml PBS, 200 µl 3% chloronaphthol solution (L5) and 20 µl 30% H_2O_2 (L6)

under agitation. After appearance of the visible protein bands, the developing solution was removed and the membrane was then washed with distilled H_2O.

Table 17: Solutions required for the immunological detection of BSS and NMS by Western blotting.

	Solution	**Composition**
L1	PBS-buffer, pH 7,4	4 mM KH_2PO_4 16 mM Na_2HPO_4 115 mM NaCl
L2	PBST-buffer, pH 7,4	PBS-buffer + 0,1 % (v/v) Tween 20
L3	5% milk powder	2,5 g milk powder in 50 ml PBST
L4	StrepMAB-classic HRP-conjugate	α-streptavidin-antibody, coupled with horseradish peroxidase
L5	chloronaphtol solution	3 % (w/v) 4-chloro-1-naphtol in methanol
L6	H_2O_2-solution	30 % (v/v) H_2O_2

4.4 Purification of (R)-benzylsuccinate synthase and naphthyl-2-(methyl) succinate synthase from E.coli

Purification of the non-active forms of BSS and NMS by Strep-Tactin affinity chromatography was performed under strictly anaerobic conditions. For this purpose, both anaerobized buffers and all material (ultracentrifuge cups, Strep-Tactin Superflow column, plastic beakers and 50 ml reaction vessels) were introduced into the anaerobic tent for 7 days before use. *E. coli* cell extract with overproduced BSS and NMS was applied to a Strep-Tactin Superflow column (10 ml; IBA, Göttingen). The column was previously equilibrated with base buffer (100 mM Tris / HCl pH 8.0, 150 mM NaCl, 10% glycerol), which was also used for the preparation of the cell extract. The column was washed after application of the cell extract with two column volumes of base buffer at a flow rate of 1 ml min^{-}1. The column was then washed with three column volumes of 0.5 M NaCl in base buffer before rinsing again with three column volumes of the base buffer. After the washing steps, Strep-tagged BSS and NMS were eluted by applying base buffer with 2.5 mM D-Desthiobiotin. The column was regenerated according to the manufacturer's instructions with 1 mM HABA (2-(4-hydroxyphenylazo)benzoate and stored at 4°C. Immediately after the elution, the protein was checked for activity by a batch activity test. Next, both proteins, purified by Strep-

affinity column were pooled, concentrated and further purified on a size-exclusion chromatography column equilibrated with 50 mM HEPES/NaOH, 150 mM NaCl. The purity of the proteins was verified by SDS-PAGE and the presence of all subunits of the enzyme complexes (α, β, γ subunits and the activating protein BssD) were detected by MALDI TOF analysis, performed in collaboration with Jörg Kahnt, Timo Glatter Group, Max Planck Institute for Terrestrial Microbiology, Marburg. The concentration of the complex was determined using the Bradford assay kit (Section 4.5).

4.5 Determination of the protein concentration

The determination of the protein concentration in the crude extract of *A. evansii* or *T. aromatica K172* and elution fractions after Strep-affinity and Size exclusion purification was carried out according to the method of (Bradford, 1976) in the 96 well plate reader at 495 nm. Bovine serum albumin (BSA, Sigma-Aldrich, Taufkirchen) was used as the standard protein for the preparation of calibration lines.

4.6 Reconstitution of the iron-sulfur clusters

Reconstitution of the iron-sulfur clusters in purified BSS and NMS was performed under strictly anaerobic conditions with a 15 µM protein solution. First, the proteins were incubated with 5 mM DTT for 1 hour at room temperature. Subsequently, both proteins were reduced with addition of Fe (III) ammonium citrate in a 3 molar equivalent to the protein solution, which was further incubated for the next 10 minutes. In the next step, lithium sulfide was added in a 3 molar equivalent and the protein solution incubated again for 1 hour with gentle rocking. For removal of the excessive iron a PD10 gel filtration column was used.

5. Analytical methods

5.1 Preparation of the cell extract from A. evansii and T. aromatica K172

T. aromatica cells were cultured in 2 L bottles (total volume – 4 L) anaerobically with toluene as substrate to an OD of 3-4. Cultures of *A. evansii* were grown in stoppered 2 l-bottles (total volume used for the preparation – 10 L) with discontinuous feeding of organic substrate and nitrate. Cultures were induced with 100 µmol of anhydrotetracycline at OD 0.7 and further grown for the next 24 hours in order to produce recombinant BSS or NMS. Both cells of *T. aromatica* and *A. evansii* were harvested under anaerobic conditions by centrifugation at 8,000 x g and 4 ° C for 10 minutes. The cell sediments (about 15-17 g of wet mass) were resuspended in 15-17 ml of 10 mM triethanolamine (pH 7.5). Subsequently, the cell suspension was forced three times through a 1.2 mm diameter syringe and then several times through a 0.8 mm diameter syringe to achieve complete homogenization and facilitate subsequent cell disruption. This was achieved by passing the cell suspension three times through a French Press cell at 110 MPa. Finally, the cells were centrifuged at 126,000 x g and 4 ° C for one hour and the resulting supernatant (cell-free extract) for EPR analyzes (Section 5.2) and activity determination of BSS and NMS (Section 5.3)

5.2 Sample preparation for the measurement of glycyl radical signal in BSS and NMS

Sample preparation for the study of glycyl radical signals of the recombinant proteins in the crude extract of *A. evansii* was also performed under strictly anaerobic conditions in the anaerobic tent. For this purpose, crude extract from anaerobically benzoate-grown *A. evansii* cells (~30 mg/ml) was incubated for 20 minutes at the room temperature with two effector compounds (inhibitors: benzyl alcohol and 2-naphthalenemethanol). All compounds were incubated for the EPR spectroscopic analyzes at a final concentration of 20 µM with crude extract from anaerobically benzoate-grown *A. evansii* cells. Subsequently, the EPR tubes used were filled with 300 µl of a crude extract. The EPR tubes were sealed, removed from the anaerobic cell, frozen in a liquid nitrogen and stored in the tube until measurement.

5.3 Activity assay of BSS and NMS

The determination of the enzyme activity in a crude extract of *A. evansii* cells (30-40 mg · ml-1) was performed in a discontinuous enzyme test. All assays were carried out under strictly anaerobic conditions and analyzed by RP-HPLC and HPLC-MS. All the material and all the necessary stock solutions (substrates, co-substrates, 20 mM TEA/ NaOH buffer pH 8.0) was anaerobized and placed into the anaerobic tent 7 days before carrying out the tests in the anaerobic tent. For the test batch, the crude extract was diluted 1: 5 in a total volume of 1 ml and first incubated for 2 minutes with the respective co-substrate (fumarate or 3-acetylacrylate). For the composition of the reaction mixture of NMS and substrate toluene and 2-methylnaphthalene, the x1 fold paraffin oil was added into the assay in order to reduce the toxicity and precipitation of the substrates in the reaction buffer (*two-phase reaction mixture*). Next, the reaction was started by addition of the substrate (toluene, *m-, o-, p*-cresol, *m-, o-, p*-xylene, 2-methylnaphthalene, 2-ethyltoluene, *p*-cymene), which was previously dissolved in 2-propanol at a concentration of 100 mM. At various time points (0 min, 2 min, 4 min, 8 min, 16 min) 120 µl of the sample was stopped by addition of 30 ul of 10% (v/v) H_2SO_4. Next, the stopped samples were removed from the anaerobic tent. Precipitated protein was removed by centrifugation (13000 rpm), metabolites were extracted with >99.8% diethyl ether and solubilized in water. The clear supernatant was filled into HPLC vials and analyzed for product formation (benzyl succinate, (hydroxy)benzylsuccinate, 2-naphthyl (methyl) succinate etc.). Benzylsuccinate eluted at 11.6 min retention time, as checked by co-chromatography of authentic standards, and was quantitated by the integration of the UV-Vis detector peaks. Using cresol isomers as substrates, more polar labeled products (elution times 4.1, 4.7, and 4 min with *o*-, *m*- and *p*-cresol, respectively), and using xylene isomers, more hydrophobic products (elution time 22.5 min for *m*-xylene) were obtained (Supplementary Fig. 1). These products were apparently correlated to the non-commercially available addition products of the cresol and xylene isomers and fumarate, based on their time-dependent accumulation, UV-Vis spectra, and migration positions on a reversed phase column. All conversion products have been confirmed by HPLC-MS analysis in a collaboration with the Team des Gerätezentrums für Massenspektrometrie und Elementanalytik, Fachbereich Chemie, Philipps Universität Marburg (Supplementary Fig. 3).

5.4 Kinetic studies of the recombinant BSS

The initial kinetic parameters and the inhibitory kinetics of the recombinant BSS were measured under strictly anaerobic conditions by using freshly prepared *A. evansii* crude extract (~ 30-40 mg / ml). All mathematical calculations were described in a Doctoral Thesis of (Hilberg, 2012) and (Verfürth, 2005). All kinetic parameters were determined by Prism 4.00, GraphPad, San Diego, Canada.

Vmax and Km for toluene and fumarate

For this, enzyme activities were required at different substrate concentrations of fumarate and substrate saturation of toluene. To conclude something with the measured values, fumarate concentrations needed to be selected in a spectrum up to fumarate saturation, because reaction rate differences in the area of fumarate saturation could not be measured with sufficient accuracy. The area of fumarate concentration was between 0.1 and 3 mM fumarate, while toluene concentration was kept constant at 2 mM. The experiment was performed in 20 mM TEA/NaOH pH 7.5 at a protein concentration of ~4 mg/ml. Toluene was added via a toluene/isopropanol stock solution. The reaction was started after providing the substrates by addition of T. aromatic cell lysate and stopped after 1 min by addition of 10% 1M H_2SO_4. The precipitated protein was sedimented at 10000xg and the supernatant analyzed by RP-HPLC. The linearity of the measured values was verified by a second reaction with a running time of 2 min. The enzyme activities were plotted in a diagram with enzyme activity and fumarate concentration as the axis and the resulting graph was mathematically adjusted with the Michaelis-Menten formula. Hereby, the asymptote at high fumarate concentrations equals the value of Vmax, while the intersection of the line at half maximum reaction rate with the graph equals the value of Km.

Enzyme inhibition curves with benzyl alcohol, CO and CN-

Inhibition studies of BSS were performed under strictly anaerobic conditions after incubation of a freshly prepared *A. evansii* crude extract (~ 30-40 mg/ml) with effector

compounds: benzyl alcohol, CO and CN^-. First, the cell extract was diluted 1: 5 in an assay volume of 1 ml with 10 mM TEA buffer and washed with different concentrations of benzyl alcohol (5 µM – 20 µM), CO was added at 10-50% of a gas phase, CN^- - 0.5-2 mM. Next, fumarate was added at a concentration of 3 mM and incubated again for 5 minutes. Enzyme activities were determined after the start of the reaction by the addition of the substrate toluene (2 mM) (Section 5.3). The volume fraction of the inhibitor replaced by adding the TEA buffer as a control.

5.5 Reversed-phase high performance liquid chromatography (RP-HPLC)

High performance chromatography was used to detect benzylsuccinate ((hydroxy) benzylsuccinate, (methyl)benzylsuccinate, 2-naphthyl (methyl) succinate etc.) as a product of the BSS and NMS reactions from the crude extract of *A. evansii*. For this purpose, an HPLC system from Agilent (Santa Clara, CA, USA) with a coupled diode array detector (UV DAD,) was used. Samples were applied on a RP-C18 column (Kinetex 5u C18, 250 mm x 4.6 mm, Phenomenex, Aschaffenburg) column and eluted at 1 ml min–1 with 20% (v/v) acetonitrile in 40 mM formic acid (pH 3.0) with simultaneous detection of the UV absorbance (210, 220, 250 nm). The samples were separated for 30 min and detected at wavelengths 210, 220 and 250 nm. The flow rate in the described runs was 1 ml · min-1.

5.6 Uv/Vis spectroscopy

UV/Vis absorption spectra of the purified BSS and NMS were obtained using a spectrophotometer Ultrospec 1100 per the company Amersham Biosciences (Freiburg). The protein solutions used were scanned at a wavelength in the range of 200-800 nm. The measurements were performed in quartz cuvettes and measured against the corresponding buffer in which the purified proteins were dissolved.

5.7 Metal analysis by ICP-OES

In order to validate the photometric measurement of the iron content of purified BSS and NMS the ICP-OES analysis was implemented in the group of Prof. Dr. med. Seubert (University of Marburg, Department of Chemistry). For a precise analysis, the samples were

separated from desthiobiotin and imidazole and contained low salt concentrations. Therefore, the purified proteins were applied onto PD-10 gel filtration column in low salt buffer (10 mM Tris/HCl, pH 8) and then concentrated by centrifugation. The protein concentrations were measured as described determined in section 4.5.

VI. RESULTS

1. Recombinant production of active benzylsuccinate synthase

1.1. Near-homologous production system of active BSS in *Azoarcus evansii*

In order to overproduce active BSS a previously developed homologous expression system of tagged benzylsuccinate synthase was applied (Seyhan, 2016). We have selected the denitrifying β-proteobacterium *Azoarcus evansii* as a host for near-homologous production of BSS, which has been reported as a closely related organism to *Thauera aromatica* K172 and is accessible via conjugation (Anders, Kaetzke *et al.,* 1995). Moreover, there are no pathways for the toluene degradation identified in *A. evansii*. This prevents the emergence of a benzylsuccinate background signal, which could interfere with the enzyme assay data.

To overexpress BSS genes, a broad host range pASG_bss_Strep_bssCD_DTxn-ori vector was designed, containing a Strep-tagged bssA gene (encoding α subunit), *bssB* (β subunit), *bssC* (α subunit) genes and a *bssD* gene (encoding an activating protein). In addition, the vector contains a *mob* site for conjugation, a tetracycline promotor and a gene for the tetracycline regulator (*tetR*) (Fig. 12). The overexpression vector was transformed into *A. evansii* by conjugation (Materials and Methods 2.8).

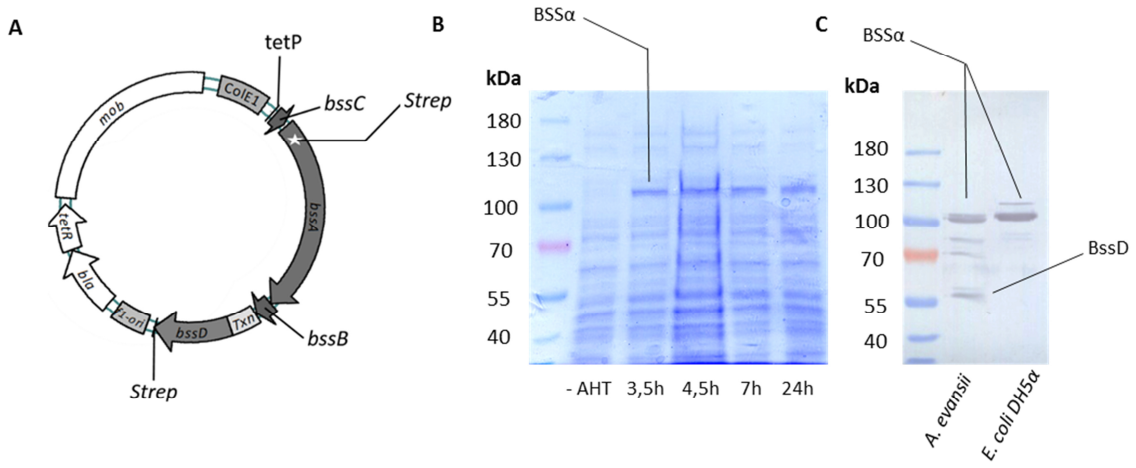

Figure 12: (A) pASG3bssstrep + bssDTxn + ori1 vector, designed for the overexpression of BSS genes. (B) SDS-PAGE: time-dependent overproduction of BSS in A.evansii cell extract (3,5h, 4,5h, 7h, 24h), including 0-time point before the induction with AHT. (C) Comparative Western Blot analysis using Strep-antibody for the detection of the activating protein BssD and double band formation of BSSα in *A. evansii* and *E. coli* DH5α.

Cultures were grown at 30 °C under denitrifying conditions in a mineral salt medium with 2mM benzoate as a sole substrate. The presence of a tetracycline promotor on the expression vector allowed induction under benzoate growing conditions (24h at 30 °C) with 100 µM of anhydrotetracycline (Seyhan, 2016), (Fig. 12, B).

Due to the extreme oxygen sensitivity and instability of activated BSS during purification, the overproduction experiment for the detection of the active benzylsuccinate synthase was performed under strictly anaerobic conditions. The production of BSS was detectable after 3,5 hours after induction with anhydrotetracycline (AHT). The characteristic double band formation, indicating the activated state of the enzyme due to the cleavage of the BSSα subunit by molecular O_2, was only detectable in the cell extracts of *A. evansii*, but not after the production of BSS in *E. coli* DH5α (Fig.12, C). This result is consistent with previous failed attempts to produce the active protein in *E. coli* hosts (Materials and Methods 4.1) (Leuthner, Leutwein *et al.,* 1998, Li and Marsh 2006, Hilberg, 2012, Seyhan, 2016).

1.2 Characterization of the specific activities of recombinant BSS

In order to confirm the identity of recombinant BSS, we have performed a set of enzyme assays in the cell extracts of *A. evansii* elucidating substrate discrimination and inhibition properties (Materials and Methods 5.3). We selected a number of substrates whose utilization pattern has been previously determined with native BSS, namely toluene, *m-, o-, p*-cresol and *m-, o-, p*-xylene (Fig. 13, 14) and determined specific BSS activities compared to those of native BSS in cell extract of toluene-grown cells of *T. aromatica* K172. The estimated specific activity of BSS with the native substrate – toluene, equaled 12 nmol*min^{-1} mg protein^{-1}. The specific activity of the native BSS in the cell extract of toluene-grown cells of *T.aromatica* K172 was assayed as a control and determined as 17 nmol*min^{-1} mg protein^{-1}. Next, we tested the conversion of all cresol isomers.

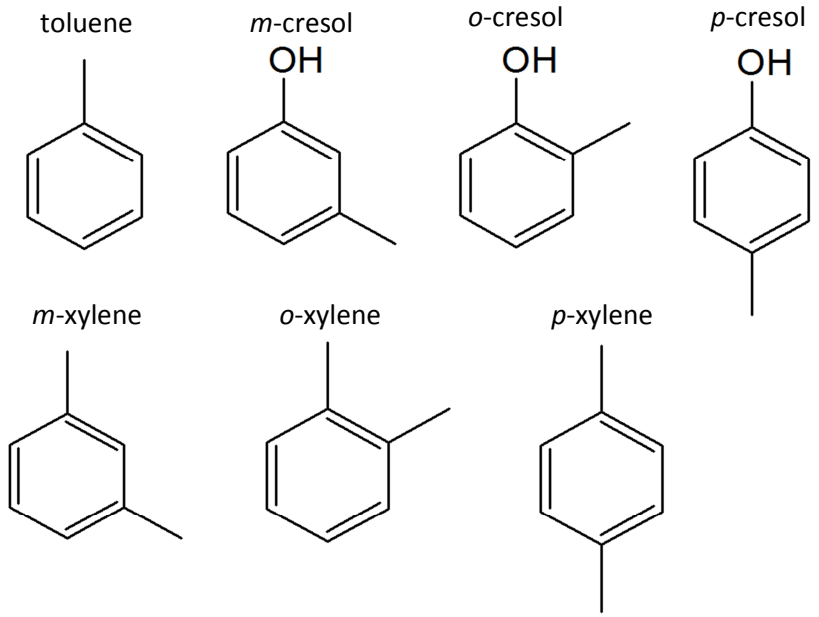

Figure 13: Aromatic hydrocarbons, used in this work as substrates for BSS.

The obtained value with *m*-cresol in the control was 10 nmol*min^{-1} mg protein^{-1}, while activity with *p*-cresol remained slightly lower at 7 nmol*min^{-1} mg protein^{-1}, and activity with *o*-cresol was determined at 8 nmol*min^{-1} mg protein^{-1}. In addition, recombinant BSS did not convert any xylene isomers *(m-, o-, p-),* which contain an additional methyl group at different positions in the aromatic ring (Table 18, Fig. 14). These

results are in accordance with the previously determined substrate conversion pattern of BSS from *T. aromatica* K172 (Supplementary Fig. 1, A- D) (Verfürth *et al.,* 2004).

Table 18: Specific activities of native BSS in cell extract of toluene grown culture of *T. aromatica* K172 with various substrates. Standard deviation values (σ) of enzyme activities are given from a total number of 3 independent activity assays.

Aromatic hydrocarbons	Recombinant BSS	BSS from *T. aromatica* K172
	nmol*min^{-1} mg protein^{-1}(σ)	
toluene	12.0 (1.0)	17.0 (1.4)
m-cresol	10.0 (1.3)	11.0 (0.5)
o-cresol	8.0 (0.6)	9.5 (0.7)
p-cresol	7.0 (1.3)	9.0 (1.0)
m-xylene	<0.1	<0.1
o-xylene	<0.1	<0.1
p-xylene	<0.1	<0.1

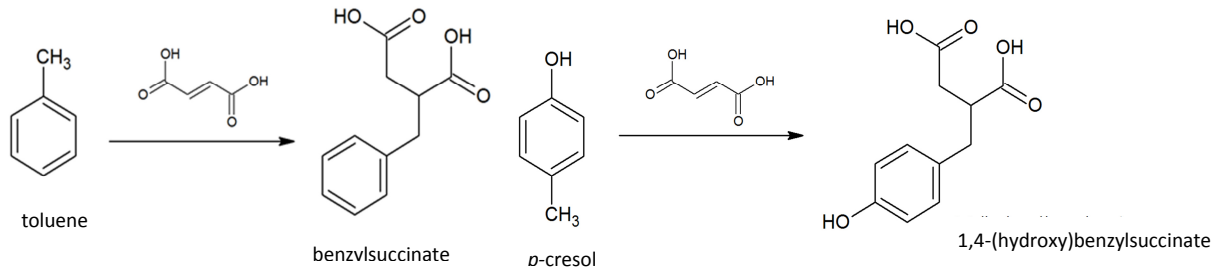

Figure 14: Fumarate addition to toluene and *p*-cresol reactions, catalyzed by BSS from *T. aromatica* K172.

The highest specific activities were observed with toluene and *m*-cresol, while *o*- and *p*-cresols were converted at lower levels and none of the xylene isomers was accepted (Table 18). Although the activities of native BSS were slightly higher than those of the recombinant enzyme and the activity ratios between the substartes were not completely identical, the data can be taken as confirmation for both enzyme sources showing the same properties. Moreover, the obtained level of recombinant production is suitable for further investigation of the reaction mechanism and mutagenesis studies of BSS.

1.3 Catalytic properties of the recombinant BSS

1.3.1 Apparent Km values for toluene and fumarate

In order to further investigate the identity of recombinant BSS we have applied a previously developed BSS enzyme activity test (Materials and Methods 5.4) allowed to determine initial kinetic parameters of benzylsuccinate synthase reaction with two substrates. To achieve this, we have set up the saturation (Michaelis-Menten) kinetic curves for toluene and fumarate for calculation of the apparent Km values for toluene and fumarate and the Vmax of the enzyme. The data obtained are shown in Fig. 15.

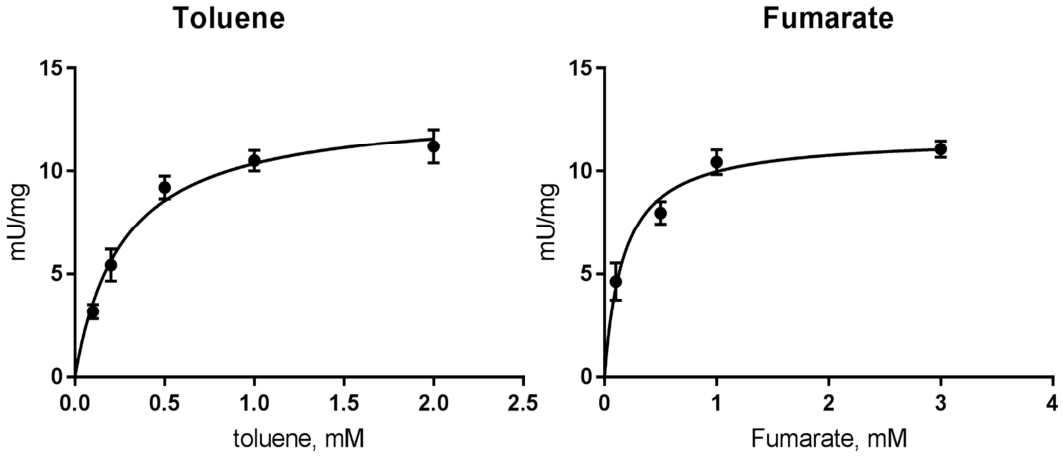

Figure 15: A) Determination of the saturation kinetics of BSS for toluene. Concentration of toluene was varied from 0,1 mM to 2 mM, while concentration of fumarate remained constant (3 mM). The determined curve is consistent with Michaelis-Menten kinetics. The specific activity of the enzyme depends on the toluene concentration. (B) Determination of the saturation kinetics of BSS for fumarate. Concentration of fumarate was varied from 0,1 mM to 3 mM, while concentration of toluene remained constant (2 mM). The determined curve is consistent with Michaelis-Menten kinetics. The specific activity of the enzyme depends on fumarate concentration.

The reaction was stopped at two-time points (after 1 and 2 min) to ensure that the initial rates of the reaction were measured. The enzyme test was carried out under fumarate saturation (or 3 mM, Fig 15). The values determined for the substrate toluene are shown in Fig. 15 (A, B).

The apparent Km value for toluene equaled 0.3 nM with a Vmax value of 21.1 nmol · (mg min) $^{-1}$. For the fumarate co-substrate, the values determined are shown in Fig. 15. The enzyme test was carried out under toluene saturation (2 mM). For fumarate, an apparent

Km value of 0.12 nM was calculated with a Vmax value of 20 nmol · (mg min) $^{-1}$, which is slightly lower than the previously determined Km and Vmax values for both substrates, as examined for the native BSS from a toluene-grown culture of *T. aromatica* K172 (toluene: Km = 0.4 nM, Vmax = 24.8 nmol·(mg·min)$^{-1}$, fumarate: Km = 0.2 nM, Vmax = 24 nmol·(mg·min)$^{-1}$) (Hilberg, 2012) (Verfürth *et al.,* 2004).

1.3.2 Inhibition by benzyl alcohol, CO and CN-

Benzylsuccinate synthase has previously been shown to be inactivated by a set of effector molecules, including substrate analogues – benzyl alcohol, benzylfumarate and benzylmaleate and reactive diatomic molecules – O_2, NO, CO and CN^- (Verfürth, *et al.,* 2004). Moreover, 10 µM benzyl alcohol decreased BSS activity by 80%, CO showed 50% enzyme activity reduction after addition of 15% of a gas phase and 1mM CN^- - 50% (Verfürth, 2005, Hilberg, 2012). In order to check whether the recombinant enzyme displays a similar inhibition pattern, we tested the effect of benzyl alcohol, CO and CN^- on the enzyme activity. For this, the inhibitors were used in three concentrations (for benzyl alcohol - 5 µM, 10 µM and 20 µM, CN^- - 0,5 mM, 1 mM, 2 mM, CO – 10%, 25% and 50% of gas phase). Activity reduction to 50% was detected with 5 µM of benzyl alcohol, and it decreased further to 10% with 20 µM. CN^- eliminated 60% of the enzyme activity at a concentration of 0,5 mM, while a 10% gas phase of CO reduced 50% of the recombinant BSS activity (Fig. 16).

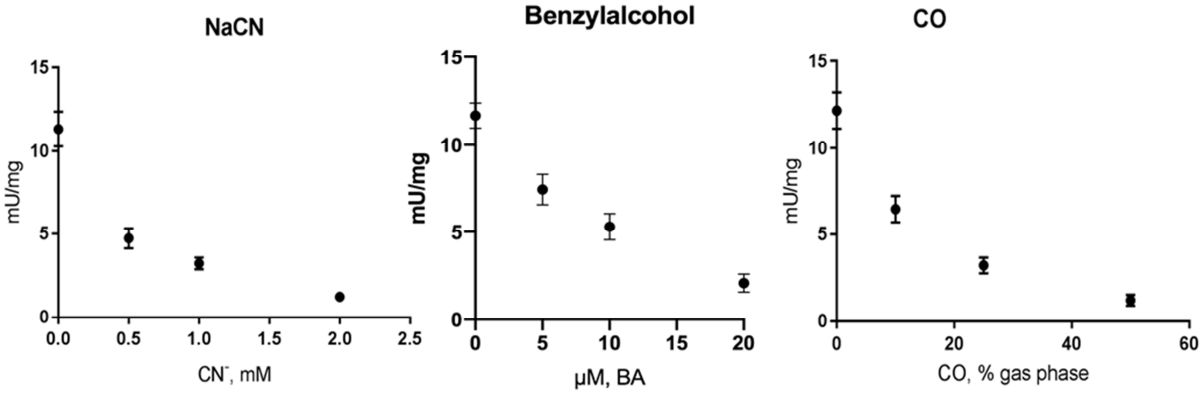

Figure 16: Effect of benzyl alcohol, CN^- and CO on the activity of benzylsuccinate synthase in the crude extract of *A. evansii*. Graphs show the correlation between the inhibitor concentration and the specific enzyme activity.

Based on these acquired results, we have further confirmed the identical behaviour of recombinant and native BSS by demonstrating their identical inhibition patterns.

1.3.3 The effect of added CO_2 on BSS activity

According to the recent X-ray structure, the active site cavity of BSS consists exclusively of hydrophobic amino acids, which create a shielded environment around the thiyl radical of Cys493 in order to isolate the toluene binding site from unwanted reactive intermediates and solvent molecules (Funk, Judd *et al.,* 2014, Funk, Marsh *et al.,* 2015). A potential problem may arise from the nature of the remaining free space in the active site after toluene and fumarate binding. While this is assumed to be filled up with water molecules in usual enzymes, a radical reaction involving hydrocarbon substrates may be disturbed by the presence of water. Therefore, we have hypothesized that neutral molecules of solvated gases, such as CO_2 or N_2, may take over the role of filling up the active site pocket and thereby may stimulate enzyme activity at higher concentrations. In order to test the impact of increased CO_2 concentrations on BSS activity, we have performed a set of activity assays with the addition of different concentrations of CO_2/bicarbonate buffer (1M HCO_3^-, with the addition of 1mg/ml carbonic anhydrase), namely 10 mM, 25 mM, and 50 mM. As shown in Fig. 17, the highest activity of the recombinant BSS with toluene was achieved in the presence of 50 mM CO_2 (14,3 mU/mg), thereby increasing the reaction rate by 20 %, compared to experiments without added CO_2. We also measured the same parameters with native BSS from *T. aromatica* as a control. Due to our experiments, the maximum specific activity of native BSS equalled 19,4 mU/mg with 50 mM of CO_2 added, which is 16% higher than the one without added CO_2.

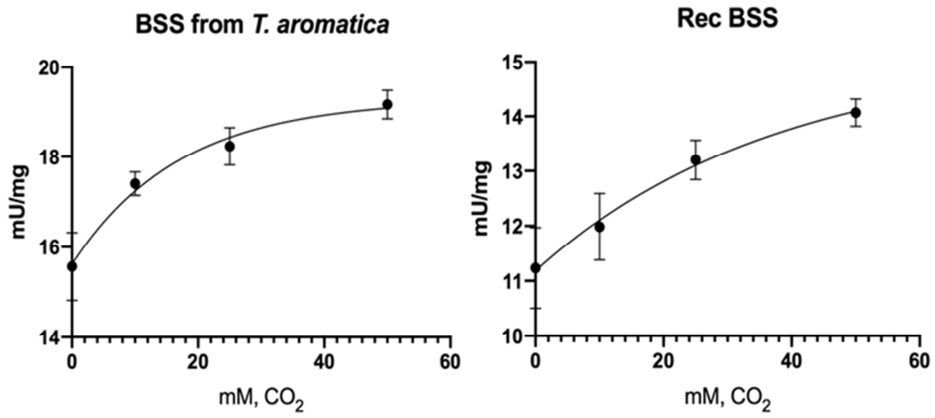

Figure 17: The effect of CO_2 on the enzyme activity of BSS. (A) Recombinant BSS (B) Native BSS from *T. aromatica* K172.

The obtained data serve as a first evidence on a putative role of neutral gaseous molecules, which may substitute for H_2O in the active site, in the enhancement of the specific activity of BSS. To confirm this hypothesis further, similar effects on the enzyme reactivity should also be followed for the addition of different gaseous compounds, such as N_2 (e.g. at increased pressures), acetylene, H_2 or noble gases.

2. Determination of the substrate recognition of BSS by target mutagenesis

2.1 Mutagenesis of the α-subunit of benzylsuccinate synthase

Potential key amino acids involved in the reaction mechanism of BSS that could be responsible for binding of the two substrates through hydrophobic interaction or through hydrogen bonding have been identified by Funk *et al.* (2015) and Szaleniec & Heider (2016). These analyses provide several targets for the generation of potential mutant variants of BSS. In addition, amino acid sequence alignments of closely related BSS isoenzymes suggest that targeted alteration of some key amino acids of the substrate binding pocket may result in changes of the available substrate spectrum.

At the same time, a decrease or loss of measurable activity in mutant variants would identify essential amino acids involved in the reaction. For our first mutagenesis attempts, we selected the amino acids highlighted in Figure 18 (A-C) of BSS from *T. aromatica* strain K172, based on sequence analysis (Fig. 18, A) and structural modeling of the active site of

the highly related BSS isoenzyme of *T. aromatica* strain T1 (81% identity; Funk, Judd *et al.,* 2014).

Mutagenesis of isoleucine 617 and isoleucine 620 to valine and glutamine

The two isoleucine residues Ile617 and Ile620 (I) were found to be conserved in the alpha subunits of most anaerobic toluene-degrading strains, such as *T. aromatica* K172, *T. aromatica* T1 and *Aromatoleum aromaticum* EbN1. Interestingly, the alpha subunits of BSS from the *m*-xylene-degrading strains *Azoarcus sp*. CIB and *Azoarcus sp*. T contained valines (Val, V) at the respective positions (Val 617 and Val 620). Moreover, BSS from *Geobacter metallireducens* contains a single Val corresponding to Ile620, but this enzyme has not yet been tested for its substrate specificity.

Since valine, compared to isoleucine, is a smaller branched amino acid containing a methyl instead of an ethyl group, we decided to substitute Ile 617 and Ile 620 to Val as single mutations and as a double mutation in order to open access to the active site cavity of BSS, which may then potentially enable access for xylenes. Additionally, we performed a substitution of Ile 620 to glutamine (Gln, Q), containing a polar amide group, to test for the effect of substituting the hydrophobic cavity wall by a more polar amino acid (Table 2, Supplementary Fig. 2).

Mutagenesis of arginine 508 to glutamine or lysine

According to the structural data and sequence alignments, it has been shown that Arginine 508 is universally conserved between all FAE (Fig. 18, C). It was proposed to be responsible for the binding of fumarate by forming an ionic bond between the charged guanidine group and one of the carboxyl groups of fumarate (Funk, Judd *et al.,* 2014; Szaleniec and Heider, 2016). By replacing arginine 508 with glutamine or lysine, which are smaller polar amino acids with or without a positive charge, we planned to see whether the resulting enzyme variants still retain activity or even gain activity to use a potential fumarate analogue, namely 3-acetylacrylic acid.

Based on these findings, we designed a set of expression plasmids based on pASG3bssstrep, which contain mutations leading to the previously indicated amino acid substitutions (Table 19). The resulting plasmids were assigned as

pASG3bssstrepArg508Lys,pASG3bssstrepArg508Gln,pASG3bssstrepIle617+620Val,pASG3bssstrepIle620Val, pASG3bssstrepIle620Gln (Seyhan, 2016) and pASG3bssstrepIle617Val. All 6 plasmids were transferred into *A.evansii* by conjugation with *E. coli* S17 strain (Materials and Methods 2.8). The presence of the expression constructs was confirmed by plasmid preparation and restriction analysis (Materials and Methods 3.9).

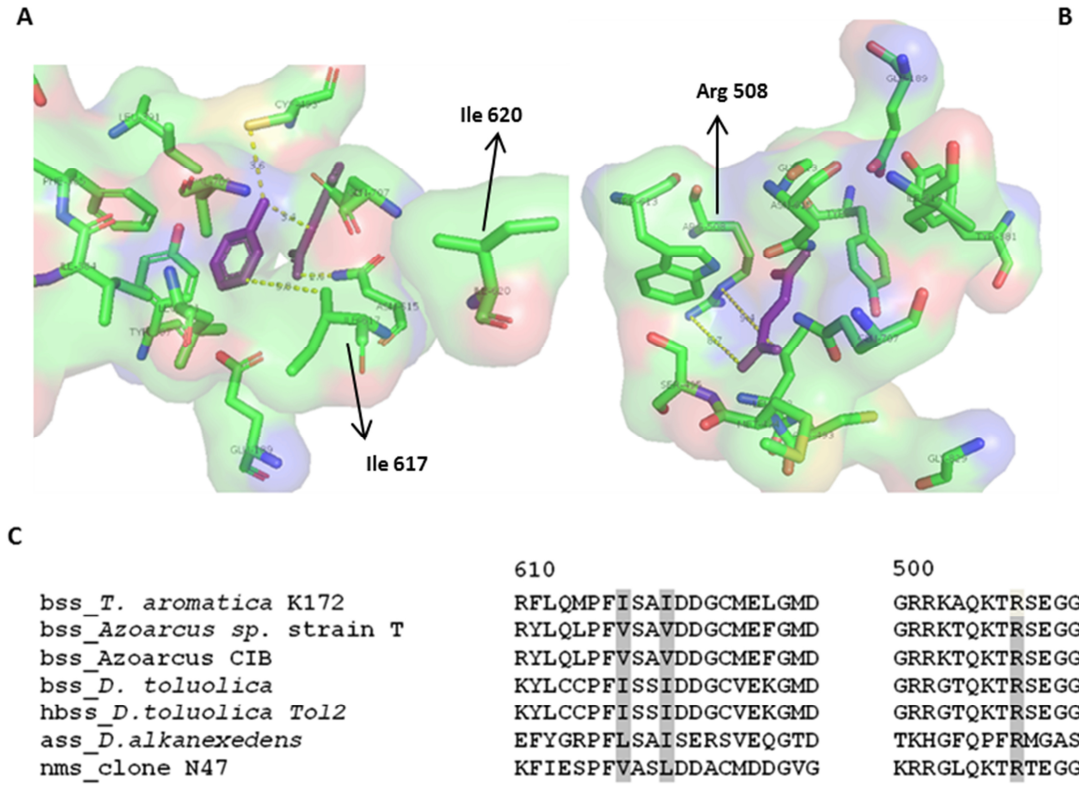

Figure 18: (A) Structural model of the active site of BSS from *Thauera aromatica* strain T1 indicating crucial amino acid residues forming the hydrophobic wall around toluene and fumarate (colored in purple, created with PyMol Software) (Leu 391, Cys 493, Gln 707, Val 709, Phe 385, Ile 384, Tyr 381, Glu 169, Ile 617, Ile 620), (B) Structural model of the active site of BSS from *Thauera aromatica* strain T1 showing fumarate anchored to the conserved Arg 508, (C) Multiple sequence alignments of the α-subunit of BSS and its paralogs between related nitrate, sulfate and metal ion reducing proteobacteria. Residues believed to be responsible for the binding of toluene and fumarate are highlighted in grey (R 508, I617, I620).

For overproducing active BSS enzyme variants, the previously developed homologous expression system of tagged BSS in *A.evansii* was used (Hilberg, 2012, Seyhan, 2016). The occurrence of double bands for the alpha subunits of all analyzed mutants on anti-strep Western Blots suggested their activation to the Gly radical state in the active site (Results 1).

Table 19: Arg 508, Ile 617, Ile 620, mutated to Lys, Gln, Val, their function in the toluene or fumarate binding, respective alternative substrates, expression vectors and BSS mutants.

Amino acid residue	Function	Replaced by	Alt. substrate	Expression vector, mutated variant
R 508	Fumarate binding	Lys, K	3-acetylacrylate	pASG3bssstrepArg508Lys, BSS R508K
		Gln, Q		pASG3bssstrepArg508Gln, BSS R508Q
I 617	Toluene binding	Val, V	xylenes	pASG3bssstrepIle617Val, BSS I617V
I 620		Val, V		pASG3bssstrepIle620Val, BSS I620V
		Gln, Q		pASG3bssstrepIle620Gln, BSS I620Q
I 617 + I 620		2x Val, V		pASG3bssstrepIle617+620Val, BSS I617+620V

The presence of Strep-Tagged BSS wild-type enzyme and its mutated variants was confirmed by Western Blot analysis. As it can be seen in Figure 19, the characteristic double band formation of the radical-containing alpha subunits can be observed, indicating an O_2-dependent breakdown at the site of the Gly radical. After confirming activation of the recombinant BSS variants, we determined their substrate specificities.

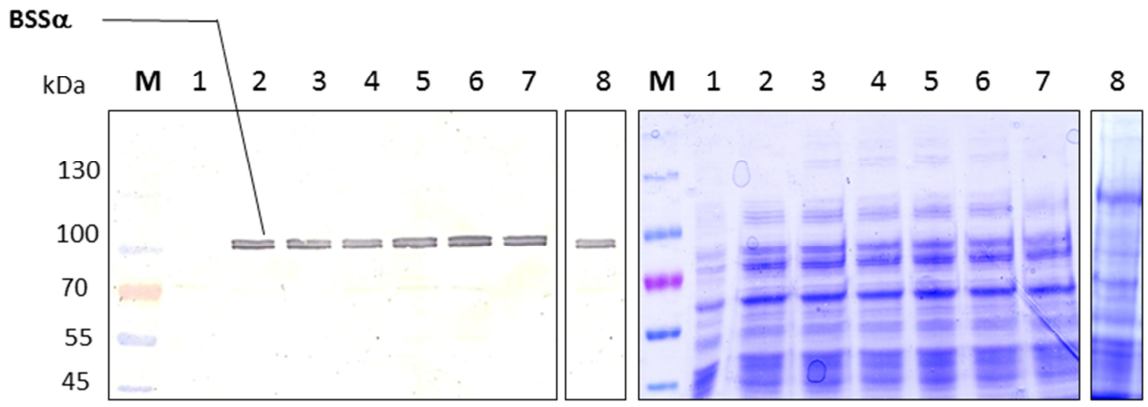

Figure 19: SDS-PAGE and Western Blot of Strep-tagged α-subunit (110kDa) of BSS variants using α-Strep antibody. Lane 1 – *A. evansii* cell extract before induction with AHT; Lane 2-8 - *A. evansii* cell extract after induction with AHT: 2- BSS WT, 3 – BSS Ile 620 Val, 4 – BSS Ile 617 + 620 Val, 5 – BSS Ile 620 Gln, 6 – BSS Arg 508 Lys, 7 – BSS Arg 508 Gln, 8 – BSS Ile 617 Val.

2.2 Isoleucine mutants: characterization of the specific activities of recombinant BSS I620V, BSS I617 + 620V, BSS I617V and BSS I620Q

In order to examine the change of substrate discrimination of the constructed isoleucine mutants of BSS, we performed a set of enzyme assays to test the turnover of toluene, *m, o-, p*-cresol and *m-, o-, p*-xylene (Fig. 13, 14, 20).

The predicted activity with *m*-xylene was indeed detected in the mutants, which either carried a single isoleucine 617 to valine mutation or a double substitution of isoleucine 617 and isoleucine 620 to valines, which exhibited specific activities of 6 and 5.5 nmol*min^{-1} mg protein^{-1} with *m*-xylene, whereas activities with toluene equalled 7 and 6.5 nmol*min^{-1} mg protein^{-1}, respectively. BSS I617V and BSS I620+I617V also showed the activity with toluene (7 nmol*min^{-1} mg protein^{-1} and 6.5 nmol*min^{-1} mg protein^{-1}), *m*-cresol (6 nmol*min^{-1} mg protein^{-1} and 4 nmol*min^{-1} mg protein^{-1}), *o*-cresol (4 nmol*min^{-1} mg protein^{-1} and 3 nmol*min^{-1} mg protein^{-1}) and *p*-cresol (3.5 nmol*min^{-1} mg protein^{-1} and 2.5 nmol*min^{-1} mg protein^{-1}), respectively (Table 20, Fig. 14, 20, Supplementary Fig. 1, E). Single substitution of isoleucine 620 to valine in BSS I620V resulted in the activity with toluene (5.5 nmol*min^{-1} mg protein^{-1}) and all cresols (for *m*-3.5, *o*- 2.5 and *p*- 3 nmol*min^{-1} mg protein^{-1}) but not with xylenes (Table 20).

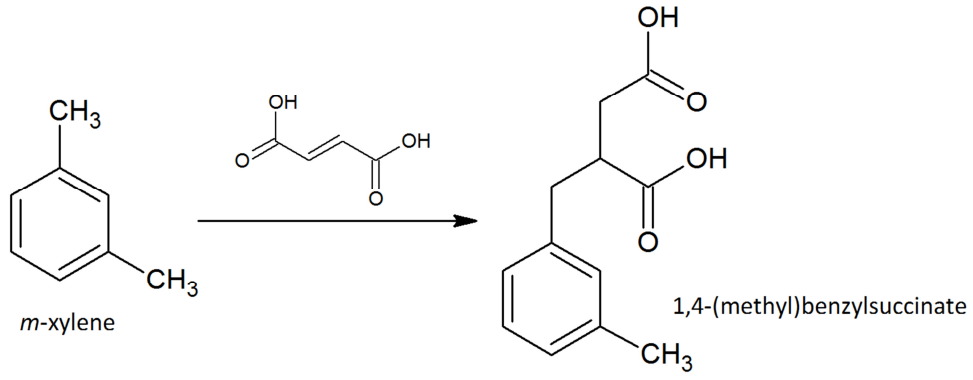

Figure 20: Fumarate addition reaction to the methyl group of *m*-xylene with formation of 1,4 – (methyl)benzylsuccinate, additionally catalyzed by BSS I617+620V and I617V.

Interestingly, both of the constructed *m*-xylene-converting mutants (BSS I620+I617V and BSS I617V) did not display observable activity with *p*- or *o*-xylene. Moreover, a single

substitution of isoleucine 620 to glutamine apparently led to a complete elimination of the enzyme activity, since BSS I620Q did not demonstrate the turnover of any of the substrates.

Table 20: Specific activities of the recombinant BSS variants (BSS I620V, BSS I620+I617V, BSS I617V) in *A. evansii* with various aromatic hydrocarbon substrates. Standard deviation values (σ) of enzyme activities are given from a total number of 3 independent activity assays.

Aromatic hydrocarbon substrates	**BSS I620V**	**BSS I620+I617V**	**BSS I617V**
	nmol*min^{-1} mg protein^{-1}(σ)		
toluene	5.5 (0.7)	6.5 (0.5)	7.0 (0.7)
m-xylene	< 0.1	5.0 (0.8)	6.0 (0.6)
o-xylene	< 0.1	< 0.1	< 0.1
p-xylene	< 0.1	< 0.1	< 0.1
m-cresol	3.5 (0.8)	4.0 (0.6)	6.0 (0.6)
o-cresol	2.5 (0.5)	3.0 (0.6)	4.0 (0.4)
p-cresol	3.0 (0.7)	2.5 (0.7)	3.5 (0.6)

Based on our experiments, we can assume that isoleucine 617 is indeed essential in the discrimination between toluene and *m*-xylene, and by changing Isoleucine 617 to valine we managed to enlarge the substrate range of BSS. Still, the absence of the activity with *p*- or *o*-xylene remains an open question, suggesting that the natural xylene-converting FAE contain additional changes to recognize these isomers.

2.3 Catalytic properties of the BSS I617V

Next, we assayed initial catalytic parameters of the BSS I617V variant, including Vmax and apparent Km values for toluene and *m*-xylene. Firstly, the enzyme test was carried out under fumarate saturation (3 mM), while the concentration of toluene and *m*-xylene was varied from 0.1 mM to 2 mM. The values determined for the substrate toluene are shown in Fig. 21. The apparent Km value for toluene equalled 1.5 nM with a Vmax value of 12 nmol · (mg.min) $^{-1}$.

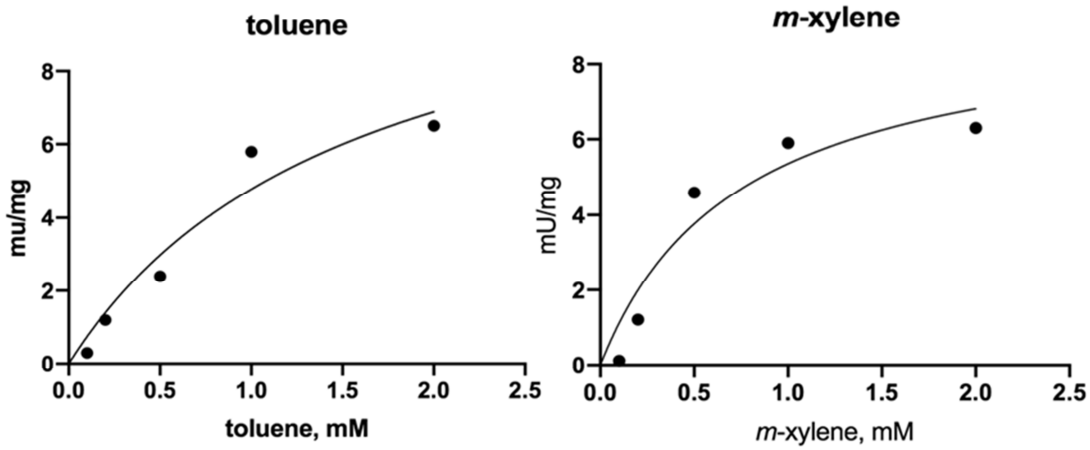

Figure 21: (A) Determination of the saturation kinetics of BSS I617V for toluene. Concentration of toluene varied from 0,1 mM to 2 mM, while concentration of fumarate remained constant (3 mM). The determined curve stands for Michaelis-Menten kinetics. The specific activity of the enzyme depending on toluene concentration. (B) Determination of the saturation kinetics of BSS for *m*-xylene. Concentration of *m*-xylene varied from 0,1 mM to 2 mM, while concentration of fumarate remained constant (3 mM). The determined curve stands for Michaelis-Menten kinetics. Constants were calculated from the mathematical adaptation of the Michaelis-Menten curve in GraphPad Prism Software.

For *m*-xylene, the values determined are shown in Fig. 21. The enzyme tests were also carried out under fumarate saturation (3 mM). For *m*-xylene, an apparent Km value of 0.7 nM was calculated with a Vmax value of 9 nmol · (mg.min)$^{-1}$, which is lower than the determined Km and Vmax values for toluene substrate, as examined for the native BSS from a toluene-grown culture of *T. aromatica* K172, for which no xylenes data is available (Verfurth, 2005).

2.4 Arginine mutants: characterization of the specific activities of the R508K and BSS R508Q mutants

Next, we tested the conversion of toluene, cresols, and xylenes with fumarate and 3-acetyl-acrylic acid by BSS variants with an arginine 508 to lysine (BSS R508K) or an arginine to glutamine (BSS R508Q) substitution. The rationale of these mutants was to see either decreased activity or changes of substrate specificity towards the conserved co-substrate fumarate, with has been replaced with the more hydrophobic analogue 3-acetyl acrylic acid, containing a ketone group instead of one of the carboxy groups (Fig. 22).

We observed a very low specific activity of 2.5 nmol*min^{-1} mg protein^{-1}with toluene and fumarate for the R508K variant, which equals to 21% of the activity of wild type BSS. No considerable product formation was detected with this BSS variant with either cresol or xylene isomers or fumarate as co-substrate.

However, we detected formation of barely detectable amounts of an apparent product in the reaction of toluene with 3-acetyl acrylate (Supplementary Fig. 4, Fig. 22) using HPLC-MS analysis in collaboration with the group of Prof. Dr Rainer Meckenstock, University Duisburg-Essen. The amount of synthesized benzylacrylic adduct was extremely low and still has to be confirmed by a second experiment (Supplementary Fig. 4), but the formation of the new adduct would be consistent with our hypothesis about the potential of arginine 508 substitutions for opening the reaction towards non-natural analogues of fumarate.

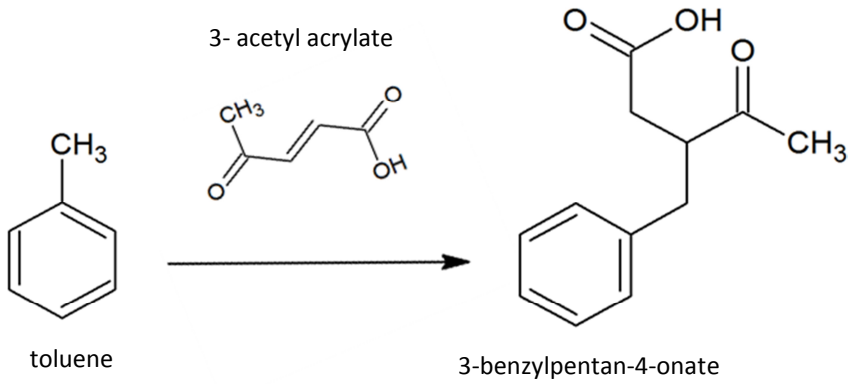

Figure 22: Plausible reaction of addition of 3-acetyl acrylic acid to toluene, catalyzed by BSS R508K with formation of 3-benzylpentan-4-onate.

The enzyme variant with an arginine to glutamine substitution, BSS R508Q, did not show any activity, even with the native substrate toluene. Thus far, it can be concluded that the presence of lysine 508 in BSS R508K still enables the turnover of toluene and fumarate at low levels. These data confirm the crucial role of a charged α-amino group (of either arginine or lysine) which has been proposed to form a salt bridge with one of the carboxyl group of fumarate (Funk, Marsh *et al.,* 2015). The observed total inactivation of BSS in the R508Q mutant is also a significant finding and may indicate that uncharged polar glutamine residue does not contribute to the fumarate binding, resulting in a complete elimination of the enzyme activity.

3. Homologous expression of naphthyl-2-methylsuccinate synthase in *A. evansii*

For the homologous expression of active naphthyl-2-methylsuccinate synthase (NMS), we implicated the earlier established overexpression system used for the production of active BSS (Results 1, Materials and Methods 4.1). After 3,5 hours of induction with anhydrotetracycline, a visible double band of Strep-tagged α-subunit of produced NMS was detected on the Western Blot (Fig. 23). Furthermore, we tested the conversion of toluene and the predicted native substrate – 2-methylnaphthalene, which have been assumed to be performed by this enzyme.

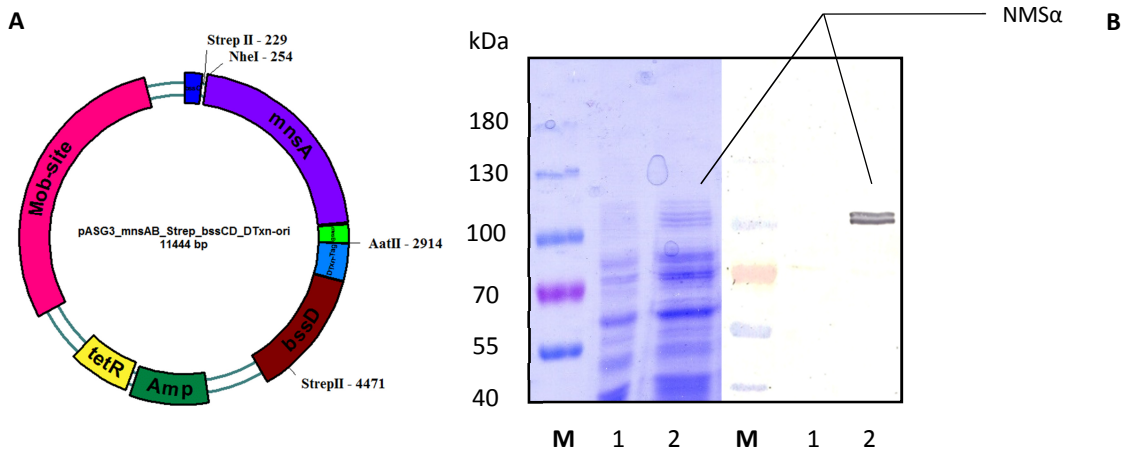

Figure 23: (A) pASG_nmsAB_Strep_bssCD_DTxn-ori vector, designed for overproduction of NMS. (B) SDS-PAGE and Western Blot of Strep-tagged α-subunit (110kDa) of NMS using α-Strep antibody: 1 – cell extract before induction.

Recombinant NMS displayed low conversion rates with toluene (2.5 nmol*min^{-1} mg protein^{-1}), but there was initially no product formation observed with 2-methylnaphthalene, probably due to its poor solubility in water as well as in the reaction buffer. Hence, we modified the reaction conditions in order to reduce 2-methylnaphthalene toxicity and improve its solubility by adding 50% paraffin oil as an insoluble hydrophobic phase to the reaction mixture (Materials and Methods 5.3).

Unfortunately, there formation of 2-naphthyl-methyl succinate was still not detectable by HPLC-MS analysis under these changed conditions. Therefore, the conditions of the enzyme assay need to be further improved for the detection of the methyl-2-naphthylsuccinate adduct. Observable activity with toluene, on the other hand, suggests that NMS is capable of catalyzing a glycyl radical type fumarate addition reaction, which has not been demonstrated in previous studies.

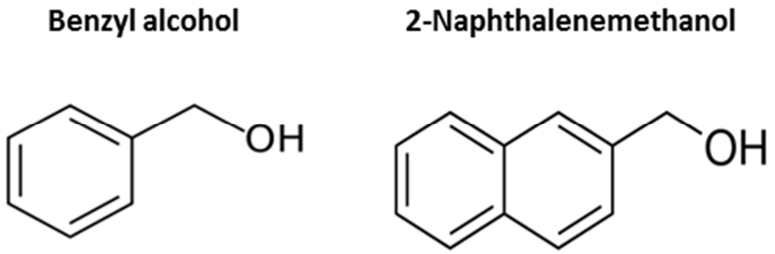

Figure 24: Benzyl alcohol and 2-naphthalenemethanol – two potential effector molecules for NMS.

Next, we have collected a set of samples for further examination via EPR spectroscopy to observe mechanistically relevant spectral changes in the presence of potential inhibitors, such as benzyl alcohol or 2-naphthalenemethanol (20 µM each) (Verfürth, 2005, Hilberg, 2012) (Fig. 24, Results 1.3.2). In order to test whether 2-naphthalenemethanol has an inhibitory effect on the reaction of NMS with toluene and 2-methylnaphthalene, as well as on the BSS reaction with toluene, similar inhibitory studies (Results 1.3.2) have to be performed.

4. Overproduction and purification of BSS, NMS and MPS in *E. coli*

In order to produce these enzymes in *E. coli* DH5α, and further in *A. evansii*, two pASG_nmsAB(mpsAB)_Strep_bssCD_DTxn-ori vectors for heterologous expression were designed, containing Strep-tagged *nms(mps)A* (encoding α subunit), *nms(mps)B* (beta subunit) genes, but retaining *bssC* (gamma subunit) of native BSS, together with the *bssD* gene (encoding activating enzyme for BSS) (Fig. 26, Materials and Methods 3.9). Due to the high sequence homology of the subunits of all three enzymes, it was assumed, that all three subunits (α, β, γ) will form a functional heterohexamer complex, similar to the one in BSS.

Furthermore, we have carried out multiple amino acid sequence alignments for homologous α subunits of MPS, MNS (clone N47), BSS from *T. aromatica* K172, *Azoarcus* strain T, hydroxybenzylsuccinate synthase from *Desulfobacula toluolica* (Hbs) and alkylsuccinate synthase from *Desulfoglaeba alkanexedens* (Fig. 25, Supplementary Fig. 5) in order to identify potentially distinctive residues in the large subunits of NMS or MPS to perform mutagenesis of the active site.

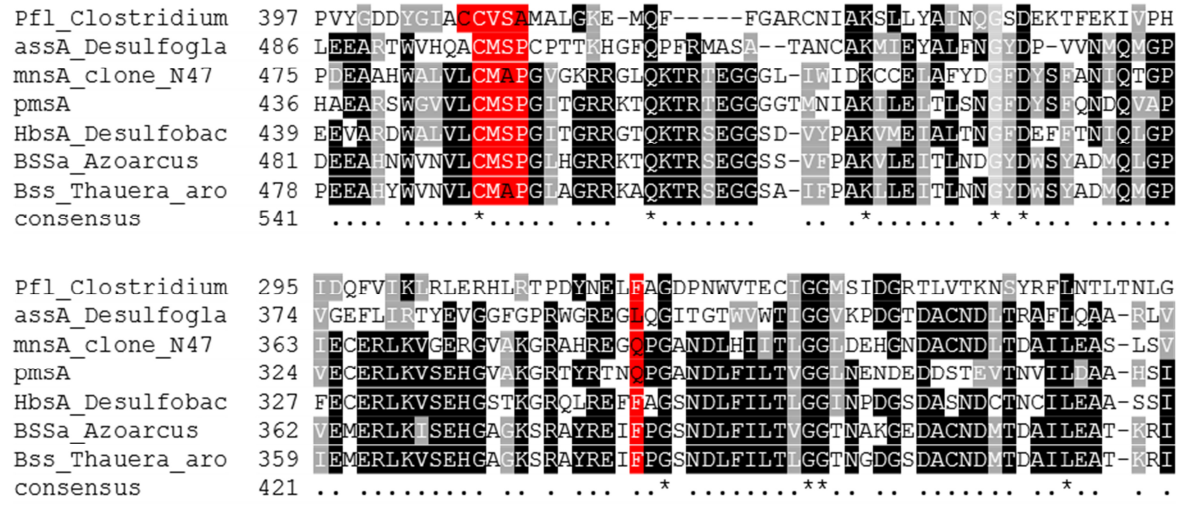

Figure 25: Amino acid residues inside the active sites of alpha subunits of MPS (pms) compared to other FAEs from δ-Proteobacteria *Desulfoglaeba alkanexedens* and *Desulfobacula toluolica* and β-Proteobacteria *Thauera aromatica* K172, *Azoarcus* strain T. 'Pfl' from *Clostridium kluyveri* (Firmicutes) is represented as a member of an outgroup. Amino acids, identified as crucial for substrate binding and glycyl radical formation are highlighted in red (S158, S160, Q346, C447, G784).

Judging from the amino acid sequence alignments, the polar residue Glu346 (Q) in NMS or MPS could be replaced by Phe (F), containing an aromatic ring in order to create a steric hindrance effect, which can possibly block the active site cavity for larger substrates,

such as methylnaphtalenes or methyphenanthrenes. Another possible target for the modification of the active centre is Ser158 (S) in MPS, which can be substituted by another aromatic amino acid Tyr (Y), which would potentially act similar to Phe (F). Hence, by introducing the described changes, it may be plausible to eliminate the conversion of both methylnaphtalene and methyphenanthrene (Fig. 25, Supplementary Fig. 5).

Both enzymes have been successfully overproduced in *E. coli* DH5α and purified via Strep-affinity column and size Exclusion chromatography (SEC) (Fig. 26 A, B). For the Strep-affinity purification, 10 g of cells were used, which yielded of purified BSS (6 mg/ml) and 7 mg/ml of NMS (7 mg/ml after subsequent concentration). Both proteins have then been loaded on a Size Exclusion column, which resulted in further enrichment, yielding BSS (3.5 mg/ml) and NMS (4.3 mg/ml). After SDS-PAGE separation of both proteins, the large α subunit was observed as a single band, indicating the non-activated state of BSS and NMS (Fig. 26 A, B). Regrettably, there was no detectable production of the MPS subunits (Fig. 26, C) (either in the cell extract or after Strep-affinity purification).

Furthermore, the presence of alpha and beta subunits of NMS together with the gamma subunit of BSS has been detected (Fig. 26, A, B) in the purified recombinant naphthyl-2-methyl-succinate synthase complex and was confirmed by MALDI TOF analysis in collaboration with Jörg Kahnt, Max Planck Institute for Terrestrial Microbiology, Marburg (data not shown). The fractions obtained after Size-Exclusion (SEC) purification of purified BSS and NMS were taken for further characterization by UV-Vis spectroscopy and ICP-OES elemental analysis in order to examine the iron-sulfur cluster content (Materials and Methods 5.6, 5.7).

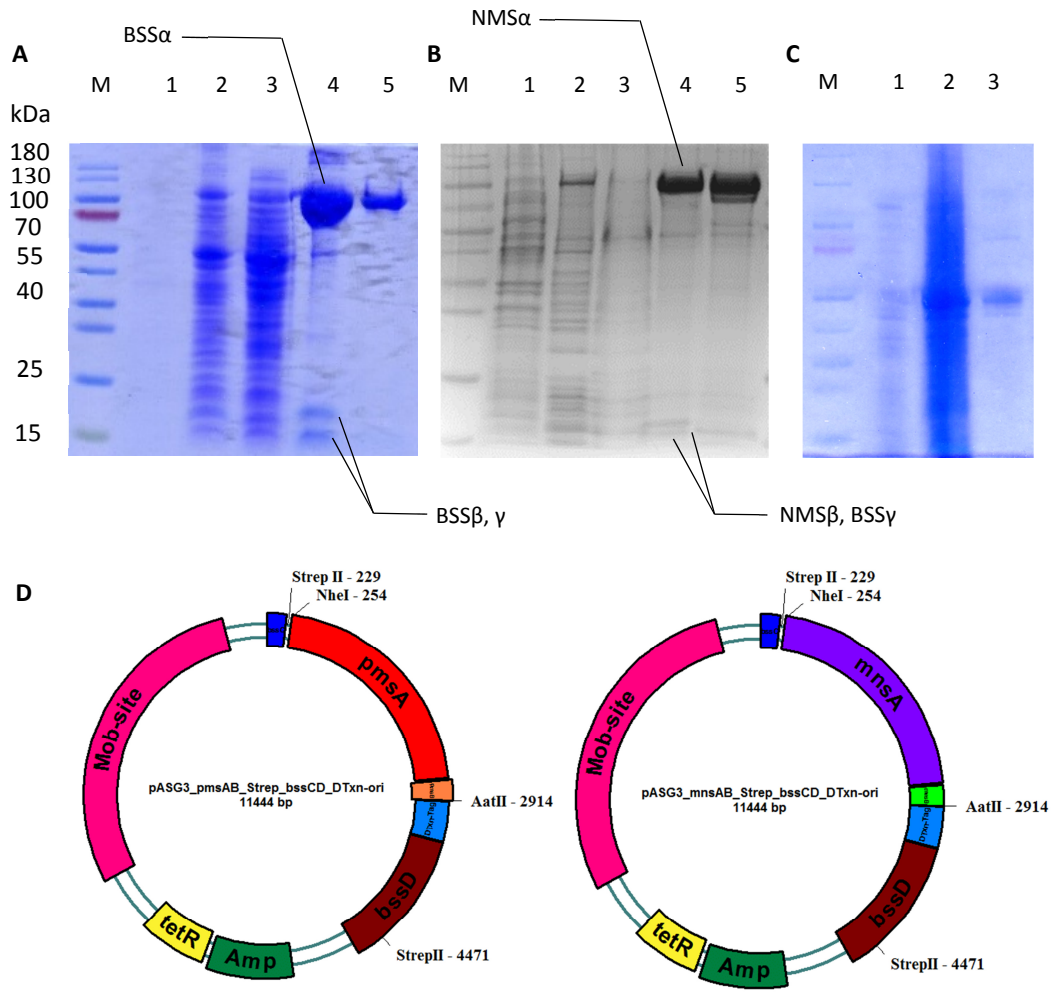

Figure 26: Overproduction and purification of BSS (A), NMS complex (NMSα, β + BSS γ) (B) and MPS in *E.coli* DH5α (C). Lane numbers correspond to: (A, B) 1 – cell extract before induction with AHT, 2 – cell extract after induction with AHT, 3 – flow through fraction, 4 – Strep-affinity elution fraction, 5 – Size Exclusion elution fraction. (C) 1 – cell extract before induction with AHT, 2 – flow through fraction, 3 – Strep-affinity elution fraction. (D) pASG_mnsAB(mpsAB)_Strep_bssCD_DTxn-ori vectors, constructed for heterologous expression of NMS and MPS.

5. Uv/Vis spectroscopy analysis and iron-sulfur cluster determination of BSS and NMS

Purified BSS and NMS were used at concentrations of 4.3 µM (BSS) and 5.1 (NMS) for a UV/Vis spectroscopic analysis in the range of 300-600 nm (Fig. 27). Both untreated BSS and NMS showed a broad absorption maximum at 420 nm, as previously reported for native BSS (Fig. 27 A, B). After treatment with increasing concentrations of sodium dithionite (NaDT) (1 mM, 1.5 mM, 2 mM, 2.5 mM) a stepwise decrease of this absorption maximum was observed (Fig. 27 A, B).

This data indicates the presence of reducible iron-sulfur clusters in the β- and γ-subunits of NMS and BSS.

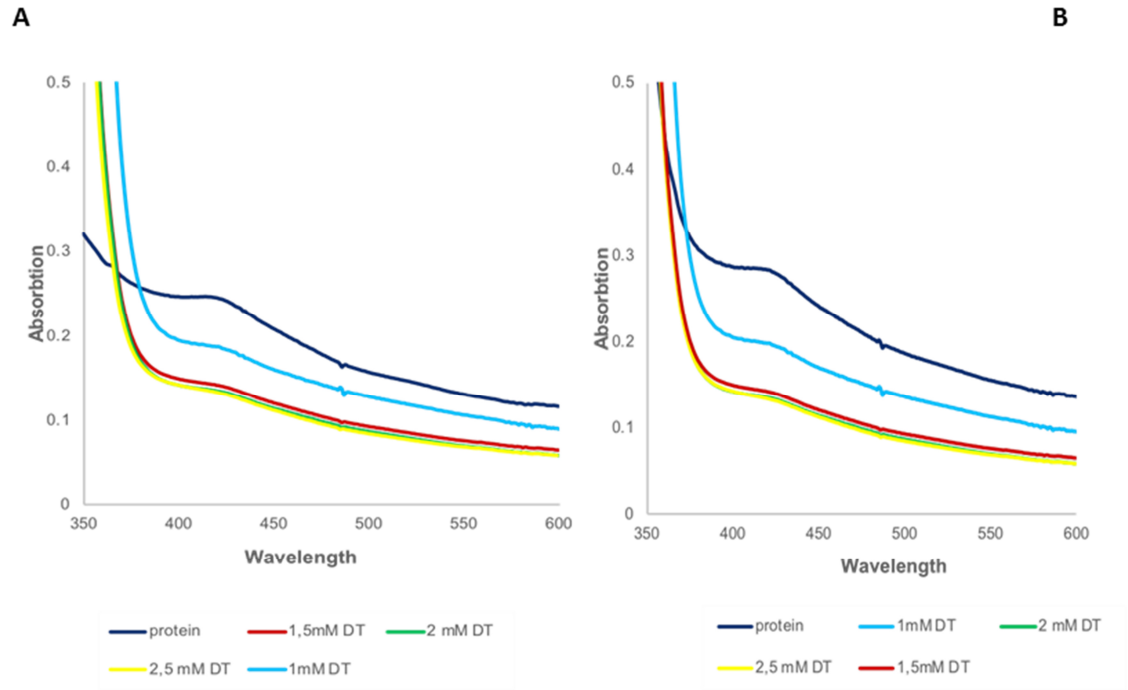

Figure 27: UV/Vis spectra of purified Strep-tagged benzylsuccinate synthase (A) and naphthyl-2-methyl succinate synthase (B): UV/Vis spectra of 4.3 µM BSS and 5.1 µM NMS, including the untreated enzymes and after gradual reduction with sodium dithionite (DT). Characteristic for iron-sulfur clusters decrease in absorption at a wavelength of 420 nm after incubation of both proteins with sodium dithionite. Enzymes were solubilized in a buffer containing 100 mM Tris, 150 mM NaCl 10% glycerol, pH 8.0.

In addition, the iron content of BSS and NMS was determined by ICP-OES elemental analysis (Materials and Methods 5.7). After chemical reconstitution of BSS and NMS with Fe (II) ammonium citrate and lithium sulfide (Materials and Methods 4.6), the metal analysis of

BSS and NMS by ICP-OES (Lovenberg *et al.,* 1963) showed iron contents of 7.4 (BSS) and 8.5 (NMS) iron atoms per holoenzyme (Table 21).

Table 21: Calculated Fe atom numbers per holoenzyme in BSS and NMS based on ICP-OES analysis after Size Exclusion chromatography.

Purification step	Fe atoms/ $\alpha_2\beta_2\gamma_2$ holoenzyme	
	BSS	NMS
Size Exclusion	7.4	8.5

The number of iron atoms, obtained with recombinant BSS, was 41% lower than previously described for Strep-tagged purified BSS in Hilberg *et al.* (2012), where the reconstituted protein contained 17.9 Fe atoms per $\alpha_2\beta_2\gamma_2$ holoenzyme. Moreover, both proteins seem to have lost significant amounts of Fe atoms during the passage through the Size Exclusion column: the evaluated Fe atom number for BSS or NMS corresponds to about half of the expected amounts (Table 21).

VII. DISCUSSION

1. Characterization of the recombinant active *(R)*-benzylsuccinate synthase

Recombinant production of BSS from various strains of anaerobic toluene-degrading bacteria has previously been established in *E. coli* strains using various gene expression systems. However, recombinant BSS was either completely inactive or showed extremely low activities (Verfürth, 2005, Li and Marsh, 2006) under these conditions, despite the presence of a co-expressed gene for the cognate activating enzyme in the expression vector (Hilberg, 2012). According to previous observations, recombinantly produced BSS activating enzyme (BssD) appears to be highly sensitive to misfolding and precipitates quantitatively as inclusion bodies (Hermuth *et al.,* 2002). Therefore, we cloned the *bssD* gene as a translational fusion with a C-terminal thioredoxin and a C-terminal Strep-tag into our expression vectors, which yielded small amounts of soluble protein containing the predicted Fe-S clusters (Hilberg, 2012). However, adding this construct into a vector containing the genes for the BSS subunits still did not yield in producing active BSS in *E.coli* hosts (Hilberg *et al.,* unpublished results). Previous attempts to achieve an active enzyme have been performed in our laboratory with *A. aromaticum* EbN1 as a host organism by (Seyhan, 2016) and led to the maximum activity of BSS with toluene at 7,2 mU/mg, which comprised only 1/3 of the native enzyme activity from toluene-grown cells of *T. aromatica* K172. Notably, the recombinant production of BSS in *A. aromaticum* was achieved without co-expressing the *bssEFGH* genes of the *bss* operon, since these genes were neither present on the plasmid nor induced during growth on benzoate. However, the presence of a separate *bss* operon in the genome still precluded clear statements on their requirement. The subsequent complete and partial deletion of the *bss* operon of *A. aromaticum* EbN1-SR7 led to unusual phenotypes of the deletion mutants, which were still capable of growing on toluene as a sole carbon source (Seyhan, 2016). Moreover, the deletion mutants also showed unusual growth behavior even without externally added substrate, further suggesting that *A. aromaticum* EbN1-SR7 is not a suitable host strain for further expression attempts.

Therefore, we have applied the same plasmid system in order to overproduce BSS in the denitrifying beta proteobacterium *Azoarcus evansii*, which is closely related to *T.*

aromatica and *A. aromaticum* EbN1 (Anders, Kaetzke *et al.,* 1995), but lacks the pathway for toluene degradation. The highest specific activities of recombinant BSS in cell extracts of *A. evansii* were observed with toluene (12 mU/mg) and *m*-cresol (10 mU/mg), while *o*- and *p*-cresols were converted at lower levels and none of the xylene isomers was accepted. Although the activities of native BSS were still slightly higher than those of the recombinant enzyme, the specific activities were very similar and consistent with the previously determined substrate pattern of BSS from *T. aromatica* K172 (Verfurth, Pierik *et al.,* 2004).

Furthermore, we have confirmed that the recombinant enzyme demonstrates a similar inhibitory pattern and catalytic properties, which have been examined for native BSS (Results 1.3.2, Fig. 16). Benzyl alcohol has been shown to be a competitive inhibitor for native BSS. It has been observed that this substrate-analogous inhibitor binds in the active site of BSS and is activated by abstraction of a hydrogen atom from the C1 atom. The resulting organic radical then adds to the fumarate co-substrate to a product radical, which then can no longer re-take the initially abstracted hydrogen from the conserved Cys493, thus blocking the active site of the enzyme. As a result of this mechanism, the catalytically active state of the enzyme cannot be restored. Information on this mechanism of inhibition was provided by EPR spectroscopic studies of *T. aromatica* crude extract after incubation with benzyl alcohol (Hilberg, 2012). Moreover, a mixture of benzyl fumarate / benzylmaleate has been demonstrated to be a non-competitive inhibitor that does not compete with toluene. In addition to benzyl alcohol, several other substrate analogues have been proven in previous studies by (Verfürth, 2005, Hilberg, 2012) to be potent inhibitors for the native BSS from *T. aromatica* K 182, such as benzaldehyde, phenylhydrazine and benzyl chloride. In order to further investigate the identity of the recombinant BSS, we have prepared a set of BSS samples, containing the untreated enzyme and the enzyme after incubation with 20 µmol of benzyl alcohol for subsequent EPR spectroscopic analysis (data not yet available). Therefore, the established overproduction system appears to be suitable for further investigations of the reaction mechanism as well as the mechanisms of action of further inhibitors, including benzaldehyde, phenylhydrazine and benzyl chloride, and mutagenesis studies of BSS.

2. Elucidation of the substrate recognition determinants by mutated BSS variants

Isoleucine mutants

Recently published crystal structures of BSS and modelling data based on these structures have made it possible to identify a number of amino acids in BssA that could play a key role in the mechanism of BSS (See Introduction).

Particular attention was paid to the mutagenesis of putative active site amino acids in three different target groups. The isoleucine residues Ile617 and Ile620 in BssA of *T. aromatica* are changed to valine in the enzymes of the *m*-xylene degrading strains *Azoarcus sp.* CIB and *Azoarcus sp. T* and could play a role in the binding and conversion of *m*-xylene (Verfurth, Pierik *et al.,* 2004). To check this, we investigated whether the substrate spectrum of the enzyme is indeed expanded, when the isoleucine residues in BSS from *T. aromatica* are replaced to valines or to glutamine.

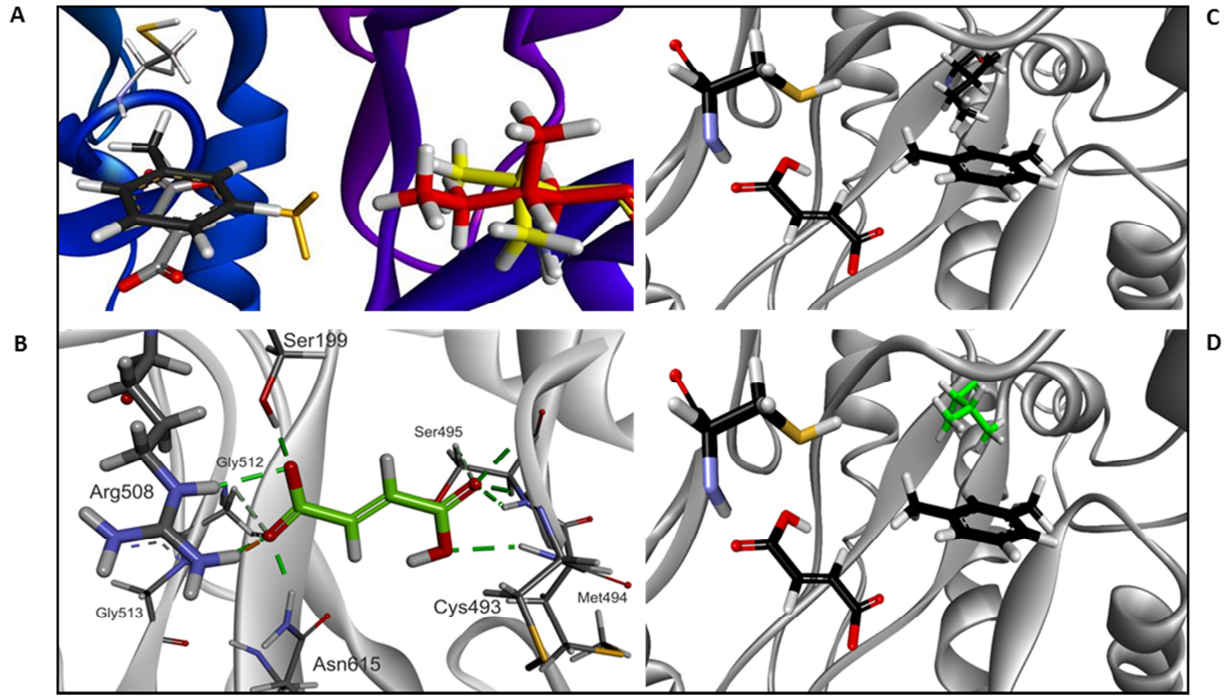

Figure 28: Predicted interactions of active site residues with the respective substrates. (A) Overlaid MD models of toluene (black) or *m*-xylene (yellow) binding at the active site with either wild type or the I617V variant of BSS. (B) Model of fumarate binding at R508. (C) MD model of *m*-xylene bound at the active site of BSS wild type. (D) Model of *m*-xylene bound at the active site of BSS I617V.

The mutant variants were produced in *A. evansii* to the same extent as the wild-type enzyme and appeared to be activated based on the presence of a double band of the α-subunit in Western blots with anti-strep antiserum (Results 2.1, Fig. 19). The specific activities of all mutants with toluene and the cresol isomers dropped to 30 – 50 % of the values recorded with the recombinant wild-type enzyme, but they were still clearly detectable. Conversely, activity with *m*-xylene was only detected in those variants, which carried an I617V substitution, whereas the I620V variant only showed turnover of toluene. The I617V single mutant showed almost the same specific activities with toluene and *m*-xylene, whereas the I617V+I629V double mutant showed an about 50% reduced activity with *m*-xylene (Results 2.2, Table 20). Surprisingly, none of the other xylene isomers was turned over by either of the constructed mutants (Table 20), in contrast to the natural BSS orthologue from *Azoarcus* strain T which accepts all xylene isomers (Verfurth, Pierik *et al.,* 2004). This suggests that the I617V exchange very likely represents the determinant to discriminate between toluene and *m*-xylene, whereas the other xylene isomers may be discriminated by additional determinants.

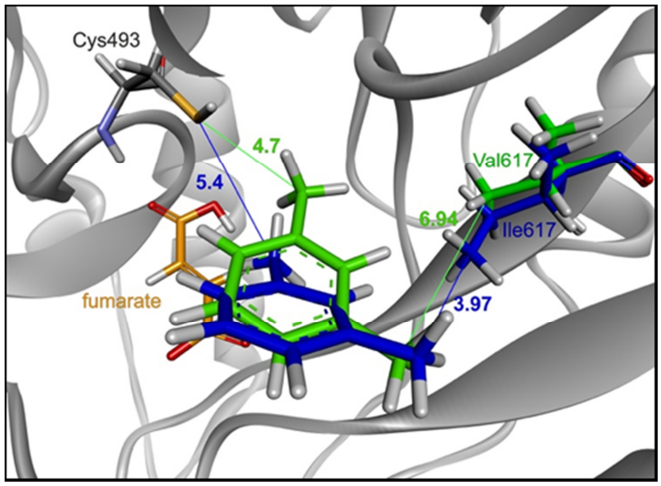

Figure 29: Most frequent position of *m*-xylene in the BSS active site from MD simulations for the wild-type (blue) and I617V mutant (green). Distances provided in Å.

The obtained substrate discrimination data have been supported by molecular dynamics and docking (MD) modelling performed by Maciej Szaleniec (Krakow) specifically for this work (Fig. 28, 29). According to the toluene docking MD simulation, in the wild-type BSS, toluene easily penetrates the active site cavity, a most frequent distance (MFD) of 4.64 Å between the C and Sγ atoms was predicted, allowing the approach of the methyl group of

toluene to the radial thiyl group (S atom of Cys493. (Fig. 28, 29). In contrast, *m*-xylene penetration to the thiyl radical of Cys493 is hindered by steric interaction between the additional methyl groups with Ile617. The methyl group of *m*-xylene is supposed to be activated to a radical stays further away from Cys493 (MFD between C and Sγ equals 5.4 Å), while the second methyl group never gets close to Cys493 (MFD equals 9.7 Å). However, after an I617V mutation, *m*-xylene is able to rotate inside the active site presenting both either of the two methyl groups at a similar distance to Cys493 as seen in the MD analysis with toluene (MFD equals 4.7 Å).

This enables an efficient activation of one of the methyl groups of *m*-xylene as is observed for toluene. Furthermore, the analysis of distances between *m*-xylene and the side chain of Ile 617 confirms higher steric clashes for wild type BSS (Fig. 29, the distance between the second methyl group (C7) and Cγ2 Ile617 is 3.97 Å) compared to I617V mutant (Fig. 29, distance between C7 of *m*-xylene and Cγ2 Val 617 is 6.94 Å). Interestingly, toluene binding in the I617V variant seems to be less constrained than in the wild-type which probably results in higher mobility in the active site and further (on average) distance to Cys493. This would be consistent with the observed decrease of activity of the BSS I617V mutant with toluene as substrate. On the other hand, the complete inactivation observed for the Ile 620 to Gln substitution (BSS I620Q) implies a potential structural role of Ile 620 in the maintenance of the hydrophobicity and integrity of the active site wall.

In order to identify likely determinants for binding of *o*- and *p*-xylene, it is necessary to perform further analysis of the structural data and sequence alignments with xylene-degrading species *Azoarcus sp.* CIB (unknown substrate spectrum for xylenes) and *Azoarcus sp. T* (turnover of all xylene isomers). Moreover, according to the sequence alignments performed in this work, BssA from the metal ion reducing bacterium *G. metallireducens* contains valine at the position 617 and isoleucine at the position 620. Therefore, it would be of interest to test the conversion of xylene isomers by the enzyme from this species.

Arginine mutants

The arginine residue Arg508 has been identified as having a key role in fumarate binding in recent studies. It most likely binds a deprotonated carboxyl group of fumarate, thereby fixing the co-substrate in the active site (Funk, Judd *et al.,* 2014, Szaleniec and

Heider, 2016). To confirm this assumption and, where appropriate, to extend the substrate scope to other fumarate-like substrates (e.g. 3-acetyl acrylate), the arginine residue was another important target of the mutagenesis studies performed in this work. Based on the activity tests, the BSS variant R508K showed drastically decreased activity with toluene, implying the essential role of Arg508 in the fumarate binding, but also demonstrating that it can principally be substituted by Lys as another basic residue.

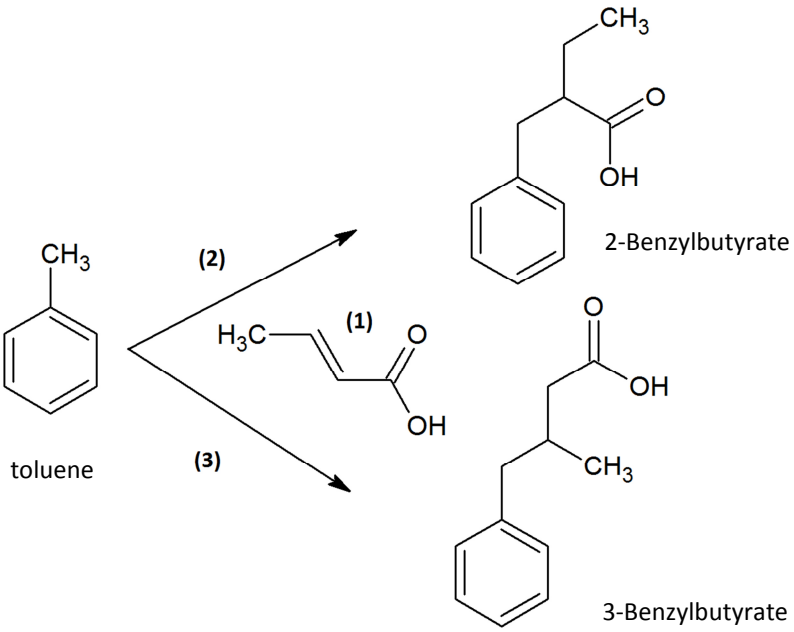

Figure 30: Two possible outcomes **(2, 3)** of the reaction of BSS R508K with toluene and alternative fumarate analogue – crotonate **(1)** with the formation of 2-Benzylbutyrate and 3-Benzylbutyrate.

Next, we hypothesized that another potential effect of substituting arginine to lysine may be the shift of specificity towards fumarate as co-substrate. The rationale of this choice was based on the higher hydrophobicity of lysine compared to arginine, which could possibly lead to productive binding of the ketone group of the fumarate analogue 3-acetylacrylate, while the remaining carboxyl-group of 3-acetylacrylate would be anchored as in the wild type enzyme. Surprisingly, we did indeed observe a conversion of toluene while using 3-acetylacrylate at very small amounts, which confirmed our initial hypothesis (Results 2.4, Supplementary Fig. 4). For further experiments, it would be highly interesting to test the effect of further arginine 508 substitutions on the acceptance of even more fumarate analogues. For example, exchange of Arg508 to hydrophobic amino acids with long side chains (e.g. Ile or Phe) might further improve interaction with the ketone group of

3-acetylacrylate, or even allow to add other analogues such as crotonate, pentenoate, or glutaconate (Fig. 30).

3. Elucidating the substrate spectrum and reaction mechanism of NMS

Naphthyl-2methyl succinate synthase (NMS), derived from a sulfate-reducing enrichment culture N47 has been suggested to catalyze of the fumarate addition reaction to the methyl group of 2-methylnaphthalene (see Introduction). This was supported by the detection of putative fumurate addition genes encoding proteins analogues to naphthyl-2-methylsuccinate synthase (NmsA) (Selesi, Jehmlich *et al.,* 2010). NMS has been suggested to be composed of alpha-, beta-, and gamma-subunits that are encoded by the genes *nmsABC*. Located directly upstream of *nmsABC*, the *nmsD* gene encodes the putative NMS-activating enzyme, which harbours the characteristic [Fe4S4] cluster sequence motifs of S-adenosylmethionine radical enzymes. The *bns* gene cluster, coding for enzymes involved in beta-oxidation reactions converting naphthyl-2-methyl-succinate to 2-naphthoyl-CoA, was found further downstream in the genome sequence after four intervening open reading frames. This cluster consists of eight genes (*bnsABCDEFGH*) corresponding to 8.1 kb, which are closely related to genes for analogous enzymes involved in anaerobic toluene degradation in the denitrifiers "*Aromatoleum aromaticum*" EbN1, *Azoarcus* sp. strain T, and *Thauera aromatica* (Selesi, Jehmlich *et al.,* 2010).

Based on these findings, we have applied the near-homologous overproduction system developed for BSS for producing active NMS in *A. evansii* under benzoate degrading conditions. We have indeed been able to demonstrate for the first time that the predicted NMS is active as fumarate-adding enzyme, catalyzing the formation of benzylsuccinate from toluene and fumarate. Although we did not yet prove the conversion of methylnaphthalene by this enzyme, we believe this to be a technical problem because of the low solubility of this substrate in water. However, the availability of this enzyme from our recombinant system will now allow to further elucidate the substrate spectrum and the reaction mechanism of NMS.

The substrate scope of NMS has been proposed based on sequence alignments with different aromatic and aliphatic hydrocarbon degrading species and homology models of

the active site (Heider, Szaleniec *et al.,* 2016), (Fig. 33). Apart from the native substrate – 2-methylnaphthalene, NMS is believed to encompass a broader substrate range compared to BSS and other FAEs due to the amino acid composition and size of the active site pocket, which provides more space for the accommodation of various aromatic and aliphatic substrates, such as toluene, xylene and cresol isomers, *p*-cymene, alkanes, fluorotoluenes or 4-ethyltoluene (Fig. 31).

In this work, we were able to overproduce active NMS (Results 3, Fig. 23) and observe the formation of benzylsuccinate in the reaction with toluene, which provided initial biochemical evidence on the fumarate addition nature of the enzyme. Moreover, we also tested the turnover of 2-methylnaphthalene, *p*-cymene and 4-ethyltoluene. Unfortunately, there was no considerable formation of the respective succinate adducts with these substrates, which should be detectable by HPLC-MS analysis. In addition, due to the low solubility of 2-methylnaphthalene in the reaction buffer, most of the substrate gets precipitated and not used by the enzyme. Therefore, the development of an improved enzyme activity assay is crucial for further studies.

A following step in elucidating the reaction mechanism of NMS would be the mechanistic modelling using QM and DFT techniques, which have been applied for the modelling of the reaction mechanism of BSS (Himo 2002, Himo 2005, Bharadwaj, Dean *et al.,* 2013, Szaleniec and Heider, 2016). Also, EPR spectroscopic experiments are aimed to initially detect the glycyl radical signal as well as to identify potential competitive inhibitory molecules, which have been extensively characterized for BSS.

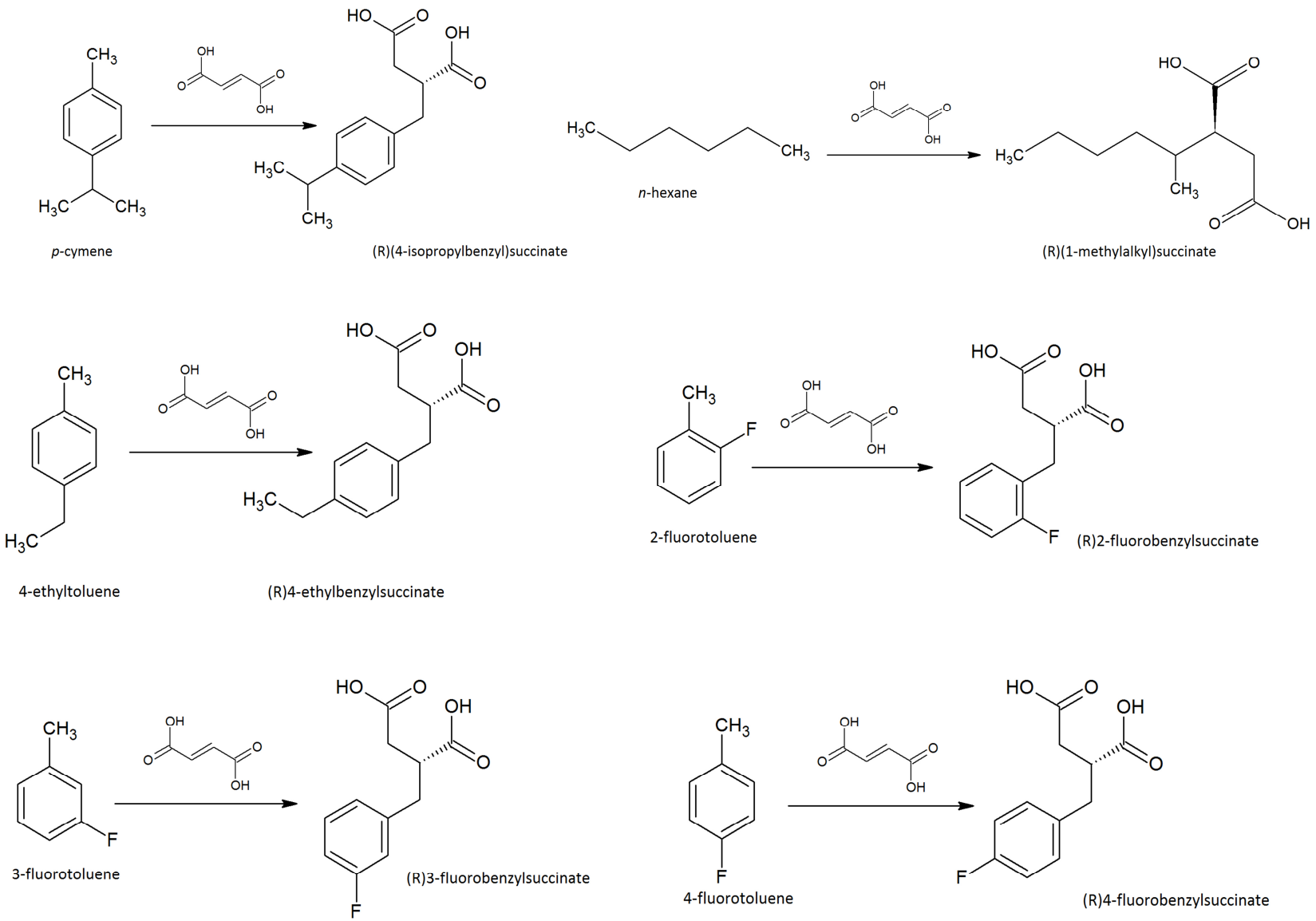

Figure 31: Plausible fumarate addition reactions, catalyzed by NMS, including *p*-cymene, *n*-hexane, 4-ethyltoluene and 2-, 3-, 4-fluorotoluene with the formation of respective adducts.

4. Structural comparison of BSS with other FAEs

Recently modelled active site conformations of HBSS, NMS and ASS were compared with those of BSS based on homology models derived from the crystal structure of BSS (Szaleniec and Heider, 2016) (Fig. 33). Model building was performed using the amino acid sequences of the large subunits of (hydroxy)benzylsuccinate synthase (HBSS) from *D. toluolica* (Wohlbrand, Jacob *et al.,* 2013), NMS from strain NaphS6 (Musat, Galushko *et al.,* 2009), alkylsuccinate synthase-1 (ASS) from *D. alkenivorans* (Callaghan, Wawrik *et al.,* 2008), (4-isopropyl)benzylsuccinate synthase (IBSS) from strain p CyN2 (Strijkstra *et al.,* 2014) and (1-methylalkyl)succinate synthase (MASS) from "*Aromatoleum*" strain HxN1 (Jarling *et al.,* 2012) (Fig. 9, 32, 33). All analyzed FAEs showed a universal conservation of the catalytic thiol/thiyl moiety (Cys493 in BSS) and the Arg508 (BSS) involved in fumarate binding, proving the important roles of these amino acids for catalysis.

HBSS displayed a relatively high amino acid sequence identity with BSS (49%) and contains only one different side chain among 14 selected highly conserved active site residues, a phenylalanine instead of tyrosine. NMS shows 45% amino acid sequence identity to BSS and displays only one different side chain the conserved active site residues, a glutamine instead of a phenylalanine. Also, ASS showed a quite low amino acid sequence identity with BSS (33%) and diverged the most from the sequence of BSS, exhibiting 8 amino acid changes in the 14 positions predicted to contribute to the active site (Heider, Szaleniec *et al.,* 2016). Notably, the more related structural models of HBSS and MNS show a very similar positioning of the key residues analogous to Cys493 and Arg508 of BSS as well as several other active site amino acids, suggesting very similar functions in fumarate binding (Fig. 33).

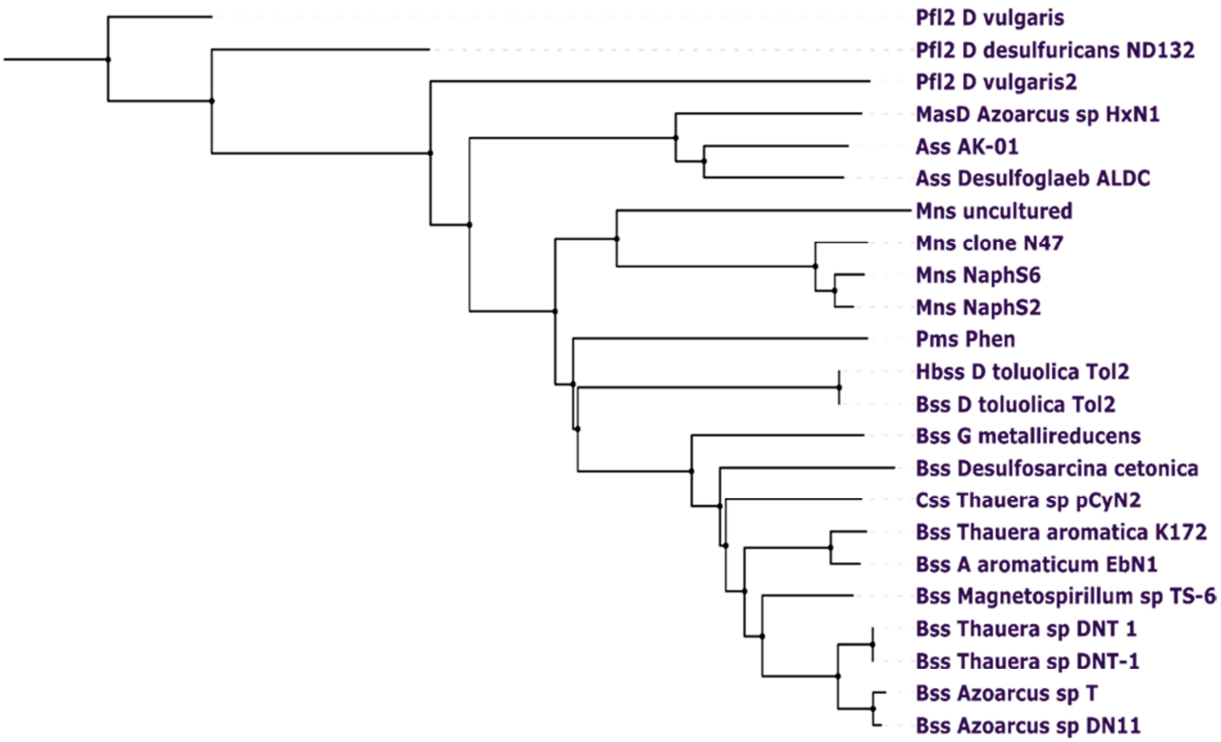

Figure 32: Phylogenetic tree of several selected FAEs, including methylphenanthrene succinate synthase (MPS). The tree was constructed by multiple alignments of the sequences of the large subunits of FAEs using the ClustalW2 program available on the EMBL-EBI website.

Several other amino acids differ in their positions, which may indicate some flexibility and repositioning during substrate binding. In the case of NMS, the most obvious amino acid exchange (Phe385 of BSS to Gln366) results in the loss of a phenyl ring, which may indeed allow the enzyme to position the two-ring structure of 2-methylnaphthalene in the opened space. The different side-chain composition observed in ASS with many exchanges of larger to smaller amino acids might allow a bigger void volume for the active site pocket in ASS compared to BSS, which may be better suited to position alkanes (Fig. 32, 33).

Additionally, the fumarate could be bound in a different angle in the active site of ASS compared to BSS to enable its attack at the methylene group of alkanes. The final examination of the side-chain geometries and the amino acids relevant for substrate binding and discrimination among BSS, HBSS, MNS and ASS still requires more detailed biochemical and structural characterization.

In this work, we have established the overproduction system for α and β subunits of NMS together with the γ subunit of BSS both in the non-active and activated form and proved the formation of the a functional heterohexamer complex (Results 4, MALDI TOF,

data not shown). Therefore, further improvement of the purification procedure of the non-activated form of NMS and BSS for crystallography studies and structural characterization are the next major tasks in this project.

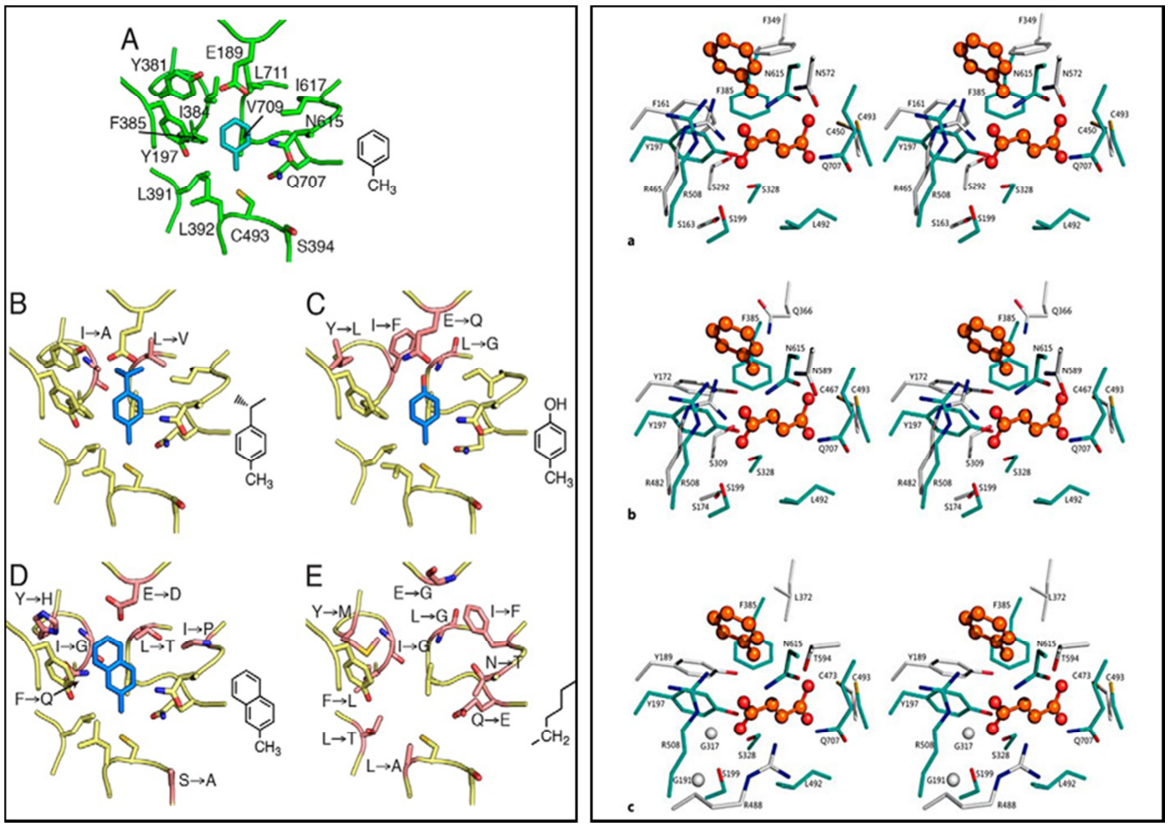

Figure 33: (Heider, Szaleniec *et al.,* 2016) (1) Homology models of XSS family members displaying the hydrocarbon binding site. (A) Crystal structure of BSS-bound to toluene alone (cyan). (B) Model of IBSS with *p*-cymene. (C) Model of HBSS with *p*-cresol. (D) Model of NMS with 2-methylnaphthalene. (E) Model of MASS without *n*-hexane. For each model, substrates (*blue*, diagramed at the *right*) were modelled according to changes in the active site due to amino acid substitutions (*pink*). (2) Substrate-binding site models of FAEs. Stereo-views of the active site pocket of BSS to accommodate binding of the substrates compared with those of HBSS (a), MNS (b) and ASS (c). The colour code for BSS is cyan (carbon), red (oxygen), blue (nitrogen) and yellow (sulfur). The overlaying homology protein models use grey for carbon. The binding mode for the substrates fumarate and toluene calculated for BSS from T. *aromatica* strain T1 is shown in ball-and-stick mode (orange for carbon and red for oxygen).

VIII. LITERATURE

1. Achong, G. R., A. M. Rodriguez and A. M. Spormann (2001). Benzylsuccinate synthase of *Azoarcus sp*. strain T: cloning, sequencing, transcriptional organization, and its role in anaerobic toluene and *m*-xylene mineralization. *J Bacteriol.* **183**: 6763-6770.
2. Aklujkar, M., J. Krushkal, G. DiBartolo, A. Lapidus, M. L. Land and D. R. Lovley (2009). The genome sequence of *Geobacter metallireducens*: features of metabolism, physiology and regulation common and dissimilar to *Geobacter sulfurreducens*. *BMC Microbiol.* **9**: 109.
3. Altenschmidt, U. and G. Fuchs (1991). Anaerobic degradation of toluene in denitrifying *Pseudomonas sp*.: indication for toluene methyl hydroxylation and benzoyl-CoA as central aromatic intermediate. *Arch Microbiol.* **156**: 152-158.
4. Anders, H. J., A. Kaetzke, P. Kampfer, W. Ludwig and G. Fuchs (1995). Taxonomic position of aromatic-degrading denitrifying Pseudomonad strains K172 and KB740 and their description as new members of the genera *Thauera*, as *Thauera aromatica sp*. nov., and *Azoarcus*, as *Azoarcus evansii sp*. nov., respectively, members of the beta subclass of the Proteobacteria. *Int J Syst Bacteriol.* **45**: 327-333.
5. Annweiler, E., A. Materna, M. Safinowski, A. Kappler, H. H. Richnow, W. Michaelis and R. U. Meckenstock (2000). Anaerobic degradation of 2-methylnaphthalene by a sulfate-reducing enrichment culture. *Appl Environ Microbiol.* **66**: 5329-5333.
6. Beller, H. R., M. Reinhard and D. Grbic-Galic (1992). Metabolic by-products of anaerobic toluene degradation by sulfate-reducing enrichment cultures. *Appl Environ Microbiol.* **58**: 3192-3195.
7. Beller, H. R. and A. M. Spormann (1997). Anaerobic activation of toluene and *o*-xylene by addition to fumarate in denitrifying strain T. *J Bacteriol.* **179**: 670-676.
8. Beller, H. R. and A. M. Spormann (1997). Benzylsuccinate formation as a means of anaerobic toluene activation by sulfate-reducing strain PRTOL1. *Appl Environ Microbiol.* **63**: 3729-3731.
9. Beller, H. R. and A. M. Spormann (1998). Analysis of the novel benzylsuccinate synthase reaction for anaerobic toluene activation based on structural studies of the product. *J Bacteriol.* **180**: 5454-5457.
10. Beller, H. R. and A. M. Spormann (1999). Substrate range of benzylsuccinate synthase from *Azoarcus sp*. strain T. *FEMS Microbiol Lett.* **178**: 147-153.
11. Beller, H. R., A. M. Spormann, P. K. Sharma, J. R. Cole and M. Reinhard (1996). Isolation and characterization of a novel toluene-degrading, sulfate-reducing bacterium. *Appl Environ Microbiol.* **62**: 1188-1196.
12. Bertani, G (1951). Studies on lysogenesis. I. The mode of phage liberation by lysogenic *Escherichia coli*. *J Bacteriol.* **62**: 293-300.
13. Bharadwaj, V. S., A. M. Dean and C. M. Maupin (2013). Insights into the glycyl radical enzyme active site of benzylsuccinate synthase: a computational study. *J Am Chem Soc.* **135**: 12279-12288.
14. Biegert, T., G. Fuchs and J. Heider (1996). Evidence that anaerobic oxidation of toluene in the denitrifying bacterium *Thauera aromatica* is initiated by formation of benzylsuccinate from toluene and fumarate. *Eur J Biochem.* **238**: 661-668.
15. Birnboim, H. C. and J. Doly (1979). A rapid alkaline extraction procedure for screening recombinant plasmid DNA. *Nucleic Acids Res.* **7**: 1513-1523.
16. Boll, M (2005). Key enzymes in the anaerobic aromatic metabolism catalysing Birch-like reductions. *Biochim Biophys Acta.* **1707**: 34-50.

17. Boll, M., S. S. Albracht and G. Fuchs (1997). Benzoyl-CoA reductase (dearomatizing), a key enzyme of anaerobic aromatic metabolism. A study of adenosinetriphosphatase activity, ATP stoichiometry of the reaction and EPR properties of the enzyme. *Eur J Biochem* **244**: 840-851.
18. Bradford, M. M (1976). A rapid and sensitive method for the quantitation of microgram quantities of protein utilizing the principle of protein-dye binding. *Anal. Biochem.***1-2**: 248-254.
19. Buckel, W. and B. T. Golding (2006). Radical enzymes in anaerobes. *Annu Rev Microbiol.* **60**: 27-49.
20. Butler, C. S. and J. R. Mason (1997). Structure-function analysis of the bacterial aromatic ring-hydroxylating dioxygenases. *Adv Microb Physiol.* **38**: 47-84.
21. Callaghan, A. V., I. A. Davidova, K. Savage-Ashlock, V. A. Parisi, L. M. Gieg, J. M. Suflita, J. J. Kukor and B. Wawrik (2010). Diversity of benzyl- and alkylsuccinate synthase genes in hydrocarbon-impacted environments and enrichment cultures. *Environ Sci Technol.* **44**: 7287-7294.
22. Callaghan, A. V., B. Wawrik, S. M. Ni Chadhain, L. Y. Young and G. J. Zylstra (2008). Anaerobic alkane-degrading strain AK-01 contains two alkylsuccinate synthase genes. *Biochem Biophys Res Commun.* **366**: 142-148.
23. Coschigano, P. W. (2000). Transcriptional analysis of the tutE tutFDGH gene cluster from *Thauera aromatica* strain T1. *Appl Environ Microbiol.* **66**: 1147-1151.
24. Coschigano, P. W., T. S. Wehrman and L. Y. Young (1998). Identification and analysis of genes involved in anaerobic toluene metabolism by strain T1: putative role of a glycine free radical. *Appl Environ Microbiol.* **64**: 1650-1656.
25. Dagley, S., W. C. Evans and D. W. Ribbons (1960). New pathways in the oxidative metabolism of aromatic compounds by microorganisms. *Nature.* **188**: 560-566.
26. Davidova, I. A., L. M. Gieg, K. E. Duncan and J. M. Suflita (2007). Anaerobic phenanthrene mineralization by a carboxylating sulfate-reducing bacterial enrichment. *ISME J* **1**: 436-442.
27. Dehio, C. and M. Meyer (1997). Maintenance of broad-host-range incompatibility group P and group Q plasmids and transposition of Tn5 in *Bartonella henselae* following conjugal plasmid transfer from *Escherichia coli*. *J Bacteriol.* **179**: 538-540.
28. Dower, W. J., J. F. Miller and C. W. Ragsdale (1988). High efficiency transformation of *E. coli* by high voltage electroporation. *Nucleic Acids Res.* **16**: 6127-6145.
29. Evans, P. J., W. Ling, B. Goldschmidt, E. R. Ritter and L. Y. Young (1992). Metabolites formed during anaerobic transformation of toluene and *o*-xylene and their proposed relationship to the initial steps of toluene mineralization. *Appl Environ Microbiol.* **58**: 496-501.
30. Frazer, A. C., P. W. Coschigano and L. Y. Young (1995). Toluene metabolism under anaerobic conditions: a review. *Anaerobe.* **1**: 293-303.
31. Fuchs, G., M. Boll and J. Heider (2011). Microbial degradation of aromatic compounds - from one strategy to four. *Nat Rev Microbiol.* **9**: 803-816.
32. Funk, M. A., E. T. Judd, E. N. Marsh, S. J. Elliott and C. L. Drennan (2014). Structures of benzylsuccinate synthase elucidate roles of accessory subunits in glycyl radical enzyme activation and activity. *Proc Natl Acad Sci U S A.* **111**: 10161-10166.
33. Funk, M. A., E. N. Marsh and C. L. Drennan (2015). Substrate-bound structures of benzylsuccinate synthase reveal how toluene is activated in anaerobic hydrocarbon degradation. *J Biol Chem* . **290**: 22398-22408.

34. Galushko, A., D. Minz, B. Schink and F. Widdel (1999). Anaerobic degradation of naphthalene by a pure culture of a novel type of marine sulfate-reducing bacterium. *Environ Microbiol.* **1**: 415-420.
35. Gibson, D. T. and R. E. Parales (2000). Aromatic hydrocarbon dioxygenases in environmental biotechnology. *Curr Opin Biotechnol.* **11**: 236-243.
36. Grundmann, O., A. Behrends, R. Rabus, J. Amann, T. Halder, J. Heider and F. Widdel (2008). Genes encoding the candidate enzyme for anaerobic activation of *n*-alkanes in the denitrifying bacterium, strain HxN1. *Environ Microbiol.* **10**: 376-385.
37. Harayama, S., M. Kok and E. L. Neidle (1992). Functional and evolutionary relationships among diverse oxygenases. *Annu Rev Microbiol.* **46**: 565-601.
38. Harwood, C. S. and R. E. Parales (1996). The beta-ketoadipate pathway and the biology of self-identity. *Annu Rev Microbiol.* **50**: 553-590.
39. Heider, J., M. Szaleniec, B. M. Martins, D. Seyhan, W. Buckel and B. T. Golding (2016). Structure and function of benzylsuccinate synthase and related fumarate-adding glycyl radical enzymes. *J Mol Microbiol Biotechnol.* **26**: 29-44.
40. Hermuth, K., B. Leuthner and J. Heider (2002). Operon structure and expression of the genes for benzylsuccinate synthase in *Thauera aromatica* strain K172. *Arch Microbiol.* **177**: 132-138.
41. Hilberg, M (2012). Anaerober Toluol-Stoffwechsel in *Thauera aromatica*: Biochemische und spektroskopische Untersuchungen zur Reaktion der *(R)*-Benzylsuccinat Synthase. *Dissertation* (Philipps-Universität Marburg).
42. Hilberg, M., A. J. Pierik, E. Bill, T. Friedrich, M. L. Lippert and J. Heider (2012). Identification of FeS clusters in the glycyl-radical enzyme benzylsuccinate synthase via EPR and Mossbauer spectroscopy. *J Biol Inorg Chem.* **17**: 49-56.
43. Himmelberg, A. M., T. Bruls, Z. Farmani, P. Weyrauch, G. Barthel, W. Schrader and R. U. Meckenstock (2018). Anaerobic degradation of phenanthrene by a sulfate-reducing enrichment culture. *Environ Microbiol.* **10**:3589-3600.
44. Himo, F (2005). C-C bond formation and cleavage in radical enzymes, a theoretical perspective. *Biochim Biophys Acta.* **1707**: 24-33.
45. Himo, F (2002). Catalytic mechanism of benzylsuccinate synthase, a theoretical study. *J. Phys. Chem. B*. **106**: 7688-7692.
46. Jarling, R., M. Sadeghi, M. Drozdovska, S. Lahme, W. Buckel (2012). Stereochemical investigations reveal the mechanism of the bacterial activation of *n*-alkanes without oxygen. *Angew. Chem. Int. Ed. Engl*. **6**: 1334-1338.
47. Knappe, J. and G. Sawers (1990). A radical-chemical route to acetyl-CoA: the anaerobically induced pyruvate formate-lyase system of *Escherichia coli*. *FEMS Microbiol Rev.* **6**: 383-398.
48. Kube, M., J. Heider, J. Amann, P. Hufnagel, S. Kuhner, A. Beck, R. Reinhardt and R. Rabus (2004). Genes involved in the anaerobic degradation of toluene in a denitrifying bacterium, strain EbN1. *Arch Microbiol.* **181**: 182-194.
49. Kuhner, S., L. Wohlbrand, I. Fritz, W. Wruck, C. Hultschig, P. Hufnagel, M. Kube, R. Reinhardt and R. Rabus (2005). Substrate-dependent regulation of anaerobic degradation pathways for toluene and ethylbenzene in a denitrifying bacterium, strain EbN1. *J Bacteriol.* **187**: 1493-1503.
50. Kummel, S., F. A. Herbst, A. Bahr, M. Duarte, D. H. Pieper, N. Jehmlich, J. Seifert, M. von Bergen, P. Bombach, H. H. Richnow and C. Vogt (2015). Anaerobic naphthalene degradation by sulfate-reducing *Desulfobacteraceae* from various anoxic aquifers. *FEMS Microbiol Ecol.* **91**. fiv006.

51. Laemmli, U. K (1970). Cleavage of structural proteins during the assembly of the head of bacteriophage T4. *Nature.* **227**: 680-685.
52. Leuthner, B. and J. Heider (2000). Anaerobic toluene catabolism of *Thauera aromatica:* the *bbs* operon codes for enzymes of beta oxidation of the intermediate benzylsuccinate. *J Bacteriol.* **182**: 272-277.
53. Leuthner, B., C. Leutwein, H. Schulz, P. Horth, W. Haehnel, E. Schiltz, H. Schagger and J. Heider (1998). Biochemical and genetic characterization of benzylsuccinate synthase from *Thauera aromatica*: a new glycyl radical enzyme catalysing the first step in anaerobic toluene metabolism. *Mol Microbiol.* **28**: 615-628.
54. Leutwein, C. and J. Heider (1999). Anaerobic toluene-catabolic pathway in denitrifying *Thauera aromatica*: activation and beta-oxidation of the first intermediate, *(R)-(+)*-benzylsuccinate. *Microbiology.* **145**: 3265-3271.
55. Li, L. and E. N. Marsh (2006). Mechanism of benzylsuccinate synthase probed by substrate and isotope exchange. *J Am Chem Soc.* **128**: 16056-16057.
56. Li, L., D. P. Patterson, C. C. Fox, B. Lin, P. W. Coschigano and E. N. Marsh (2009). Subunit structure of benzylsuccinate synthase. *Biochemistry.* **48**: 1284-1292.
57. Lipscomb, J. D. (2008). Mechanism of extradiol aromatic ring-cleaving dioxygenases. *Curr Opin Struct Biol.* **18**: 644-649.
58. Lovley, D. R. and D. J. Lonergan (1990). Anaerobic oxidation of toluene, phenol, and *p*-cresol by the dissimilatory iron-reducing organism, GS-15. *Appl Environ Microbiol.* **56**: 1858-1864.
59. Meckenstock, R. U., E. Annweiler, W. Michaelis, H. H. Richnow and B. Schink (2000). Anaerobic naphthalene degradation by a sulfate-reducing enrichment culture. *Appl Environ Microbiol.* **66**: 2743-2747.
60. Mullis, K., F. Faloona, S. Scharf, R. Saiki, G. Horn and H. Erlich (1986). Specific enzymatic amplification of DNA in vitro: the polymerase chain reaction. *Cold Spring Harb Symp Quant Biol.* **51**: 263-273.
61. Musat, F., A. Galushko, J. Jacob, F. Widdel, M. Kube, R. Reinhardt, H. Wilkes, B. Schink and R. Rabus (2009). Anaerobic degradation of naphthalene and 2-methylnaphthalene by strains of marine sulfate-reducing bacteria. *Environ Microbiol.* **11**: 209-219.
62. Peters, F., Y. Shinoda, M. J. McInerney and M. Boll (2007). Cyclohexa-1,5-diene-1-carbonyl-coenzyme A (CoA) hydratases of *Geobacter metallireducens* and *Syntrophus aciditrophicus*: Evidence for a common benzoyl-CoA degradation pathway in facultative and strict anaerobes. *J Bacteriol.* **189**: 1055-1060.
63. Qiao, C. and E. N. Marsh (2005). Mechanism of benzylsuccinate synthase: stereochemistry of toluene addition to fumarate and maleate. *J Am Chem Soc.* **127**: 8608-8609.
64. Rabus, R., M. Fukui, H. Wilkes and F. Widdle (1996). Degradative capacities and 16S rRNA-targeted whole-cell hybridization of sulfate-reducing bacteria in an anaerobic enrichment culture utilizing alkylbenzenes from crude oil. *Appl Environ Microbiol.* **62**: 3605-3613.
65. Rabus, R. and F. Widdel (1995). Conversion studies with substrate analogues of toluene in a sulfate-reducing bacterium, strain Tol2. *Arch Microbiol.* **164**: 448-451.
66. Rabus, R., H. Wilkes, A. Behrends, A. Armstroff, T. Fischer, A. J. Pierik and F. Widdel (2001). Anaerobic initial reaction of *n*-alkanes in a denitrifying bacterium: evidence for (1-methylpentyl)succinate as initial product and for involvement of an organic radical in *n*-hexane metabolism. *J Bacteriol.* **183**: 1707-1715.

67. Safinovski, M., Meckenstock R. U (2004). Enzymatic reactions in anaerobic 2-methylnaphthalene degradation by the sulfate-reducing enrichment culture N47. *FEMS Microbiol. Lett*. **240**: 99-104.
68. Sambrook, J., Fritsch, E.F. & Maniatis, T (1989). Molecular Cloning: A Laboratory Manual. *Cold Spring Harbor Laboratory Press*, Plainview, NY.
69. Sanger, F., S. Nicklen and A. R. Coulson (1977). DNA sequencing with chain-terminating inhibitors. *Proc Natl Acad Sci U S A.* **74**: 5463-5467.
70. Selesi, D., N. Jehmlich, M. von Bergen, F. Schmidt, T. Rattei, P. Tischler, T. Lueders and R. U. Meckenstock (2010). Combined genomic and proteomic approaches identify gene clusters involved in anaerobic 2-methylnaphthalene degradation in the sulfate-reducing enrichment culture N47. *J Bacteriol.* **192**: 295-306.
71. Selmer, T., A. J. Pierik and J. Heider (2005). New glycyl radical enzymes catalysing key metabolic steps in anaerobic bacteria. *Biol Chem.* **386**: 981-988.
72. Seyfried, B., G. Glod, R. Schocher, A. Tschech and J. Zeyer (1994). Initial reactions in the anaerobic oxidation of toluene and *m*-xylene by denitrifying bacteria. *Appl Environ Microbiol.* **60**: 4047-4052.
73. Seyhan, D (2016). Neue Einblicke in den Reaktionsmechanismus der Benzylsuccinat-Synthase. *Dissertation* (Philipps Universität Marburg).
74. Seyhan, D., P. Friedrich, M. Szaleniec, M. Hilberg, W. Buckel, B. T. Golding and J. Heider (2016). Elucidating the stereochemistry of enzymatic benzylsuccinate synthesis with chirally labeled toluene. *Angew Chem Int Ed Engl.* **55**: 11664-11667.
75. Sofia, H. J., G. Chen, B. G. Hetzler, J. F. Reyes-Spindola and N. E. Miller (2001). Radical SAM, a novel protein superfamily linking unresolved steps in familiar biosynthetic pathways with radical mechanisms: functional characterization using new analysis and information visualization methods. *Nucleic Acids Res.* **29**: 1097-1106.
76. Strijkstra, A., K. Trautwein, R. Jarling, L. Wöhlbrand, M. Dörries (2014). Anaerobic activation of *p*-cymene in denitrifying betaproteobacteria: methyl group hydroxylation versus addition to fumarate. *Appl. Environ. Microbiol.* **80**: 7592-603.
77. Szaleniec, M. and J. Heider (2016). Modeling of the reaction mechanism of enzymatic radical C-C coupling by benzylsuccinate synthase. *Int J Mol Sci.* **17**: 514.
78. Towbin, H., T. Staehelin and J. Gordon (1979). Electrophoretic transfer of proteins from polyacrylamide gels to nitrocellulose sheets: procedure and some applications. *Proc Natl Acad Sci U S A.* **76**: 4350-4354.
79. Verfürth, K (2005). Untersuchungen zur Reaktion der Benzylsuccinat Synthase, des ersten Enzyms des anaeroben Toluol-Stoffwechsels. *Dissertation*(Albert-Ludwigs-Universität Freiburg).
80. Verfurth, K., A. J. Pierik, C. Leutwein, S. Zorn and J. Heider (2004). Substrate specificities and electron paramagnetic resonance properties of benzylsuccinate synthases in anaerobic toluene and *m*-xylene metabolism. *Arch Microbiol.* **181**: 155-162.
81. Vogel, T. M. and D. Grbic-Galic (1986). Incorporation of oxygen from water into toluene and benzene during anaerobic fermentative transformation. *Appl Environ Microbiol.* **52**: 200-202.
82. Weelink, S. A., W. van Doesburg, F. T. Saia, W. I. Rijpstra, W. F. Roling, H. Smidt and A. J. Stams (2009). A strictly anaerobic betaproteobacterium *Georgfuchsia toluolica* gen. nov., *sp*. nov. degrades aromatic compounds with Fe(III), Mn(IV) or nitrate as an electron acceptor. *FEMS Microbiol Ecol.* **70**: 575-585.
83. Wohlbrand, L., J. H. Jacob, M. Kube, M. Mussmann, R. Jarling, A. Beck, R. Amann, H. Wilkes, R. Reinhardt and R. Rabus (2013). Complete genome, catabolic sub-proteomes and

key-metabolites of *Desulfobacula toluolica* Tol2, a marine, aromatic compound-degrading, sulfate-reducing bacterium. *Environ Microbiol.* **15**: 1334-1355.

84. Wohlbrand, L. and R. Rabus (2009). Development of a genetic system for the denitrifying bacterium '*Aromatoleum aromaticum'* strain EbN1. *J Mol Microbiol Biotechnol.* **17**: 41-52.

85. Zengler, K., J. Heider, R. Rossello-Mora and F. Widdel (1999). Phototrophic utilization of toluene under anoxic conditions by a new strain of *Blastochloris sulfoviridis*. *Arch Microbiol.* **172**: 204-212.

86. Zhang, X. and L. Y. Young (1997). Carboxylation as an initial reaction in the anaerobic metabolism of naphthalene and phenanthrene by sulfidogenic consortia. *Appl Environ Microbiol.* **12**:4759-64.

IX. SUPPLEMENTARY MATERIAL

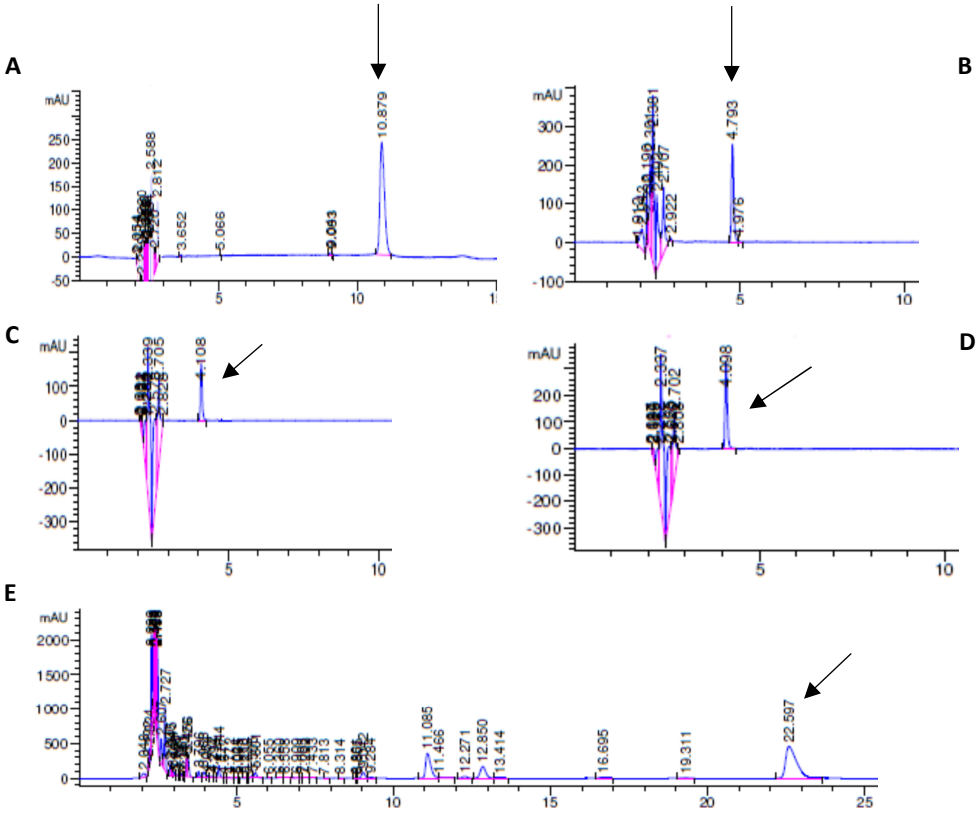

Supplementary Figure 1: RP-HPLC chromatograms with respective products of conversion of (A) toluene (benzylsuccinate), (B) *m*-cresol, (C) *o*-cresol, (D) *p*-cresol (hydroxyl)benzylsuccinate, (E) *m*-xylene (methyl)benzylsuccinate.

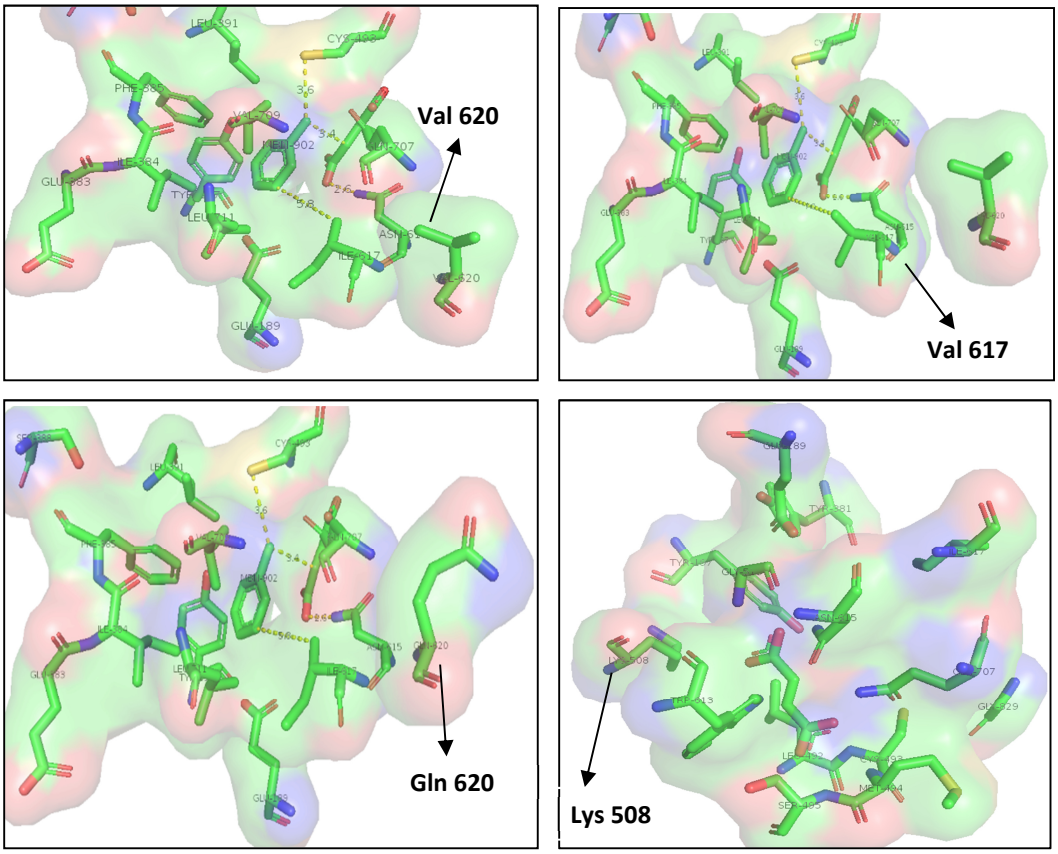

Supplementary Figure 2: Structure models of the active centre of BSS Isoleucine (617, 620) and Arginine 508 mutants together with bound substrates: toluene and fumarate (shown as sticks, coloured in green). (A) BSS I620V (B) BSS I617 + 620V (C) BSS I620Q (D) BSS R508K (E) BSS R508Q. Arrows indicate respective amino acid substitutions of Isoleucine 617, 620 and Arginine 508.

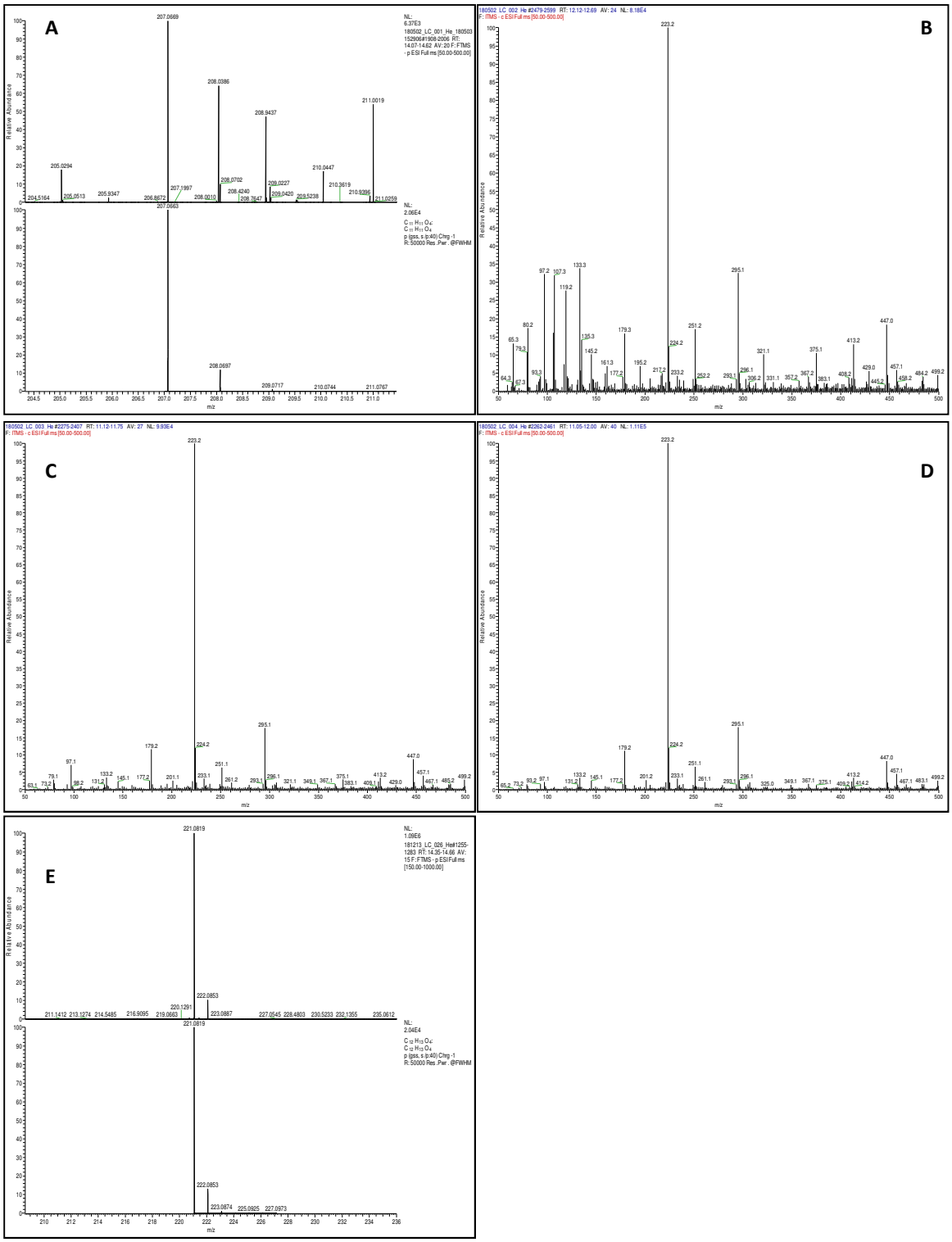

Supplementary Figure 3: HPLC-MS analysis of the samples, containing reaction products of recombinant wild type BSS and its variants with toluene, *m-, o-, p*-cresol and *m*-xylene, respectively: (A) benzylsuccinate (m/z = 207.067), (B, C, D) hydroxybenzylsuccinate (m/z = 223.2), (E) (methyl)benzylsuccinate (m/z = 221.08) Conversion assays with unlabeled substrates were adjusted to pH 3, the precipitated proteins were removed by centrifugation, metabolites were extracted with >99,8% diethyl ether and solubilized in water. Samples, containing reaction products were separated by HPLC-MS on a RP-C4 column) with an aqueous mobile phase containing 20% acetonitrile and 40mM formic acid. The samples were analyzed in collaboration with the Team des Gerätezentrums für Massenspektrometrie und Elementanalytik, Fachbereich Chemie, Philipps Universität Marburg.

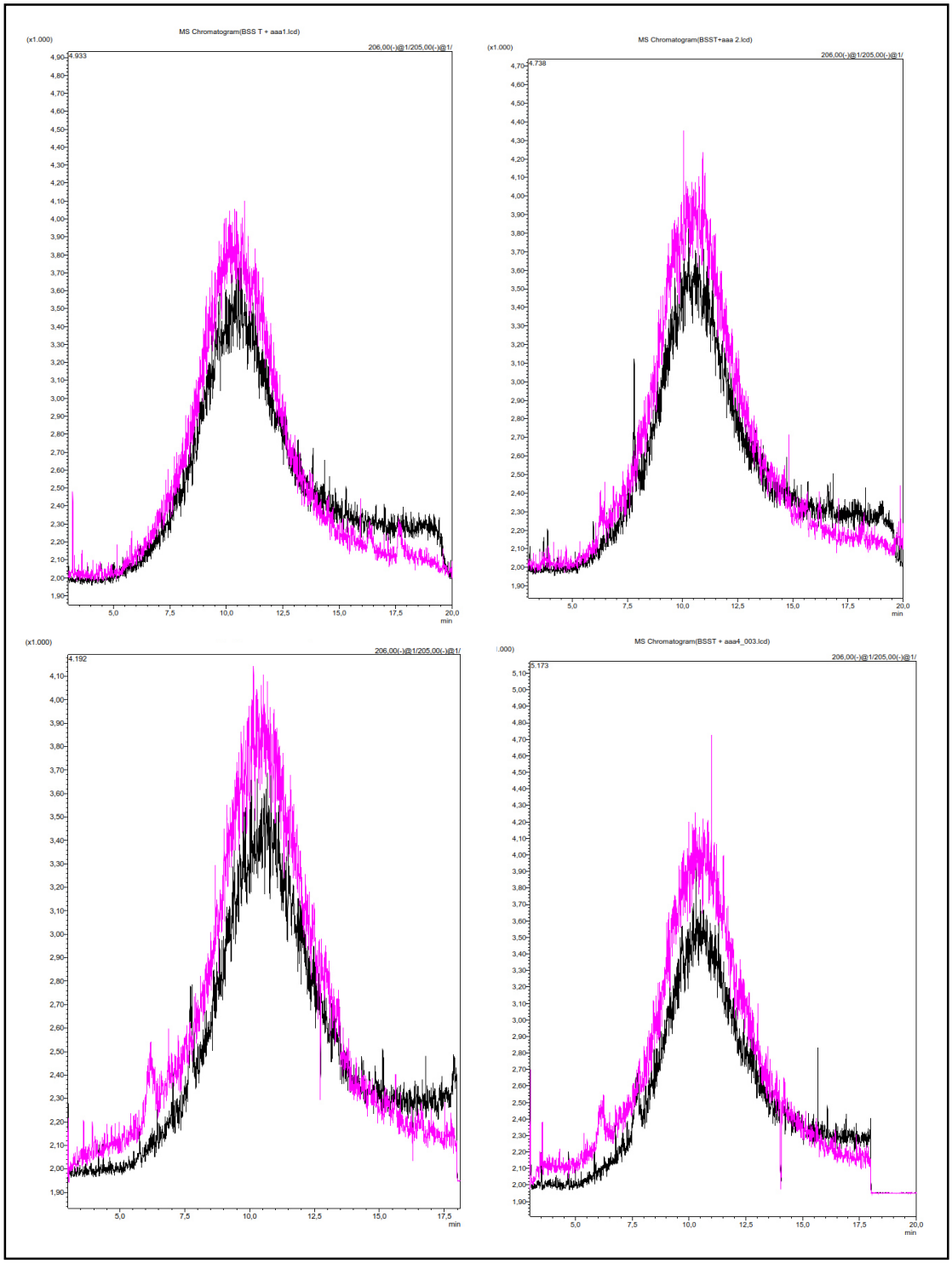

Supplementary Figure 4: HPLC-MS analysis for the detection of 3-benzylpentan-4-onate (m/z = 206.00). (m/z = 206.0)

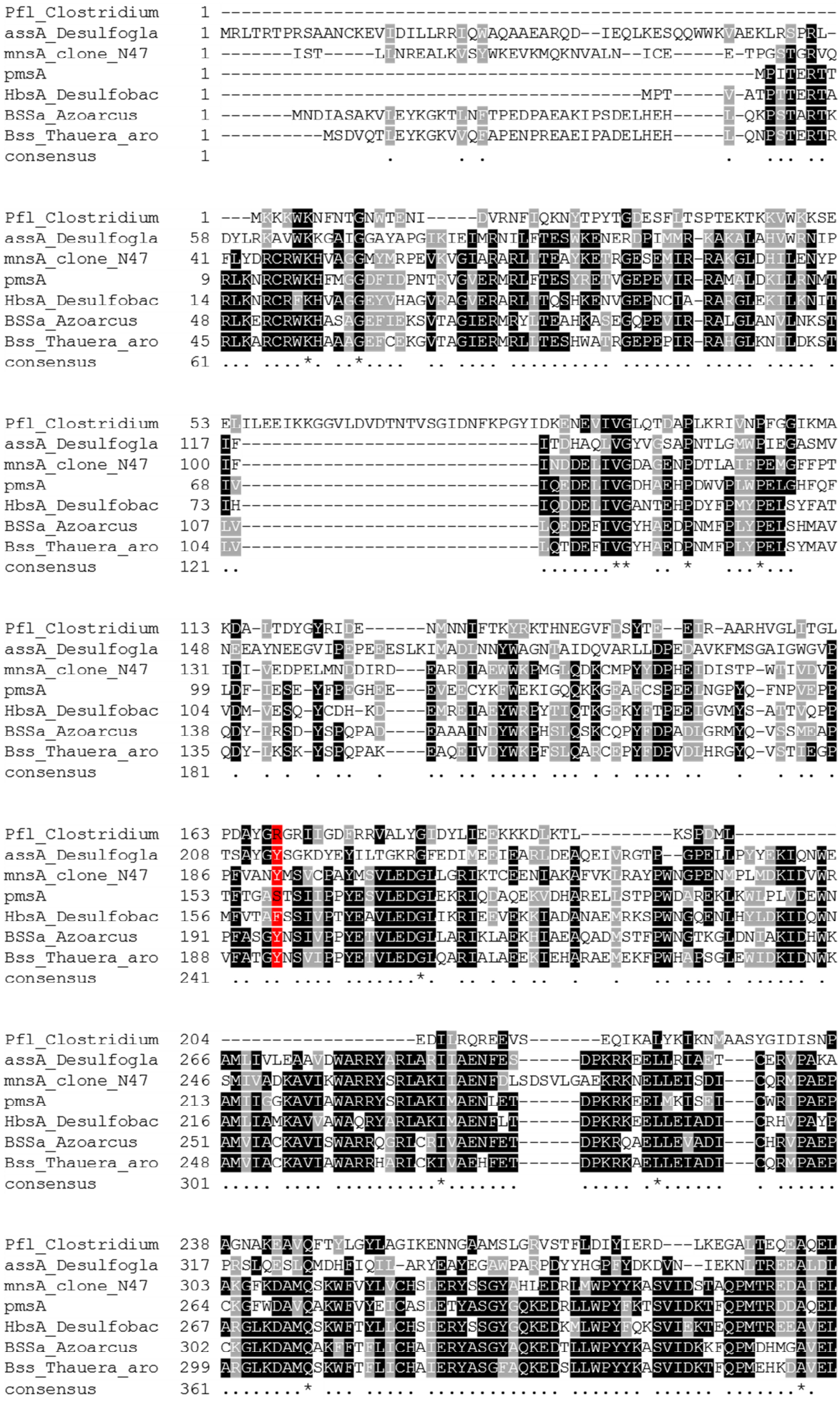
Pfl_Clostridium
assA_Desulfogla
mnsA_clone_N47
pmsA
HbsA_Desulfobac
BSSa_Azoarcus
Bss_Thauera_aro
consensus

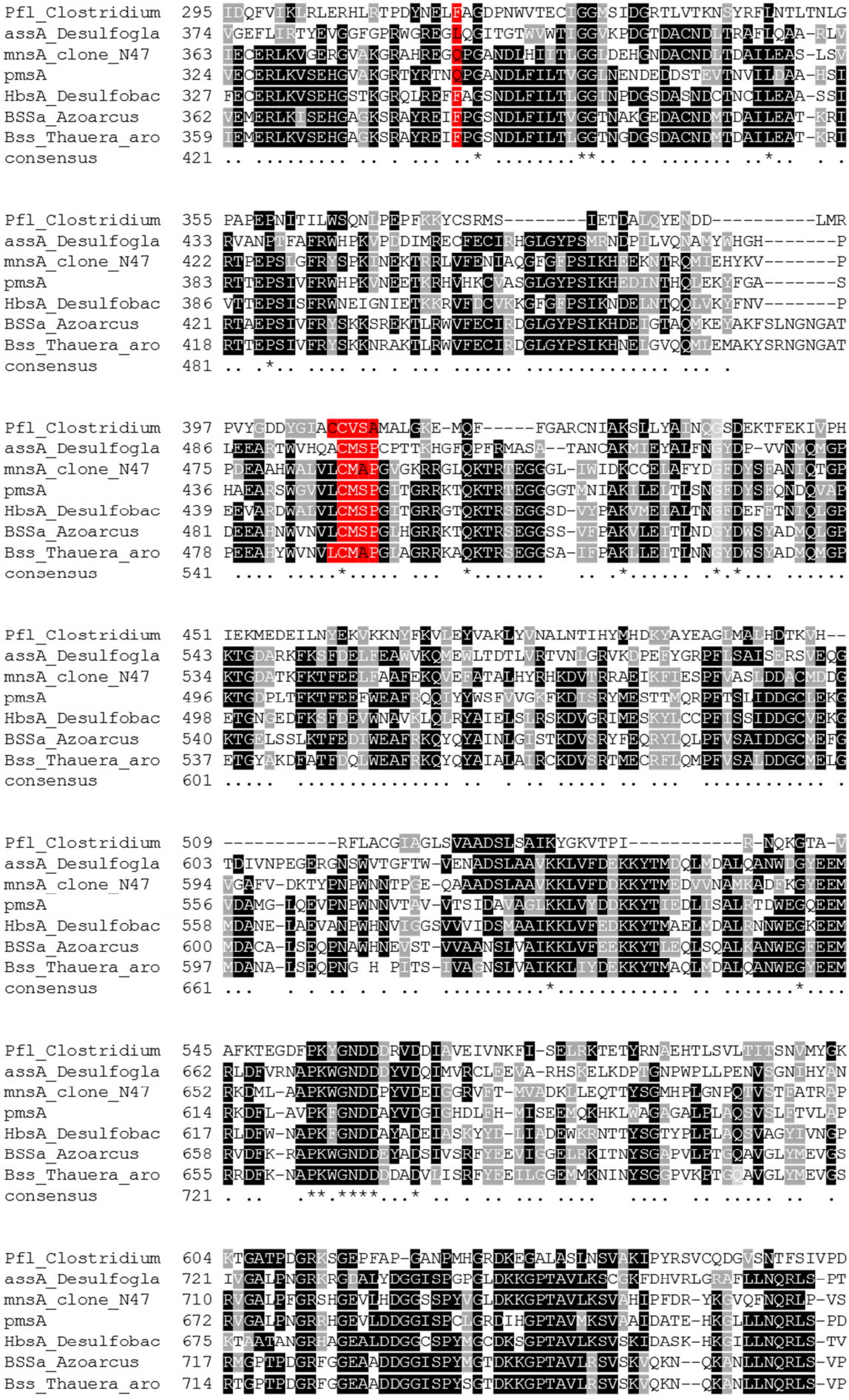
Pfl_Clostridium 295
assA_Desulfogla 374
mnsA_clone_N47 363
pmsA 324
HbsA_Desulfobac 327
BSSa_Azoarcus 362
Bss_Thauera_aro 359
consensus 421
Pfl_Clostridium 355
assA_Desulfogla 433
mnsA_clone_N47 422
pmsA 383
HbsA_Desulfobac 386
BSSa_Azoarcus 421
Bss_Thauera_aro 418
consensus 481
Pfl_Clostridium 397
assA_Desulfogla 486
mnsA_clone_N47 475
pmsA 436
HbsA_Desulfobac 439
BSSa_Azoarcus 481
Bss_Thauera_aro 478
consensus 541
Pfl_Clostridium 451
assA_Desulfogla 543
mnsA_clone_N47 534
pmsA 496
HbsA_Desulfobac 498
BSSa_Azoarcus 540
Bss_Thauera_aro 537
consensus 601
Pfl_Clostridium 509
assA_Desulfogla 603
mnsA_clone_N47 594
pmsA 556
HbsA_Desulfobac 558
BSSa_Azoarcus 600
Bss_Thauera_aro 597
consensus 661
Pfl_Clostridium 545
assA_Desulfogla 662
mnsA_clone_N47 652
pmsA 614
HbsA_Desulfobac 617
BSSa_Azoarcus 658
Bss_Thauera_aro 655
consensus 721
Pfl_Clostridium 604
assA_Desulfogla 721
mnsA_clone_N47 710
pmsA 672
HbsA_Desulfobac 675
BSSa_Azoarcus 717
Bss_Thauera_aro 714

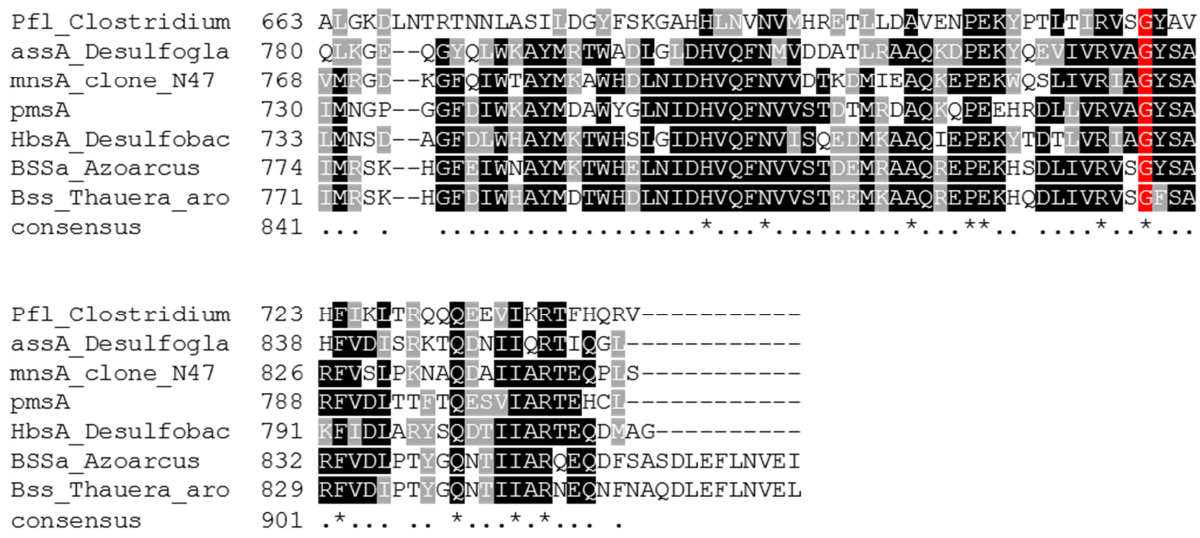

Supplementary Figure 5: Amino acid residues inside the active sites of alpha subunits of MPS (PMS) compared to other FAEs from δ-Proteobacteria *Desulfoglaeba alkanexedens*, *Desulfobacula toluolica* and β-Proteobacteria *Thauera aromatica* K172*, Azoarcus* strain T. Amino acids, identified as crucial for substrate binding and glycyl radical formation are highlighted in red (S158, S160, Q346, C447, G784).

X. List of abbreviations

%	percent
°C	grad Celsius
µ	micro (10^{-6})
A	adenine
Å	Angstrom
A.	*Aromatoleum, Azoarcus*
AHT	anhydrotetracycline
Amp	ampicillin
APS	ammonium persulfate
ATP	adenosine-5´-triphosphate
bbs	operon for the β-oxidation of (R)-benzylsuccinate
bla	gene for β-lactamase
bp	basepairs
BSA	bovine serum albumine
BSS	(R)-benzylsuccinate synthase
CoA	coenzyme A
C-terminal	carboxyterminal
Da	Dalton
DFT	*density function theoretical* (-model)
DMSO	dimethyl sulfoxide
DNA	deoxyribonucleic acid
DNase	desoxyrionuclease
E.	*Escherichia*
EDTA	ethylendiamintetraacetatic acid
EPR	'Electron Paramagnetic Resonance'-(spectroscopy)
Et al.,	*et al*ii; and others
FAE	fumarate addition enzyme
Fig.	figure
g	gram, gravity (acceleration of gravity)
G	guanine
h	hour
HEPES	4-(2-hydroxyethyl)-1-piperazineethanesulfonic acid
HPLC	high performance liquid chromatography
ICP-OES	optical emission spectrometry
K	Kelvin
k	kilo (10^{3})
kBp	kilo base pair
kDa	kilo Dalton
Km	Michaelis-Menten constant
l	liter
m	meter, milli (10^{-3}), messenger
M	molarity, mega (10^{6})
m/z	mass to charge ratio

MALDI	matrix-assisted laser desorption/ionization
MD	molecular dynamics and docking
min	minute
MPS/PMS	methylphenanthrene succinate synthase
MS	mass spectrometry
mU/mg	mili units per miligram
n	nano (10^{-9})
NMS	naphthyl-2(methyl)succinate synthase
N-terminal	aminoterminal
OD_{578}	optical density at 578 nm
PAGE	polyacrylamid gel electrophoresis
PAH	polycyclic aromatic hydrocarbons
PCR	polymerase chain reaction
pH	negative decadal logarithm of the proton concentration
QM	quantum modelling
RNA	ribonucleic acid
RNase	ribonuclease
RP	reversed-phase
rpm	revolutions per minute
RT	room temperature
s	seconds
SAM	S-adenosylmethionine
SDS	sodium dodecyl sulphate
T	thymine
T.	*Thauera (aromatica)*
TAE	tris-acetate EDTA-buffer
TEMED	tetramethylethylenediamine
TOF	time-of-flight
Tris	tris-(hydroxymethyl)-aminomethane
V	Volt
v/v	volume per volume
Vmax	maximum velocity
w/v	weight per volume

XI. Acknowledgements

I would like to express my sincere gratitude to my Doctoral Thesis supervisor, Prof. Dr. Johann Heider for his encouragement, mentoring and throughout the course of this work. I would also like to thank him for his patience and motivation during the time of research and writing of the thesis. I am grateful to Prof. Dr. Wolfgang Buckel and Dr. Seigo Shima for their guidance, suggestion and the time we spent on all the wonderful scientific discussions. I also take this opportunity to thank all the past and present members of the Prof. Dr. Heider laboratory, for their help, support and the wonderful working environment during the course of this work. I would like to say a big thank you to all the wonderful friends and people I have met at the Philipps University Marburg and at the Max Planck Institute. A special thank you needs to be mentioned to Dr. Karola Schühle and Dr. Georg Schmitt for all the help and advice in the laboratory during the last few years. Lastly, I would like to thank my beloved partner, Daniel Gleditzsch and his family, all my friends: Fabian Arndt, Agnieszka Winiarska, Ammar Alhaj Zein, Anastasiya Sybirna and Oleksii Lyzak. Special thanks to my family and friends in Ukraine for constant emotional support during my time in Marburg. Without the understanding and encouragement of all these wonderful people, this work would not have been possible.

I would also like to thank the IMPRS Graduate School and it's organizers for the research guidance, financial funding during the first 2 years of my PhD studies and providing the excellent opportunity for young scientists all over the world to work in first-class laboratories and working groups, as it is represented at the Philipps University Marburg and the Max Planck Institute for Terrestrial Microbiology.

XII. Erklärung

Ich versichere, dass ich meine Dissertation selbstständig, ohne unerlaubte Hilfe angefertigt und mich keiner anderen als der von mir ausdrücklich bezeichneten Quellen Hilfen bedient habe.

Die Dissertation wurde in der jetzigen oder einer ähnlichen Form noch bei keiner anderen Hochschule eingereicht und hat noch keinen sonstigen Prüfungszwecken gedient.

_____ _____

(Datum) (Unterschrift)

XIII. Lebenslauf

Ausbildung

Seit 10/2015	**Promotion**, International Max Planck Research School, Philipps-Universität Marburg • Arbeitsgruppe für Mikrobielle Biochemie • Arbeiten mit anaeroben Mikroorganismen • Protein-Aufreinigung und –Bioanalytik • Entwicklung und Durchführung von Enzymaktivitäts-Assays • Betreiben, Wartung und Validierung von Analytik Geräten wie von z.B. HPLC, FPLC (Äkta), HPLC-MS, MALDI-TOF
Dissertation:	‚Substrate recognition determinants of benzylsuccinate synthase and other fumarate-adding glycyl radical enzymes‘
09/2012 – 06/2013	**M.Sc. Biochemie,** Nationale Iwan-Franko-Universität Lwiw
Praktika:	• Metabolic Engineering in Hefe, Alkoholische Gärung, Enzymologie, **Molekulare Genetik**
Master-Thesis:	• Development of the multicopy gene integration system in *Saccharomyces cerevisiae* and *Hansenula polymorpha*
09/2008 – 07/2012	**B.Sc. Biologie**, Nationale Iwan-Franko-Universität Lwiw
Vertiefungen:	• Mikrobiologie, Genetik, Biochemie, Bioinformatik und Statistik, Biotechnologie, Zellbiologie, Radiobiologie, Botanik, Zoologie
Bachelor-Thesis:	• Futile cycles generation by overexpression of *TPS* and *NTH g*enes, encoding trehalose-6-phosphate synthase and neutral trehalase for improvement of ethanol production in Saccharomyces *cerevisiae*

Berufserfahrung

05/2015 – 09/2015	**Assistentin in Personalvermittlung**, Indeema Software, Lwiw, Ukraine
09/2012 – 09/2015	**Wissenschaftliche Hilfskraft**, Institut für Zellbiologie, Lwiw, Ukraine • Metabolic Engineering in Hefe, Enzymologie, Alkoholische Gärung
06/2012 – 09/2012	**Verkaufsberaterin** für Kosmetikprodukte, Lwiw, Ukraine
09/2011 – 08/2012	**Wissenschaftliche Hilfskraft**, Institut für Zellbiologie, Lwiw, Ukraine • Biochemie, Molekulare Genetik, Kultivierung von Mikroorganismen

Fortbildungen

12/2017	• Fortbildung in **GMP & GLP** (PDM-Consulting, apceth GmbH & Co.KG) Grundlagen und erweiterte Anforderungen in der pharmazeutischen Industrie. MARA Research Academy, Philipps-Universität Marburg, Deutschland
11/2017	• Fortbildung für Projektleiter und Beauftragte für **biologische Sicherheit nach § 15 GenTSV**. MPI für Biochemie, Martinsried, Deutschland
05/2017	• Workshop der International Max Planck Research School: „**Einführung in Massenspektroskopie-basierte Proteomik**“
05/2017	• Workshop der International Max Planck Research School: „**Datenanalyse und Computermodellierung in Mikrobiologie**“
11/2016	• Workshop der International Max Planck Research School: „**Quantitative Metabolomik in verschiedenen Mikroben**“
02/2016	• Workshop der International Max Planck Research School: „**Funktionelle Analyse von mikrobiellen Gemeinschaften**“
05/2014	• Workshop Universität von Rzeszów (Polen): “**Molekulare Methoden zur Herstellung von Stämmen zur Detoxifizierung der Umwelt**”